

Supporting Information

Abnormal NHC Ruthenium Catalysts: Mechanistic Investigations of their Preparation and Steric Influence on Catalytic Performance

Alexander D. Böth,¹ Michael J. Sauer,¹ Walter Baratta^{*2} and Fritz E. Kühn^{*1}

*Corresponding authors, walter.baratta@uniud.it, fritz.kuehn@ch.tum.de

¹Technische Universität München, Catalysis Research Center and Department of Chemistry, Professorship of Molecular Catalysis, Lichtenbergstr. 4, 85748 Garching b. München, Germany

²Università di Udine, Dipartimento DI4A, Via Cotonificio 108, 33100 Udine, Italy

Abstract

The bis-abnormal *N*-heterocyclic carbene (aNHC) ruthenium complexes [Ru(OAc)(aNHC-ethyl-PPh₂)₂]Br **1** and **3** are obtained from Ru(OAc)₂(PPh₃)₂ with the ligands 1-(2-diphenylphosphino-ethyl)-3-aryl-imidazolium bromide (aryl = phenyl, di-*iso*-propylphenyl) **L^{Ph}** and **L^{Dipp}** in THF at 60 °C and in the presence of NaOAc *via* displacement of PPh₃ and carbene deprotonation. Mechanistic studies on the formation of the di-*iso*-propylphenyl derivative **3** reveal the preceding generation of mono-aNHC intermediate isomers **3a** and **3b** as kinetic and thermodynamic products. Complexes **1** and **3** exhibit exceptionally high activity in the transfer hydrogenation (TH) of acetophenone and *Oppenauer*-type oxidation of α -tetralol, **1** showing turn-over frequencies (TOF) of up to 550 000 h⁻¹ in the TH of acetophenone and **3** showing TOFs up to 280 000 h⁻¹ in the *Oppenauer*-type oxidation of α -tetralol. The comparison of the catalytic activity of the phenyl **1**, mesityl **2** and di-*iso*-propylphenyl **3** complexes follows the order **1** > **2** > **3** for TH, likely due to accessibility of the active center, whilst following the inverse **3** > **2** > **1** order in *Oppenauer*-type oxidation. This inversion appears to be dependent on steric influences. These observations are in line with buried volume calculations based on density functional theory (DFT) optimized structures.

KEYWORDS: *N*-heterocyclic carbenes, Ruthenium, Transfer Hydrogenation, *Oppenauer*-type Oxidation

Table of Content

General Remarks	3
Ligand Syntheses	4
Synthesis of L _{Ph}	4
Synthesis of L ^{Dipp}	8
Complex Syntheses.....	13
Synthesis of 1.....	13
Synthesis of 3.....	14
Synthesis of 3a.....	16
NMR evidence of 3b	17
NMR Spectra.....	18
Single Crystal X-Ray Structure Determination	33
General Procedure for Catalytic Transfer Hydrogenation Reactions	35
General Procedure for Catalytic Oppenauer-type Oxidation Reactions.....	35
TOF Calculations	35
Catalytic Results	36
Transfer Hydrogenation	36
Oppenauer-Type Oxidation.....	43
DFT - Computational Structure Calculations.....	47
General Remarks	47
Coordinate Tables	47
Calculated Structures	63
DFT - Buried Volume and Steric Map Calculations	65
General Remarks	65
Buried Volume Tables	67
Steric Maps.....	73
Mechanisms	75
References.....	77
Author Contributions	78

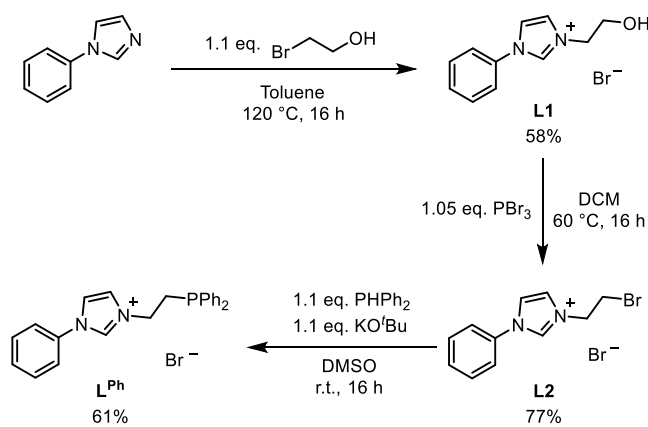
General Remarks

Unless otherwise specified, all reactions were performed under oxygen free, dry conditions in an argon atmosphere using standard Schlenk conditions and glovebox techniques. All solvents, unless described otherwise, were purified, degassed and dried according to standard purification techniques or obtained from a *M. Braun SPS* purification system. If not noted differently, all further chemicals were purchased from commercial sources and used as received. Substrates for catalysis were distilled prior to degassing. Ru(OAc)₂(PPh₃)₂ was prepared according to a literature method.¹ NMR spectra were acquired on a *Bruker Avance Ultrashield 400 MHz* and a *Bruker DPX 400 MHz* spectrometer. Data was processed with *MestreNova* from *Mestrelab Research*. All ¹H and ¹³C chemical shifts are reported in parts per million (ppm) relative to TMS, with the residual solvent peak serving as internal reference. ³¹P NMR spectra are referenced to 85% H₃PO₄ as external standard. Single crystals were measured in the SC-XRD laboratory of the *Catalysis Research Center at Technische Universität München*. Electron spray ionization mass spectrometry (ESI-MS) was conducted on a Finnigan MAT SSQ 7000 (MS-EI, 70 eV; CI, 100 eV) equipped with a ThermoFisher Scientific LTQ Orbitrap XL. Liquid Injection Field Desorption Ionization Mass Spectrometry (LIFDI-MS) was measured directly from an inert atmosphere glovebox with a Thermo Fisher Scientific Exactive Plus Orbitrap equipped with an ion source from Linden CMS. GC analysis was performed with an *Agilent Technologies 7890B* GC system using an *Agilent VF-200ms* column (30 m × 250 µm × 0.25µm). CHN analyses were carried out in the microanalytical laboratory at *Technische Universität München*.

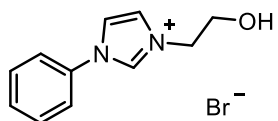
Ligand Syntheses

Synthesis of L^{Ph}

Ligand L^{Ph} is prepared applying a similar synthetic pathway to the preparation of the mesityl and di-isopropylphenyl analogues (Scheme S1), albeit adapted regarding the workup procedures. *N*-phenylimidazole is chosen as starting point for the synthesis, as this is available commercially. Whilst L1 has merely been reported previously in correlation with a patent,² both L2 and L^{Ph} represent novel compounds, to the best of our knowledge.



Scheme S1: Synthetic pathway for the preparation of L^{Ph} from *N*-phenylimidazole.



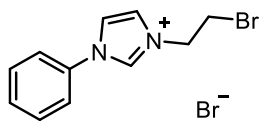
L1

C₁₁H₁₃BrN₂O
269.14 g/mol

N-phenylimidazole (6.84 g, 47.4 mmol, 1.00 eq.) is added to toluene (20.0 mL) at 60 °C. 2-Bromoethanol (6.53 g, 52.2 mmol, 1.10 eq.) is added slowly and the reaction mixture and stirred at 120 °C for 16 h. The work-up is performed under atmospheric conditions. The reaction mixture is cooled to r.t., the formed precipitate isolated and washed with toluene (3 x 10.0 mL) and diethylether (3 x 10.0 mL). Acetonitrile (15 mL) is added to the crude brown solid from which a white solid is consequently isolated by separation from the brown solution *via* filtration, yielding compound **L1** as a white solid (7.43 g, 27.5 mmol, 58%).

¹H NMR (300 MHz, CD₃OD, 300 K) δ [ppm] = 9.59 (s, 1H, NCHN), 8.14 (t, ⁴J = 1.9 Hz, 1H, NCHCHN), 7.91 (t, ⁴J = 1.9 Hz, 1H, NCHCHN), 7.82 - 7.59 (m, 5H, Ph), 4.47 (t, ³J = 4.4 Hz, 2H, NCH₂CH₂O), 4.01 (t, ³J = 4.0 Hz, 2H, NCH₂CH₂O).

¹³C NMR (101 MHz, CD₃OD, 300 K) δ [ppm] = 136.9 (NCHN), 136.4, 131.5 (2C), 131.3, 125.0 (NCHCHN), 123.4 (2C), 122.8 (NCHCHN), 60.98 (NCH₂CH₂O), 53.81 (NCH₂CH₂O).



L2

C₁₁H₁₂Br₂N₂

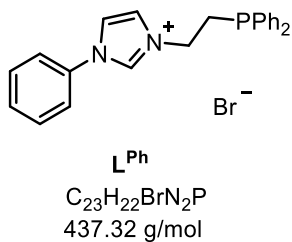
332.03 g/mol

Compound **L1** (4.84 g, 17.9 mmol, 1.00 eq.) is suspended in DCM (60 mL) and cooled to 0 °C. A solution of phosphorus tribromide (5.11 g, 18.9 mmol, 1.05 eq.) in DCM (20.0 mL) is added slowly, the reaction mixture heated to 60 °C and stirred for 16 h. The work-up is performed under atmospheric conditions. The solvent is removed under reduced pressure and methanol (20 mL) added. A yellow solid is removed *via* centrifugation and decanting, resulting in a clear solution. Addition of diethyl ether results in precipitation of a white solid. This is dissolved in methanol and filtered over a plug with basic aluminum oxide and consequently a PTFE whatman filter (0.2 µm). Removing of the solvent yields compound **L2** as a white solid (4.60 g, 13.9 mmol, 77%).

ESI-MS (EI, 70 eV): m/z (%) = 252 (100) [**L2**-Br]⁺.

¹H NMR (300 MHz, CD₃OD, 300 K) δ [ppm] = 9.73 (t, ⁴J = 1.4 Hz, 1H, NCHN), 8.18 (t, ⁴J = 1.8 Hz, 1H, NCHCHN), 7.98 (t, ⁴J = 1.8 Hz, 1H, NCHCHN), 7.81 - 7.73 (m, 2H, Ph), 7.73 - 7.61 (m, 3H, Ph), 4.81 (t, ³J = 5.9 Hz, 2H, NCH₂CH₂Br), 3.99 (t, ³J = 5.9 Hz, 2H, NCH₂CH₂Br).

¹³C NMR (101 MHz, CD₃OD, 300 K) δ [ppm] = 137.1 (NCHN), 136.3, 131.6 (2C), 131.5, 124.7 (NCHCHN), 123.3 (2C), 123.1 (NCHCHN), 52.53 (NCH₂CH₂O), 30.67 (NCH₂CH₂O).



Potassium *tert*-butoxide (1.64 g, 14.6 mmol, 1.10 eq.) and diphenylphosphine (2.72 g, 14.6 mmol, 1.10 eq.) are dissolved in dimethyl sulfoxide (40 mL) and slowly added to a solution of compound **L2** (4.41 g, 13.3 mmol, 1.00 eq.) in dimethyl sulfoxide (50 mL). The reaction mixture is stirred at 60 °C for 3 h. After removal of the solvent under reduced pressure ($1 \cdot 10^{-3}$ mbar) at 90 °C the crude product is dissolved in DCM (20 mL), filtrated, concentrated to approximately 2.00 mL and precipitated with diethylether. After filtration and drying under reduced pressure compound **L^{Ph}** is obtained as a white solid (3.55 g, 8.11 mmol, 61%).

MS (LIFDI): m/z (%): 357 (100) [$\text{L}^{\text{Ph}}\text{-Br}^-$]⁺.

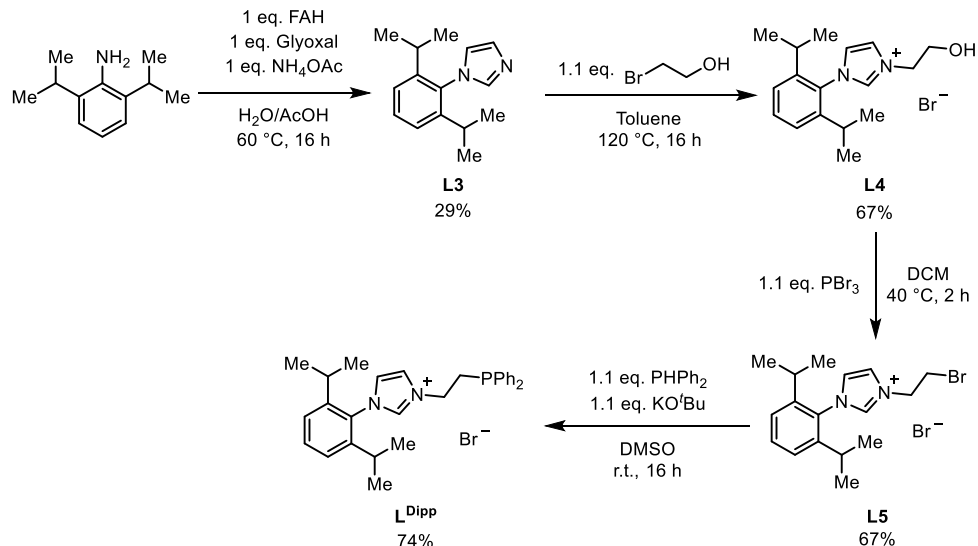
¹H NMR (300 MHz, CD₃OD, 300 K) δ [ppm] = 11.25 (s, 1H, NCHN), 7.75 (t, ⁴J = 1.9 Hz, 1H, NCHCHN), 7.74 (t, ⁴J = 1.9 Hz, 1H, NCHCHN), 7.62 – 7.46 (m, 8H, Ph), 7.45 (t, ⁴J = 1.9 Hz, 1H, Ph), 7.38 – 7.27 (m, 6H, Ph), 4.69 (dt, ^{2,3}J = 10.6, 7.3 Hz, 2H, NCH₂CH₂P), 2.95 (t, ³J = 7.3 Hz, 2H, NCH₂CH₂P).

¹³C NMR (101 MHz, CDCl₃, 300 K) δ [ppm] = 137.1, 137.0 (NCHN), 135.1, 133.5 (2C), 133.3 (2C), 131.0 (2C), 130.7, 129.7 (2C), 129.3 (2C), 129.2 (2C), 123.6, 123.5 (2C), 122.3, 120.4, 48.92 (d, J = 22.7 Hz, NCH₂CH₂P), 29.50 (d, J = 16.0 Hz, NCH₂CH₂P).

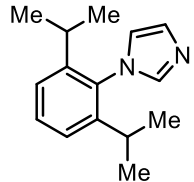
³¹P NMR (162 MHz, CD₂Cl₂, 300 K) δ [ppm] = -21.4 (s, 1P).

Synthesis of L^{Dipp}

Ligand L^{Dipp} was prepared applying a similar synthetic pathway to the preparation of the mesityl analogue (Scheme S2).³ Analytical data is in agreement with that reported in literature.^{3d, 4}



Scheme S2: Synthetic pathway for the preparation of L^{Dipp} from 2,6-di-isopropylaniline.



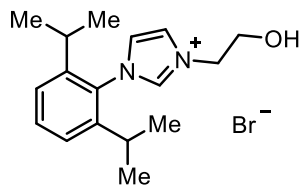
L3

C₁₅H₂₀N₂
228.34 g/mol

A mixture of aqueous formaldehyde (37 wt.%, 18.3 g, 226 mmol, 1.00 eq.), aqueous glyoxal (40 wt.%, 30.5 g, 226 mmol, 1.00 eq.) and glacial acetic acid (80.0 mL) is heated to 70 °C under atmospheric conditions. A mixture of 2,6-di-isopropylphenylaniline (40.0 g, 226 mmol, 1.00 eq.) and ammonium acetate (17.4 g, 226 mmol, 1.00 eq.) in water (16.0 mL) and glacial acetic acid (80.0 mL) is slowly added and the combined reaction mixture stirred overnight at 70 °C. After cooling to r.t. the solution is slowly neutralized with saturated NaHCO₃ solution. The precipitating brown solid is isolated by filtration, dissolved in DCM (300 mL), added to a separatory funnel and the impurities extracted with water (10.0 mL). The organic layer is isolated and the aqueous layer extracted with DCM (3 x 50.0 mL). The solvent is evaporated under reduced pressure and the crude black product purified by sublimation (160 °C, 5 x 10⁻³ mbar), yielding compound **L3** as a white solid (15.0 g, 65.5 mmol, 29%).

¹H NMR (400 MHz, CDCl₃, 300 K) δ [ppm] = 7.46 (s, 1H, NCHN), 7.43 (t, ³J = 7.8 Hz, 1H, NCHCHN), 7.25 (s, 1H, NCHCHN), 7.23 (s, 2H, Dipp_{meta}), 6.93 (t, ⁴J = 1.2 Hz, 1H, Dipp_{para}), 2.39 (hept, ³J = 6.9 Hz, 2H, Dipp_{CH3CHCH3}), 1.12 (d, ³J = 6.9 Hz, 12H, Dipp_{Me}).

¹³C NMR (101 MHz, CDCl₃, 300 K) δ [ppm] = 146.7 (2C), 138.6 (NCHN), 133.0, 129.9 (NCHCHN), 129.5 (NCHCHN), 123.9 (2C), 121.7, 28.23 (2C), 24.56 (2C, Dipp_{Me}), 24.48 (2C, Dipp_{Me}).



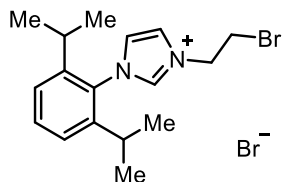
L4

C₁₇H₂₅BrN₂O
353.30 g/mol

Compound **L3** (1.88 g, 8.23 mmol, 1.00 eq.) is dissolved in toluene (20.0 mL) at 60 °C. 2-Bromoethanol (1.13 g, 9.05 mmol, 1.10 eq.) is added slowly and the reaction mixture is stirred at 120 °C for 16 h. The work-up is performed under atmospheric conditions. The reaction mixture is cooled to r.t., the formed precipitate isolated and washed with toluene (3 x 10.0 mL) and diethylether (3 x 10.0 mL). The crude red-brown solid is dissolved in acetone (10.0 mL) and precipitated with diethylether (15.0 mL). Isolation and washing with diethylether (3 x 5.00 mL) yields compound **L4** as a white solid (2.31 g, 5.51 mmol, 67%).

¹H NMR (400 MHz, CDCl₃, 300 K) δ [ppm] = 8.56 (s, 1H, NCHN), 7.71 (t, ⁴J = 1.7 Hz, 1H, NCHCHN), 7.56 (t, ³J = 7.8 Hz, 1H, NCHCHN), 7.32 (d, ³J = 7.9 Hz, 2H, Dipp_{meta}), 7.21 (t, ⁴J = 1.8 Hz, 1H, Dipp_{para}), 4.56 (t, ³J = 4.9 Hz, 2H, NCH₂CH₂P), 4.03 (t, ³J = 4.9 Hz, 2H, NCH₂CH₂P), 2.69 (s, 1H, OH), 2.30 (hept, ³J = 6.5 Hz, 2H, Dipp_{CH3CHCH3}), 1.17 (t, ³J = 6.4 Hz, 12H, Dipp_{Me}).

¹³C NMR (101 MHz, CDCl₃, 300 K) δ [ppm] = 145.7 (2C), 137.1 (NCHN), 132.2, 130.0, 124.9 (2C), 124.5 (NCHCHN), 123.8 (NCHCHN), 60.62 (NCH₂CH₂O), 52.61 (NCH₂CH₂O), 28.75 (2C), 24.31 (2C, Dipp_{Me}), 24.20 (2C, Dipp_{Me}).



L5

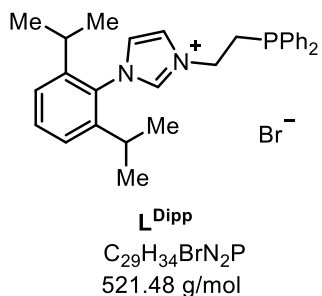
C₁₇H₂₄Br₂N₂
416.20 g/mol

Compound **L4** (1.99 g, 5.29 mmol, 1.00 eq.) is dissolved in DCM (15.0 mL) and cooled to 0 °C. A solution of phosphorus tribromide (2.17 g, 8.00 mmol, 1.10 eq.) in DCM (12.0 mL) is added slowly, the reaction mixture heated to 40 °C and stirred for 2 h. The work-up is performed under atmospheric conditions. After diluting with DCM (30.0 mL) the reaction mixture is slowly neutralized with sat. NaHCO₃ (30.0 mL) solution in a separatory funnel. The organic phase is isolated and the aqueous phase extracted with DCM (3 x 30.0 mL). The combined organic phase is dried over MgSO₄ and the solvent removed under reduced pressure, yielding compound **L5** as a white solid (1.47 g, 3.53 mmol, 67%).

ESI-MS (EI, 70 eV): m/z (%) = 336 (100) [**L5**-Br]⁺.

¹H NMR (400 MHz, CDCl₃, 300 K) δ [ppm] = 9.58 (t, ⁴J = 1.6 Hz, 1H, NCHN), 8.24 (t, ⁴J = 1.7 Hz, 1H, NCHCHN), 7.55 (t, ³J = 7.8 Hz, 1H, NCHCHN), 7.32 (d, ³J = 7.8 Hz, 2H, Dipp_{meta}), 7.21 (t, ⁴J = 1.8 Hz, 1H, Dipp_{para}), 5.16 (t, ³J = 5.3 Hz, 2H, NCH₂CH₂P), 4.01 (t, ³J = 5.4 Hz, 2H, NCH₂CH₂P), 2.34 (hept, ³J = 6.8 Hz, 2H, Dipp_{CH₃CHCH₃}), 1.19 (dd, ^{2,3}J = 19.7, 6.8 Hz, 12H, Dipp_{Me}).

¹³C NMR (101 MHz, CDCl₃, 300 K) δ [ppm] = 145.6 (2C), 137.9 (NCHN), 132.2, 130.0, 124.9 (2C), 124.3 (NCHCHN), 124.1 (NCHCHN), 53.57 (NCH₂CH₂Br), 51.71 (NCH₂CH₂Br), 32.02, 28.77, 24.47 (2C, Dipp_{Me}), 24.32 (2C, Dipp_{Me}).



Potassium *tert*-butoxide (418 mg, 3.73 mmol, 1.10 eq.) and diphenylphosphine (694 mg, 3.73 mmol, 1.10 eq.) are dissolved in dimethyl sulfoxide (10.0 mL) and slowly added to a solution of compound **L5** (1.41 g, 3.39 mmol, 1.00 eq.) in dimethyl sulfoxide (10.0 mL). The reaction mixture is stirred at r.t. for 3 h. After removal of the solvent under reduced pressure ($1 \cdot 10^{-3}$ mbar) at 90 °C the crude product is dissolved in DCM (6.00 mL), filtrated, concentrated to approximately 2.00 mL and precipitated with diethylether (5.00 mL). After filtration and drying under reduced pressure compound **L^{Dipp}** is obtained as a white solid (1.31 g, 2.51 mmol, 74%).

MS (LIFDI): m/z (%): 441 (100) [$\text{L}^{\text{Dipp}}\text{-Br}^-$]⁺.

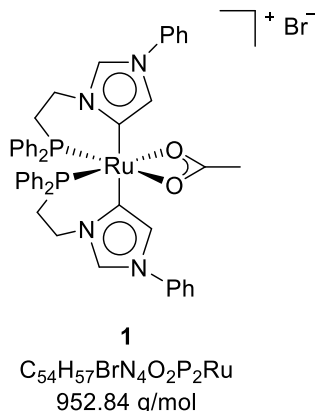
¹H NMR (400 MHz, CD₂Cl₂, 300 K) δ [ppm] = 10.34 (s, 1H, NCHN), 7.81 (t, 4J = 1.7 Hz, 1H, NCHCHN), 7.58 (t, 3J = 7.9 Hz, 1H, NCHCHN), 7.54 - 7.47 (m, 5H, Ph), 7.44 - 7.37 (m, 5H, Ph), 7.35 (d, 3J = 7.9 Hz, 2H, Dipp_{meta}), 7.17 (t, 4J = 1.8 Hz, 1H, Dipp_{para}), 4.80 (dt, $^{2,3}J$ = 11.0, 7.1 Hz, 2H, NCH₂CH₂P), 2.91 (t, 3J = 7.1 Hz, 2H, NCH₂CH₂P), 2.34 (hept, 3J = 6.6 Hz, 2H, Dipp_{CH3CHCH3}), 1.20 (dd, 3J = 35.7, 6.9 Hz, 12H, Dipp_{Me}).

¹³C NMR (101 MHz, CDCl₃, 300 K) δ [ppm] = 146.1 (2C), 138.9 (NCHN), 136.9 (d, J = 11.4 Hz, 2C) 133.5 (2C), 133.3 (2C), 132.4, 129.9 (2C), 129.5 (2C), 129.4 (2C), 125.3 (3C), 124.6 (NCHCHN), 123.9 (NCHCHN), 48.70 (d, J = 21.2 Hz, NCH₂CH₂P), 30.25 (d, J = 15.4 Hz, NCH₂CH₂P), 29.22 (2C), 24.72 (2C, Dipp_{Me}), 24.52 (2C, Dipp_{Me}).

³¹P NMR (162 MHz, CD₂Cl₂, 300 K) δ [ppm] = -23.8 (s, 1P).

Complex Syntheses

Synthesis of 1



$\text{Ru(OAc)}_2(\text{PPh}_3)_2$ (500 mg, 670 μmol , 1.00 eq), L^{Ph} (603 mg, 1.38 mmol, 2.05 eq) and anhydrous NaOAc (113 mg, 1.38 mmol, 2.05 eq) are dissolved in THF (90 mL) and stirred for 4 h at 60 °C. The precipitating black and yellow solids are dispersed in the THF by vigorous stirring. After termination of stirring, the yellow solid is transferred to a new Schlenk-flask *via* a cannula as dispersion in THF, whilst the black solid mostly remains at the reaction flask wall. The solvent is removed under reduced pressure and the residue dissolved in DCM (10 mL). The solution is filtered off *via* a whatman-filtration; precipitation is performed by addition of Et_2O . The residual black precipitate is separated from the yellow precipitate applying the above technique, repeated until no black residue remained. The solution is filtered off *via* a whatman-filtration and the residual yellow solid washed with Et_2O (10 mL) and *n*-pentane (10 mL). Product **1** is obtained as a yellow powder (0.20 g, 0.21 mmol, 31%).

Elemental analysis calcd (%) for $\text{C}_{48}\text{H}_{45}\text{BrN}_4\text{O}_2\text{P}_2\text{Ru}$: C, 60.51; H, 4.76; N, 5.88. Found: C, 60.01; H, 4.72; N, 5.77.

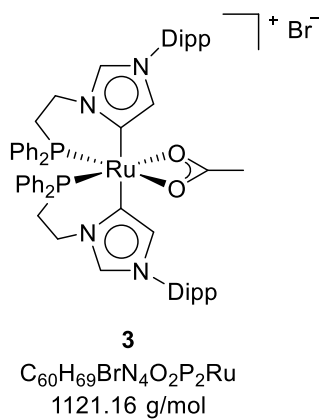
MS (LIFDI): m/z (%): 873.2 (100) [**1-Br**]⁺.

¹H NMR (400 MHz, CD_2Cl_2 , 300 K): δ 9.38 (d, $^4J = 1.9$ Hz, 2 H, NCHN), 7.81 (m, 4 H, Ph_{ortho}), 7.47 (m, 12 H, $\text{Ph}_{\text{meta/para}}$), 7.38 (m, 2 H, $\text{Ph}_{\text{meta/para}}$), 7.31 (m, 4 H, $\text{Ph}_{\text{meta/para}}$), 7.18 (m, 4 H, $\text{Ph}_{\text{meta/para}}$) 7.05 (d, $^4J = 1.8$ Hz, 2 H, NCCHN), 6.47 (m, 4 H, Ph_{ortho}), 5.58 (m, 2 H, $\text{NCH}_2\text{CH}_2\text{P}$), 3.98 (m, 2 H, $\text{NCH}_2\text{CH}_2\text{P}$), 1.92 (s, 3 H, OAc_{Me}), 1.89 (m, 2 H, $\text{NCH}_2\text{CH}_2\text{P}$), 1.36 (m, 2 H, $\text{NCH}_2\text{CH}_2\text{P}$).

¹³C NMR (125 MHz, CD_2Cl_2 , 300 K): δ 184.7 (s, OAc), 165.3 (s, NCCHN), 138.4-138.0 (m, Ph_{quart}), 136.5 (s, NCN), 134.1 (t, $^3J_{CP} = 4.6$ Hz), 133.6 (s), 132.1 (s, br), 130.6 (s), 130.2 (s), 130.0 (s), 129.2 (s), 128.7 (t, $^3J_{CP} = 3.8$ Hz), 128.4 (t, $^3J_{CP} = 4.2$ Hz), 124.3 (s), 121.9 (s), 46.1 (s, $\text{NCH}_2\text{CH}_2\text{P}$), 25.9 (s), 25.7 (t, $^3J_{CP} = 6.4$ Hz, $\text{NCH}_2\text{CH}_2\text{P}$).

³¹P NMR (162 MHz, CD_2Cl_2 , 300 K): δ 55.8 (s).

Synthesis of 3



1) Method from $Ru(OAc)_2(PPh_3)_2$

$Ru(OAc)_2(PPh_3)_2$ (4.70 g, 6.32 mmol, 1.00 eq), L^{Dipp} (6.75 g, 12.9 mmol, 2.05 eq) and anhydrous NaOAc (1.04 g, 12.6 mmol, 2.00 eq) are dissolved in THF (100 mL) and stirred for 6 h at 60 °C. The solvent is removed under reduced pressure and the residue dissolved in DCM (25 mL). The solution is filtered off *via* a whatman-filtration; fractionated precipitation is performed by addition of Et_2O and the resulting solid washed with *n*-hexane (30 mL). Product **3** is obtained as a yellow powder (5.74 g, 5.12 mmol, 81%).

2) Method from Compound **3b**

Compound **3b** (1.50 g, 1.25 mmol, 1 eq) and anhydrous NaOAc (205 mg, 2.5 mmol, 2.00 eq) are dissolved in THF (50 mL) and stirred for 6 h at 60 °C. The resulting precipitate is isolated *via* a whatman-filtration, washed with THF (5 mL) and dissolved in DCM (10 mL). The yellow solution is filtered off, the solvent removed under reduced pressure and the resulting solid washed with *n*-hexane (10 mL). Product **3** is obtained as a yellow powder (1.18 g, 1.05 mmol, 84%).

Elemental analysis calcd (%) for $C_{60}H_{69}BrN_4O_2P_2Ru$: C, 64.28; H, 6.20; N, 5.00. **Found:** C, 62.93; H, 6.33; N, 4.94.

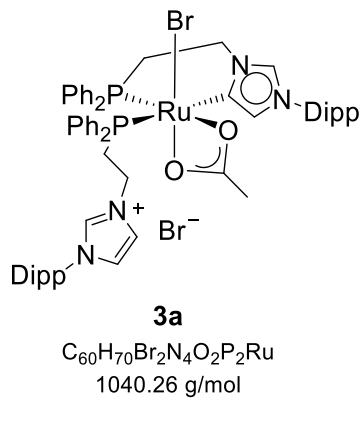
MS (LIFDI): m/z (%): 1041.3 (100) [**3**-Br]⁺.

¹H NMR (400 MHz, CD_2Cl_2 , 300 K): δ 8.59 (d, $^4J = 1.8$ Hz, 2H, $NCHN$), 7.97-7.68 (m, 4H, Ph_{ortho}), 7.44 (dt, $^{2,3}J = 15.0, 7.6$ Hz, 4H, Ph_{para}), 7.30 (d, $^3J = 7.8$ Hz, 2H, $Dipp_{p-CH}$), 7.25-7.00 (m, 12H, $Ph_{meta+Dipp_{m-CH}}$), 6.64 (s, 2H, $NCCHN$), 6.51 (t, $^3J = 7.7$ Hz, 4H, Ph_{ortho}), 4.75-4.55 (m, 2H, NCH_2CH_2P), 4.16 (q, $^2J = 12.7$ Hz, 2H, NCH_2CH_2P), 2.48 (hept, $^3J = 6.3$ Hz, 2H, $Dipp_{CH_3CHCH_3}$), 2.29 (hept, $^3J = 6.8$ Hz, 2H, $Dipp_{CH_3CHCH_3}$), 1.95 (td, $^{2,3}J = 14.7, 4.6$ Hz, 2H, NCH_2CH_2P), 1.78 (s, 3H, $OAcMe$), 1.70 (t, $^2J = 13.0$ Hz, 2H, NCH_2CH_2P), 1.20 (q, $^3J = 7.4, 6.9$ Hz, 18H, $Dipp_{Me}$), 0.43 (d, $^3J = 6.8$ Hz, 6H, $Dipp_{Me}$).

^{13}C NMR (125 MHz, CD_2Cl_2 , 300 K): δ 184.2 (s, OAc), 165.1 (t, ${}^2J_{CP} = 12.5$ Hz, NCCHN), 146.2 (s, Dipp_{quart}), 145.8 (s, Dipp_{quart}), 138.9-137.6 (m, Ph_{quart}), 134.8 (s, NCN), 134.2 (s, Dipp_{quart}), 134.1 (s, Dipp_{quart}), 134.0 (t, ${}^3J_{CP} = 4.4$ Hz, Ph_{ortho}), 132.4 (s, br, Ph_{ortho}), 132.3 (s, Dipp_{arom/Ph_{arom}}), 131.0 (s, Dipp_{arom/Ph_{arom}}), 130.2 (s, Dipp_{arom/Ph_{arom}}), 129.8 (s, Dipp_{arom/Ph_{arom}}), 129.4 (s, Dipp_{arom/Ph_{arom}}), 129.2 (s, Dipp_{arom/Ph_{arom}}), 129.0 (s, Dipp_{arom/Ph_{arom}}), 128.9 (d, ${}^3J_{CP} = 6.9$ Hz, Dipp_{arom/Ph_{arom}}), 128.3 (q, ${}^3J_{CP} = 4.5$ Hz, Dipp_{arom/Ph_{arom}}), 124.6 (s, Dipp_{arom/Ph_{arom}}), 124.3 (s, Dipp_{arom/Ph_{arom}}), 45.8 (s, NCH₂CH₂P), 28.9 (s, Dipp_{CH₃CHCH₃}), 26.4-26.1 (m, NCH₂CH₂P), 25.2 (s, OAc_{Me}), 24.4 (d, ${}^3J = 7.5$ Hz, Dipp_{Me}), 24.2 (s, Dipp_{Me}), 23.2 (s, Dipp_{Me}), 21.8 (s, Dipp_{Me}), 14.4 (s, Dipp_{Me}).

^{31}P NMR (162 MHz, CD_2Cl_2 , 300 K): δ 56.1 (s).

Synthesis of **3a**



$Ru(OAc)_2(PPh_3)_2$ (696 mg, 935 μ mol, 1.00 eq) and L^{Dipp} (1.00 g, 1.92 mmol, 2.05 eq) are dissolved in THF (100 mL) and stirred for 6 h at r.t. The solution is filtered off *via* a whatman-filtration and the residual pink precipitate washed with THF (10 mL). Product **3a** is obtained as a pink powder (876 mg, 729 μ mol, 78%).

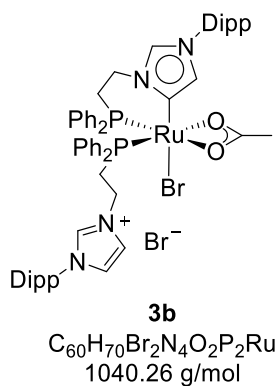
Elemental analysis calcd (%) for $C_{60}H_{70}Br_2N_4O_2P_2Ru$: C, 59.95; H, 5.87; N, 4.66. Found: C, 58.27; H, 5.81; N 4.54.

1H NMR (400 MHz, CD_2Cl_2 , 300 K): δ 9.72 (t, $^4J = 1.6$ Hz, 1H), 8.37 (t, $^4J = 1.7$ Hz, 1H), 8.01 (t, $^4J = 1.4$ Hz, 1H), 7.77-7.66 (m, 2H), 7.55 (t, $^3J = 7.8$ Hz, 1H), 7.53-7.39 (m, 4H), 7.37-7.23 (m, 11/12H), 7.21-7.06 (m, 4/5H), 7.00 (t, $^3J = 8.4$ Hz, 2H), 6.89 (t, $^3J = 8.5$ Hz, 2H), 4.80-4.53 (m, 1H, CH_2), 4.19 (q, $^2J = 13.1$ Hz, 1H, CH_2), 3.98-3.79 (m, 1H, CH_2), 3.65-3.54 (m, 1H, CH_2), 3.24-3.07 (m, 2H, CH_2), 3.05-2.88 (m, 1H, CH_2), 2.67-2.49 (m, 2H, $Dipp_{CH_3CHCH_3}$), 2.42 (td, $^{2,3}J = 13.2$, 5.7 Hz, 1H, CH_2), 2.33-2.16 (m, 2H, $Dipp_{CH_3CHCH_3}$), 1.29-1.12 (m, 24H, $Dipp_{Me}$), 1.08 (s, 3H, OAc_{Me}).

^{13}C NMR (125 MHz, CD_2Cl_2 , 300 K): δ 184.5 (s, OAc), 164.4 (dd, $J_{PC} = 101.3$, 15.8 Hz, $NCCHN_{bound}$), 146.0 (s, $NCCHN_{dangl}$), 145.5 (d, $J_{PC} = 4.1$ Hz), 145.4 (s), 140.9 (s), 140.6 (s), 137.9 (s), 137.6 (s), 136.9 (s), 135.8 (s), 135.6 (s), 134.4 (d, $J_{PC} = 11.9$ Hz), 134.2 (d, $J_{PC} = 10.0$ Hz), 134.0 (s), 133.7 (s), 133.6 (s), 132.8 (d, $J_{PC} = 9.3$ Hz), 132.5 (d, $J_{PC} = 4.2$ Hz), 132.4 (d, $J_{PC} = 7.8$ Hz), 132.0 (s), 131.7 (s), 130.4 (s), 130.3 (s), 129.6 (s), 128.9 (d, $J_{PC} = 4.9$ Hz), 128.8 (d, $J_{PC} = 2.0$ Hz), 128.7 (s), 128.5 (d, $J_{PC} = 7.0$ Hz), 128.2 (s), 128.1 (d, $J_{PC} = 8.6$ Hz), 127.8-127.4 (m), 124.6 (d, $J_{PC} = 1.4$ Hz), 123.9 (d, $J_{PC} = 9.9$ Hz), 123.8 (s), 123.6 (s), 46.3 (s, $NCH_2CH_2P_{bound}$), 44.4 (d, $J_{PC} = 8.6$ Hz, $NCH_2CH_2P_{dangl}$), 31.6 (d, $J_{PC} = 30.6$ Hz, $NCH_2CH_2P_{bound}$), 29.2 (d, $J_{PC} = 16.8$ Hz, $NCH_2CH_2P_{dangl}$), 28.6 (d, $J_{PC} = 6.1$ Hz), 28.3 (d, $J_{PC} = 6.2$ Hz), 24.6-23.6 (m, $Dipp_{Me}$).

^{31}P NMR (162 MHz, CD_2Cl_2 , 300 K): δ 56.9 (d, $J_{PP} = 24.7$ Hz, P_{transC}), 25.1 (d, $J_{PP} = 24.6$ Hz, P_{transO}).

NMR evidence of 3b



Compound **3b** was prepared and analyzed as an intermediate species. Compound **3a** (30.0 mg, 25.0 μ mol, 1 eq) is dissolved in CD_2Cl_2 (4 mL) in an NMR tube at r.t. 1H , ^{13}C , ^{31}P and 2D NMR measurements are performed at 1 h, 5 h, 17 h and 24 h for the NMR study (Manuscript, Figure 2). Characterization of **3b** was evaluated for measurements at 24 h excluding complex **3** as side-product.

1H NMR (400 MHz, CD_2Cl_2 , 300 K): δ 9.86 (t, $^4J = 1.5$ Hz, 1H, $NCHN_{dangl}$), 8.24 (t, $^4J = 1.7$ Hz, 1H, $NCHCHN_{dangl}$), 8.15 (d, $^4J = 1.8$ Hz, 1H, $NCHN_{bound}$), 8.05 (ddd, $^{2,3}J = 9.9, 6.8, 3.1$ Hz, 2H, Ph_{ortho}), 7.91-7.80 (m, 2H, Ph_{ortho}), 7.62 (t, $^3J = 8.5$ Hz, 2H, Ph_{para}), 7.56 (t, $^3J = 7.8$ Hz, 1H, $NCHCHN_{dangl}$), 7.45 (t, $^3J = 7.8$ Hz, 2H, Ph_{para}), 7.39 (td, $^{3,4}J = 7.3, 1.3$ Hz, 2H, $Ph_{meta}/Dipp_{arom}$), 7.38-7.07 (m, 20H, $Ph_{meta}/Dipp_{arom}$), 6.50 (d, $^4J = 1.8$ Hz, 1H, $NCCHN$), 6.43 (t, $^3J = 8.4$ Hz, 2H, Ph_{ortho}), 4.51-4.31 (m, 1H, CH_2), 3.98 (q, $^2J = 13.3$ Hz, 1H, CH_2), 3.50 (td, $^{2,3}J = 12.0, 6.5$ Hz, 1H, CH_2), 2.75 (qd, $^{2,3}J = 12.2, 6.6$ Hz, 1H, CH_2), 2.66-2.52 (m, 1H, CH_2), 2.43-2.28 (m, 3H, CH_2 , $Dipp_{CH_3CHCH_3}$), 2.31-2.15 (m, 2H, $Dipp_{CH_3CHCH_3}$), 1.88 (s, 3H, OAc_{Me}), 1.29-1.12 (m, 23H, $Dipp_{Me}$), 1.11 (d, $^3J = 6.8$ Hz, 3H, $Dipp_{Me}$), 0.54 (d, $^3J = 6.8$ Hz, 3H, $Dipp_{Me}$).

^{13}C NMR (125 MHz, CD_2Cl_2 , 300 K): δ 186.3 (s, OAc), 158.1 (t, $J_{PC} = 14.6$ Hz, $NCCHN_{bound}$), 146.4 (s), 145.9 (d, $J_{PC} = 14.7$ Hz), 145.5 (s), 139.1-137.9 (m), 137.4 (s), 136.5 (dd, $J_{PC} = 38.2, 21.9$ Hz), 134.6 (d, $J_{PC} = 9.6$ Hz), 134.4 (d, $J_{PC} = 9.8$ Hz), 133.9 (s), 132.9 (d, $J_{PC} = 8.4$ Hz), 132.5 (d, $J_{PC} = 8.0$ Hz), 132.3 (s), 131.9 (s), 131.2 (s), 130.7 (s), 130.3-129.8 (m), 128.6 (d, $J_{PC} = 9.0$ Hz), 128.5 (s), 128.4 (s), 128.3 (s), 128.2 (s), 128.1 (d, $J_{PC} = 2.9$ Hz), 128.1 (s), 125.2 (d, $J_{PC} = 3.3$ Hz), 124.7 (s), 124.6 (s), 124.5 (s), 124.4 (s), 47.8 (d, $J_{PC} = 7.4$ Hz, $NCH_2CH_2P_{dangl}$), 45.9 (s, $NCH_2CH_2P_{bound}$), 32.9 (d, $J_{PC} = 21.5$ Hz, $NCH_2CH_2P_{bound}$), 29.2 (d, $J_{PC} = 4.1$ Hz), 28.9 (d, $J_{PC} = 13.4$ Hz, $NCH_2CH_2P_{dangl}$), 26.1 (s), 25.1 (s), 24.8 (s), 24.8 (s), 24.7 (s), 24.6 (d, $J_{PC} = 2.6$ Hz), 24.5 (s), 24.3 (s), 23.5 (s), 23.2 (s).

^{31}P NMR (162 MHz, CD_2Cl_2 , 300 K): δ 50.1 (d, $J_{PP} = 43.3$ Hz), 49.6 (d, $J_{PP} = 43.3$ Hz).

NMR Spectra

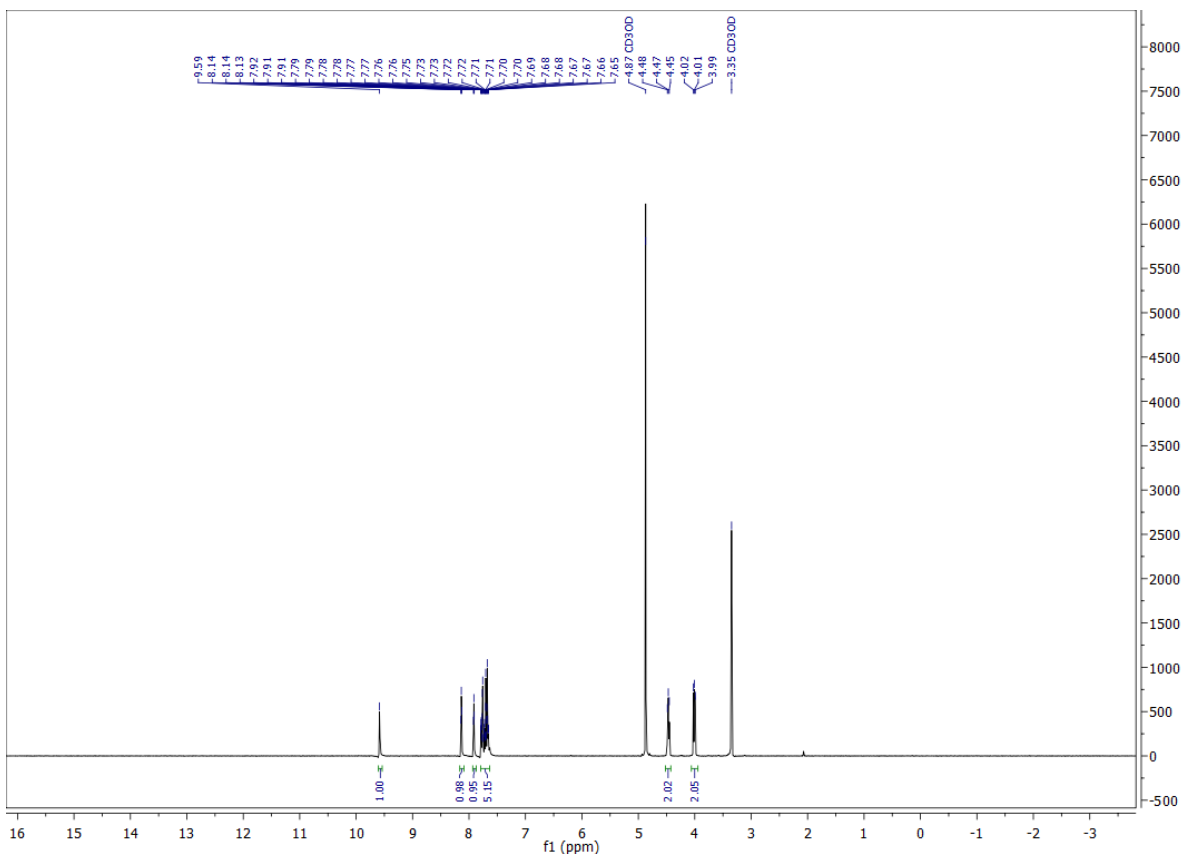


Figure S1: ^1H NMR (400 MHz, CD_3OD , 300 K) spectrum of **L1**.

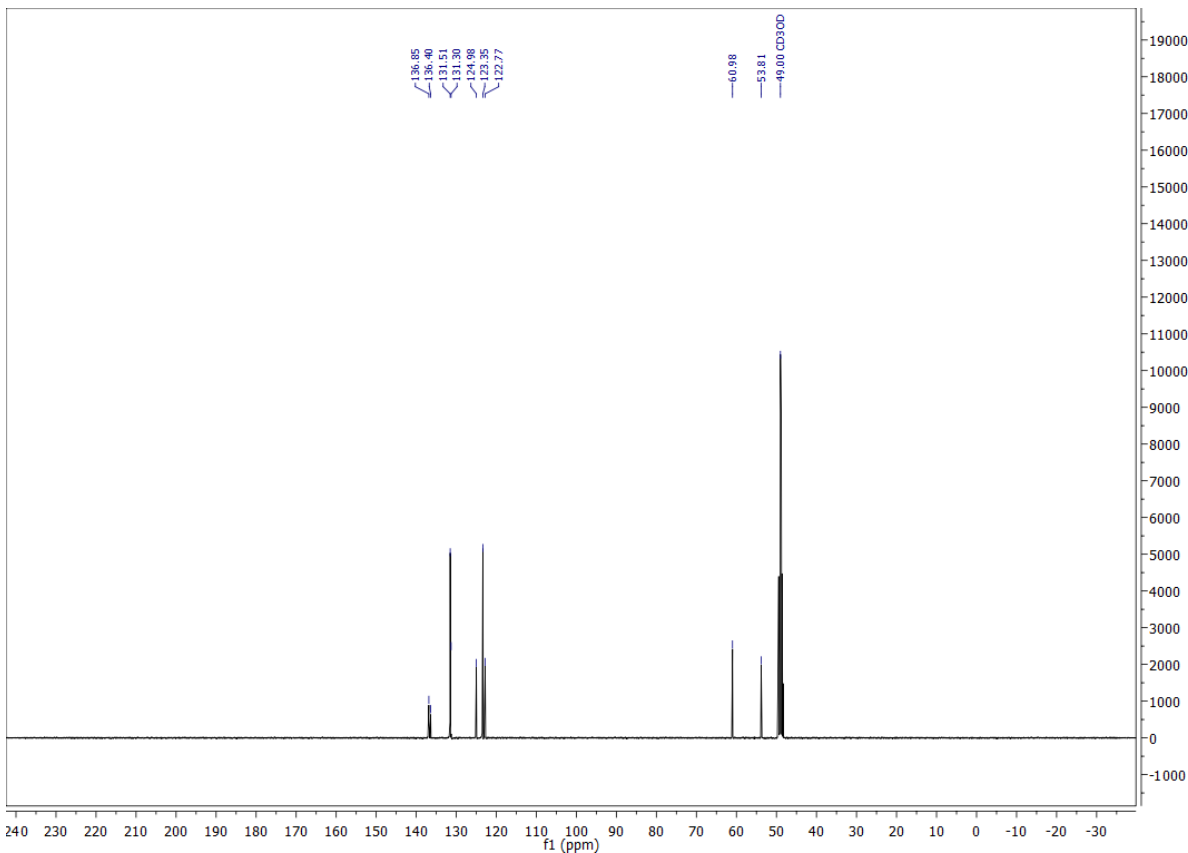


Figure S2: ^{13}C NMR (101 MHz, CD_3OD , 300 K) spectrum of **L1**.

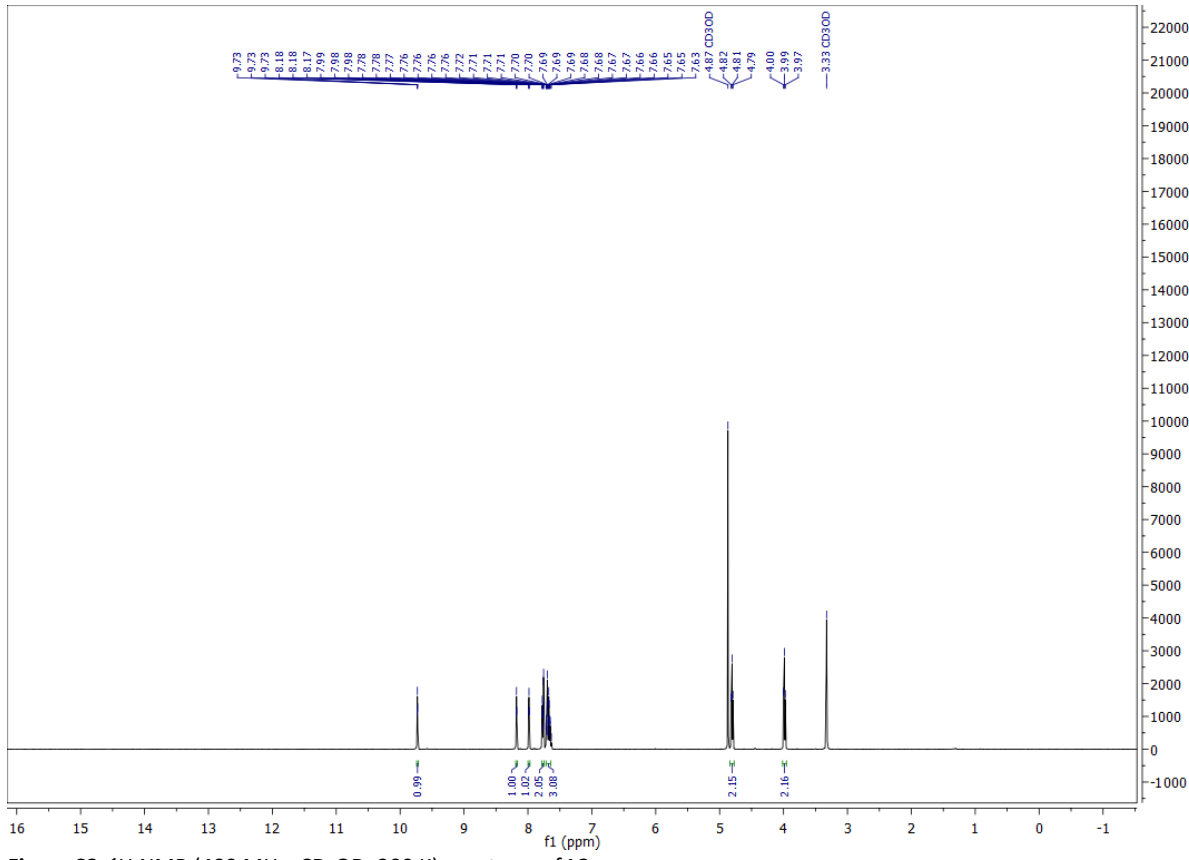


Figure S3: ^1H NMR (400 MHz, CD_3OD , 300 K) spectrum of **L2**.

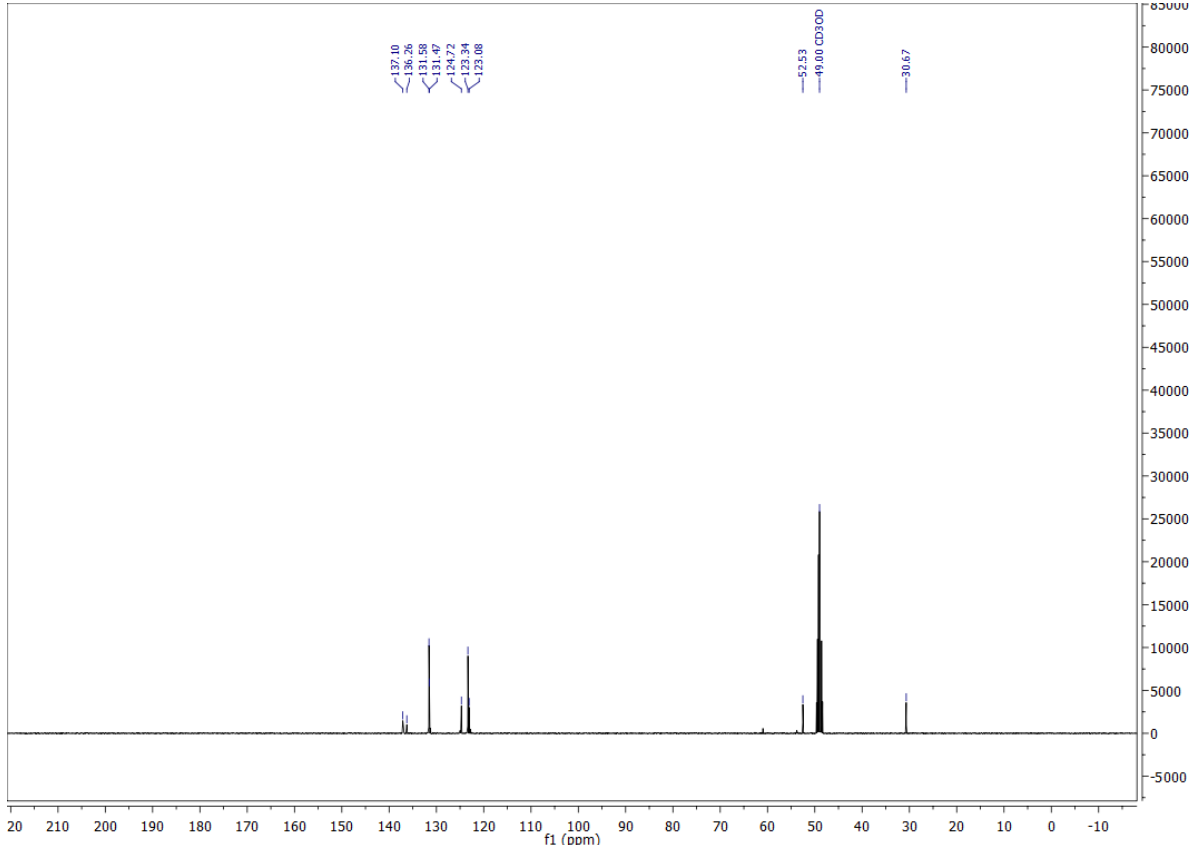


Figure S4: ^{13}C NMR (101 MHz, CD_3OD , 300 K) spectrum of **L2**.

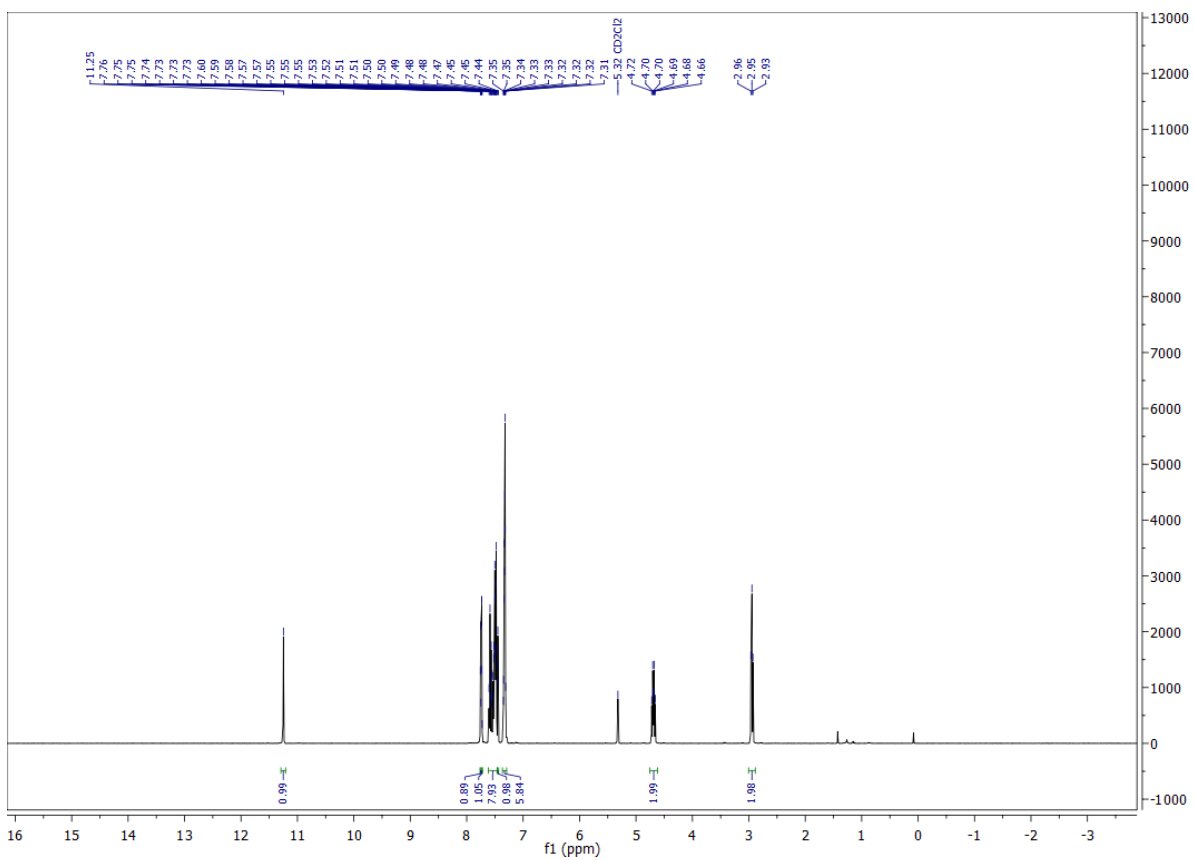


Figure S5: ^1H NMR (400 MHz, CD_2Cl_2 , 300 K) spectrum of L^{Ph} .

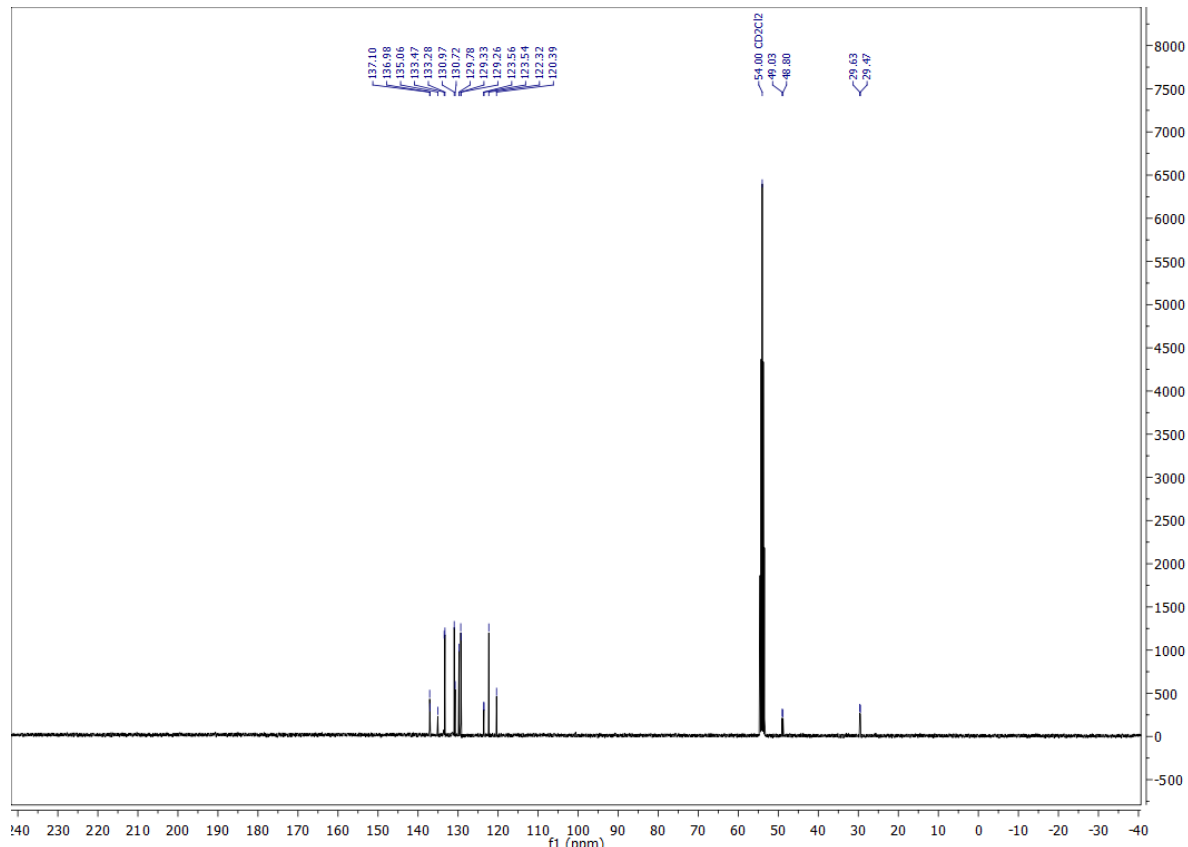


Figure S6: ^{13}C NMR (101 MHz, CD_2Cl_2 , 300 K) spectrum of L^{Ph} .

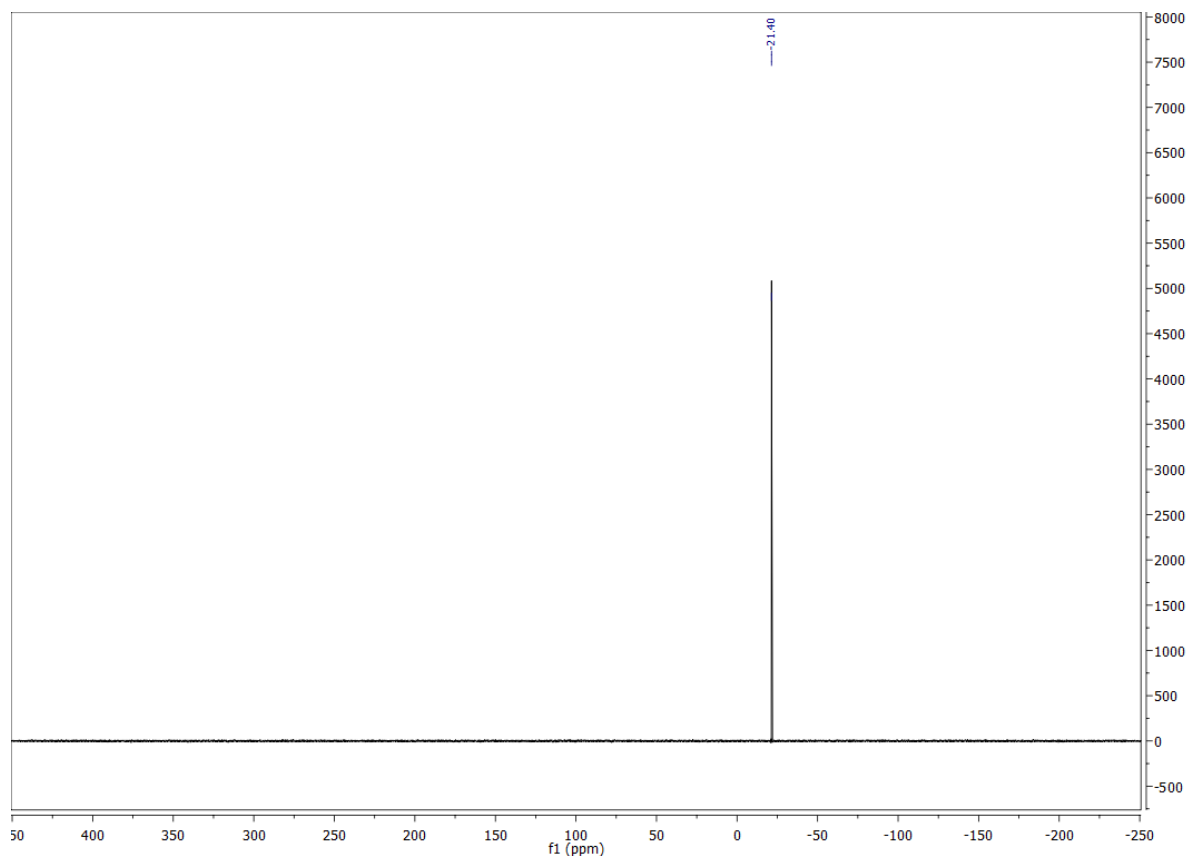


Figure S7: ^{31}P NMR (162 MHz, CD_2Cl_2 , 300 K) spectrum of L^{Ph} .

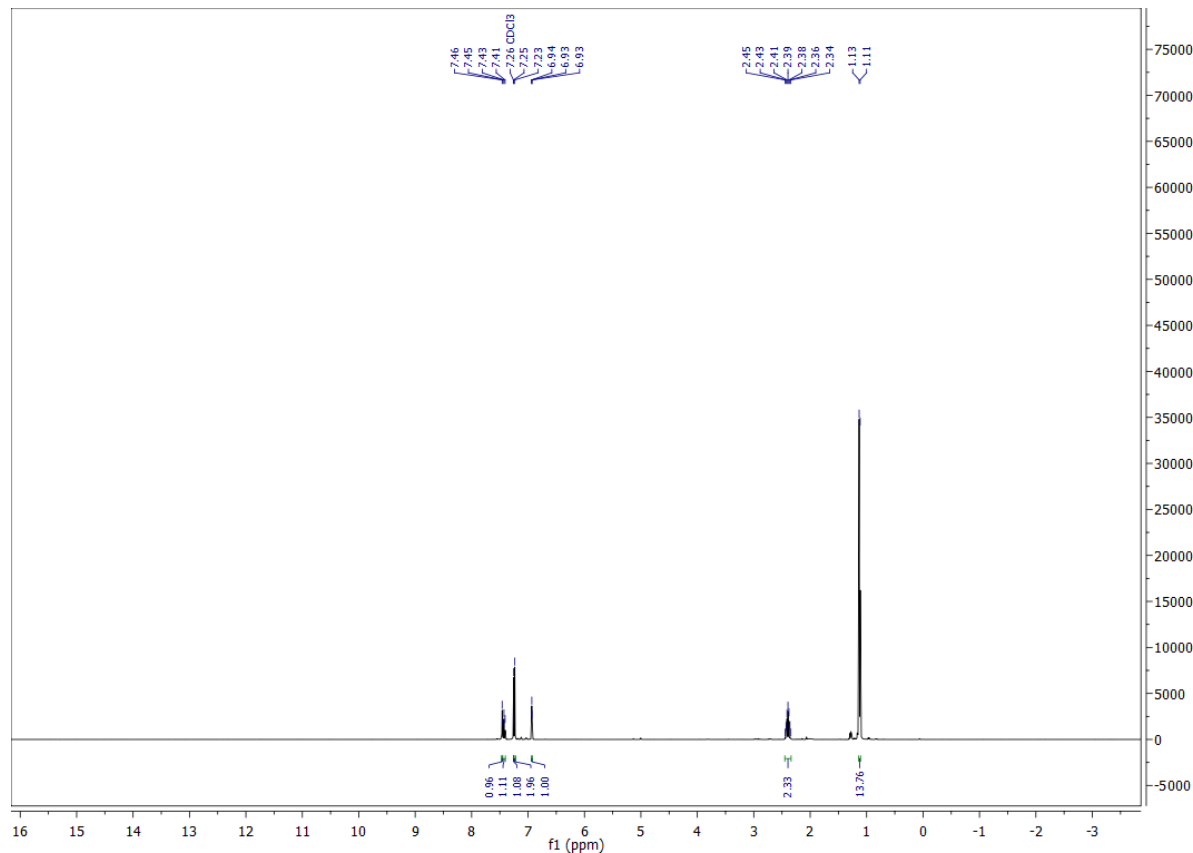


Figure S8: ^1H NMR (400 MHz, CDCl_3 , 300 K) spectrum of L^{3} .

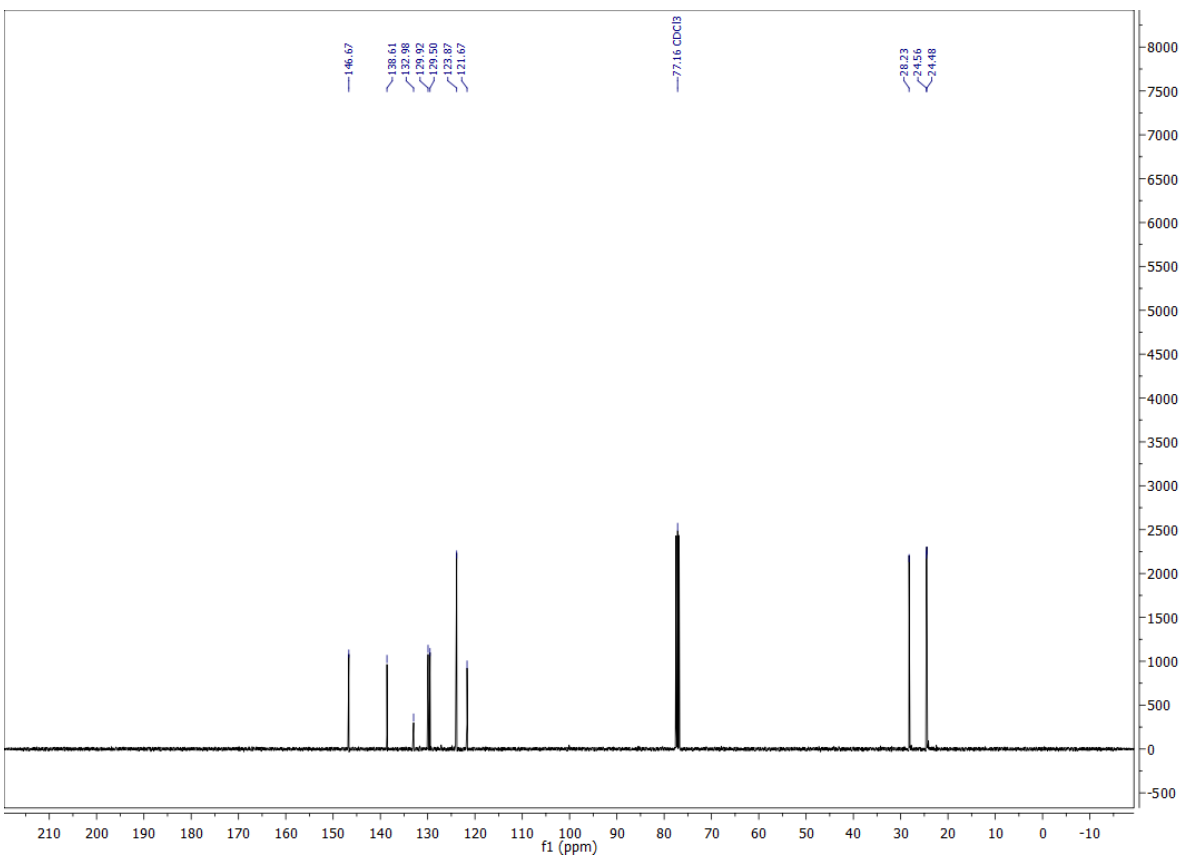


Figure S9: ^{13}C NMR (101 MHz, CDCl_3 , 300 K) spectrum of **L3**.

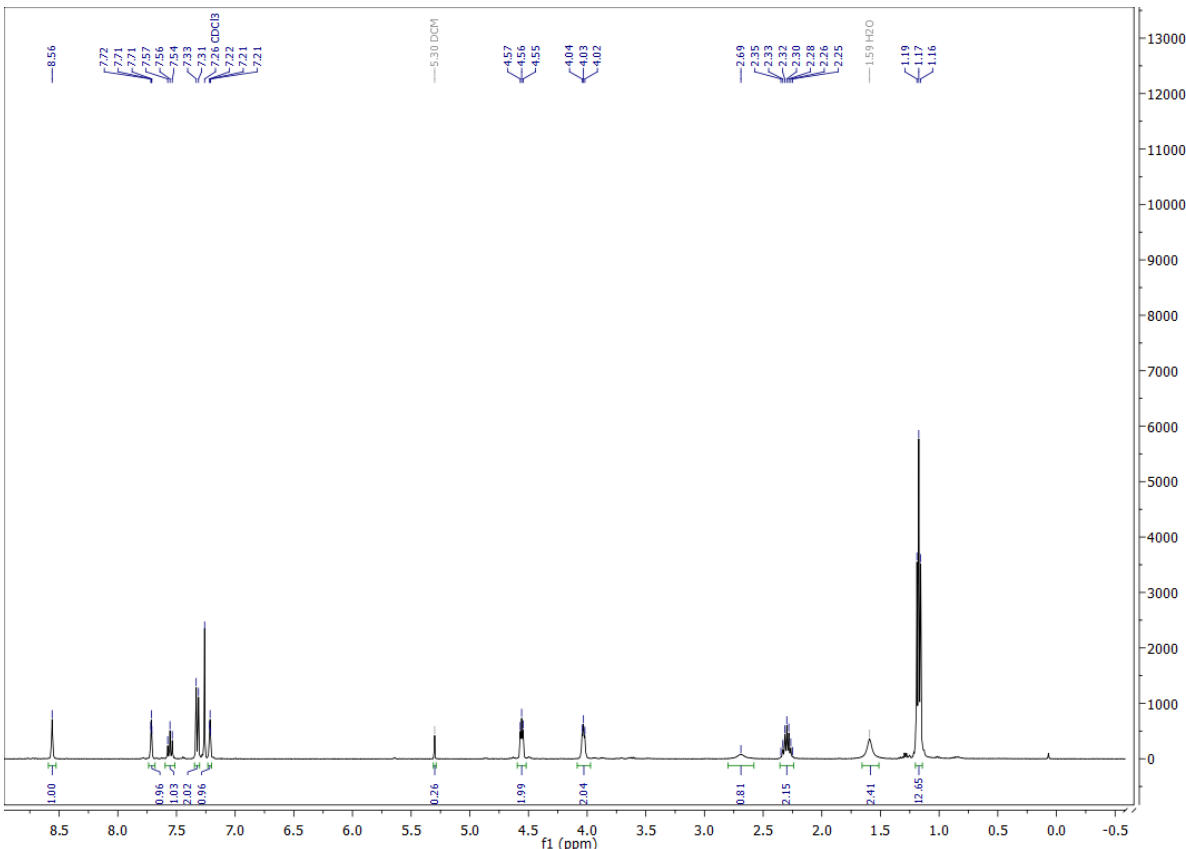


Figure S10: ^1H NMR (400 MHz, CD_2Cl_2 , 300 K) spectrum of **L4**.

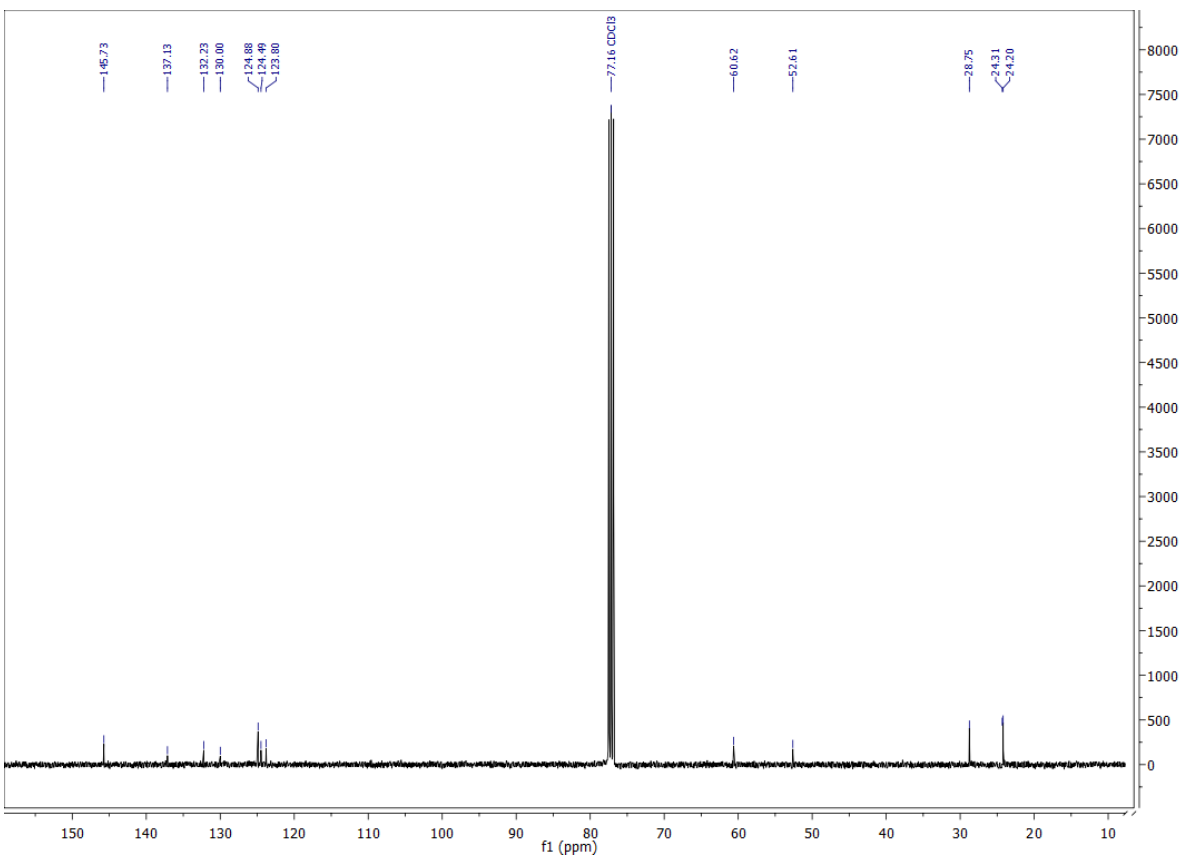


Figure S11: ^{13}C NMR (101 MHz, CDCl_3 , 300 K) spectrum of **L4**.

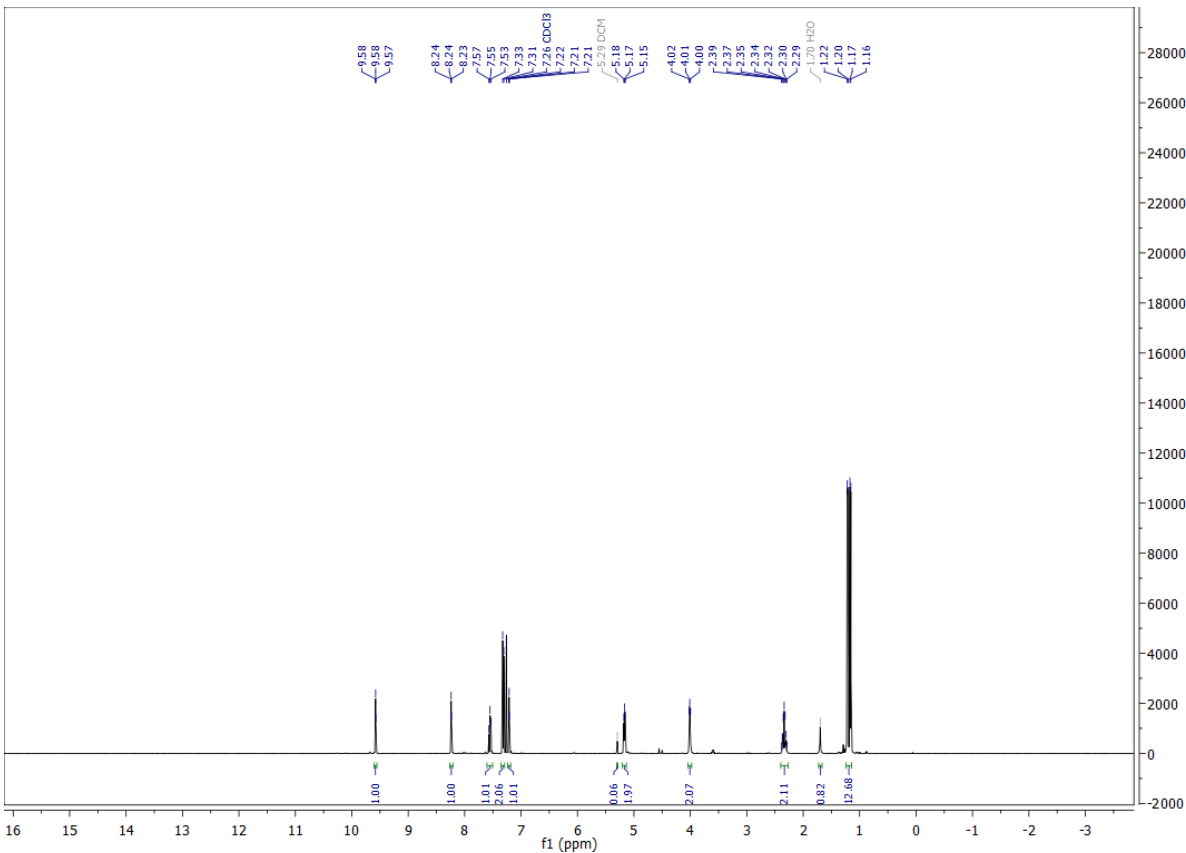


Figure S12: ^1H NMR (400 MHz, CDCl_3 , 300 K) spectrum of **L5**.

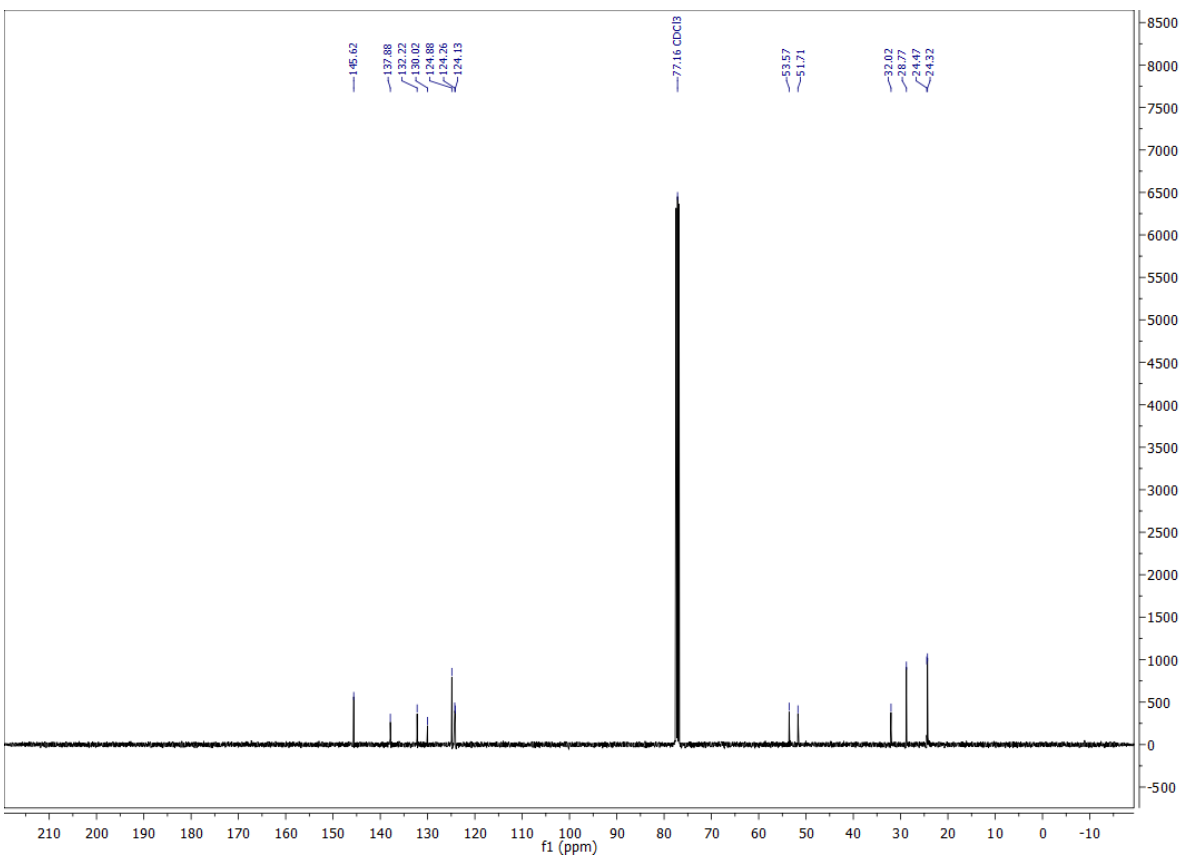


Figure S13: ^{13}C NMR (101 MHz, CDCl_3 , 300 K) spectrum of L5.

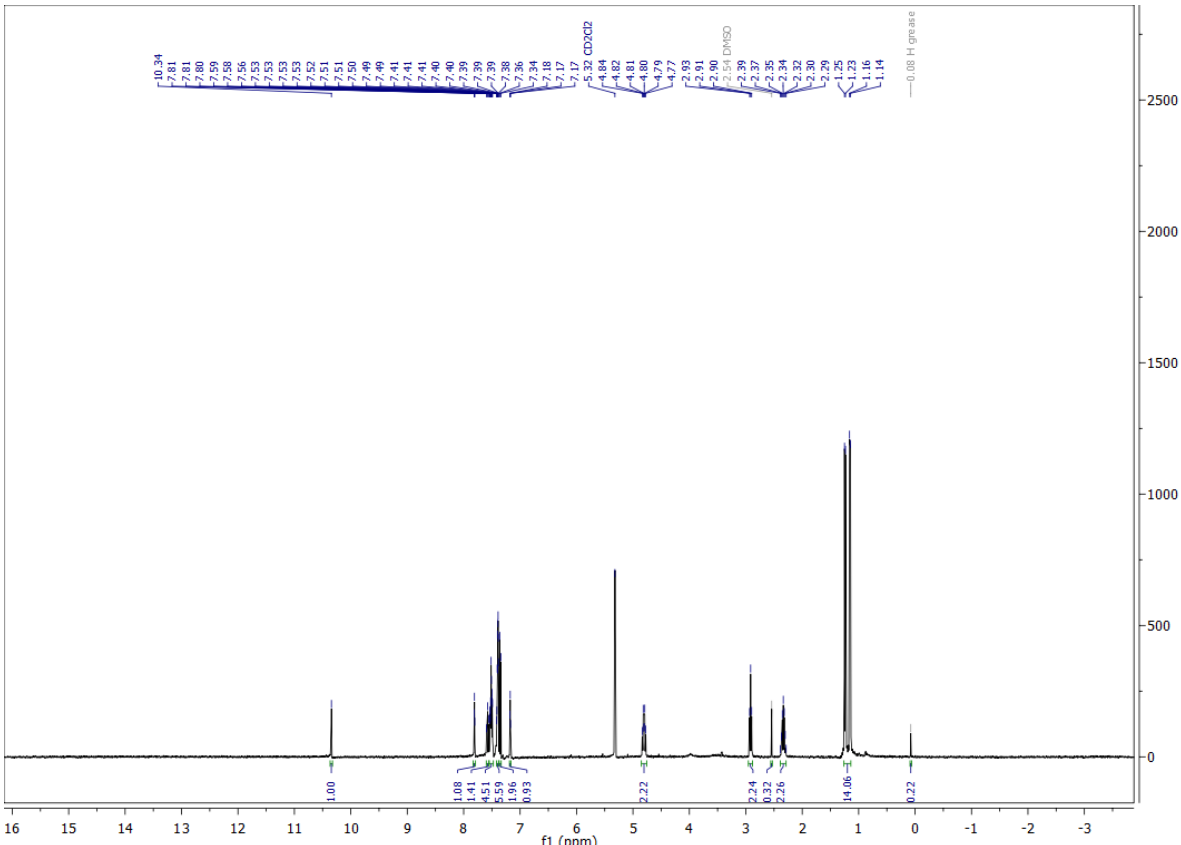


Figure S14: ^1H NMR (400 MHz, CD_2Cl_2 , 300 K) spectrum of LDipp.

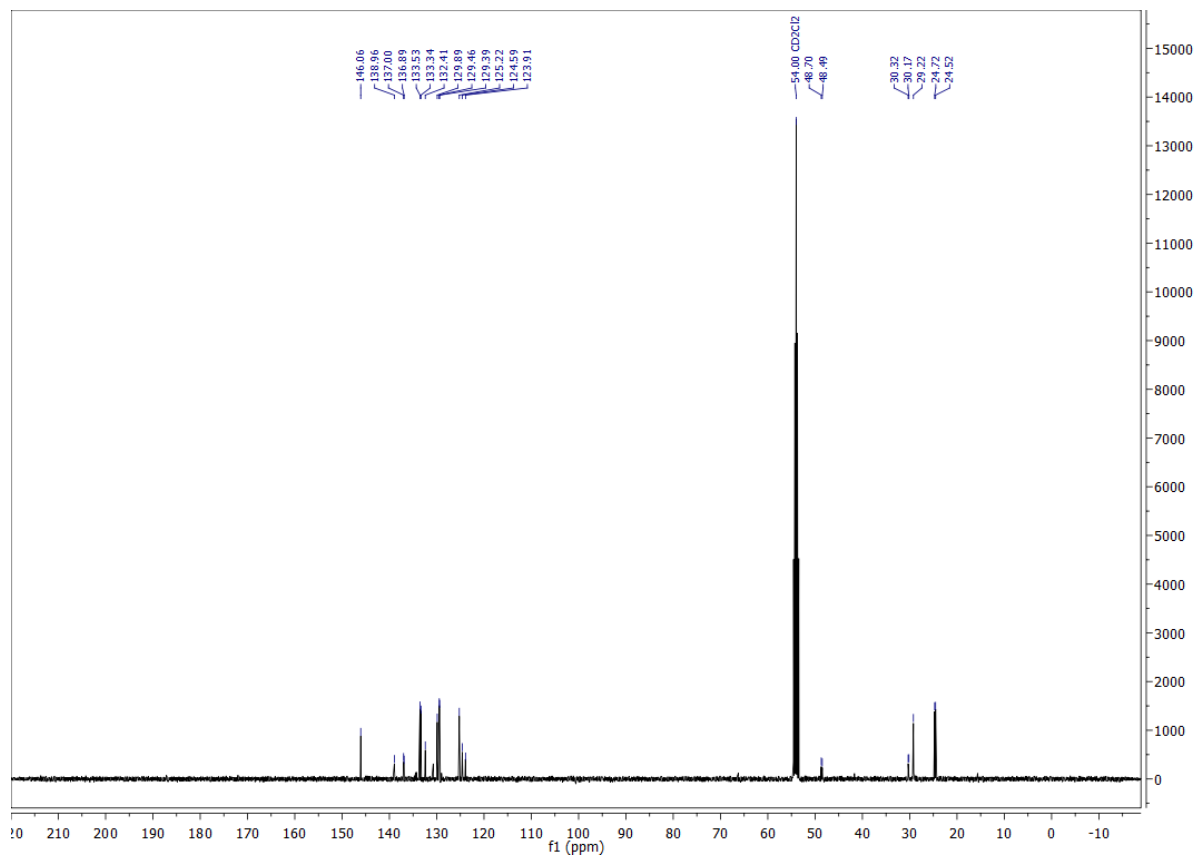


Figure S15: ^{13}C NMR (101 MHz, CD_2Cl_2 , 300 K) spectrum of L^{Dipp} .

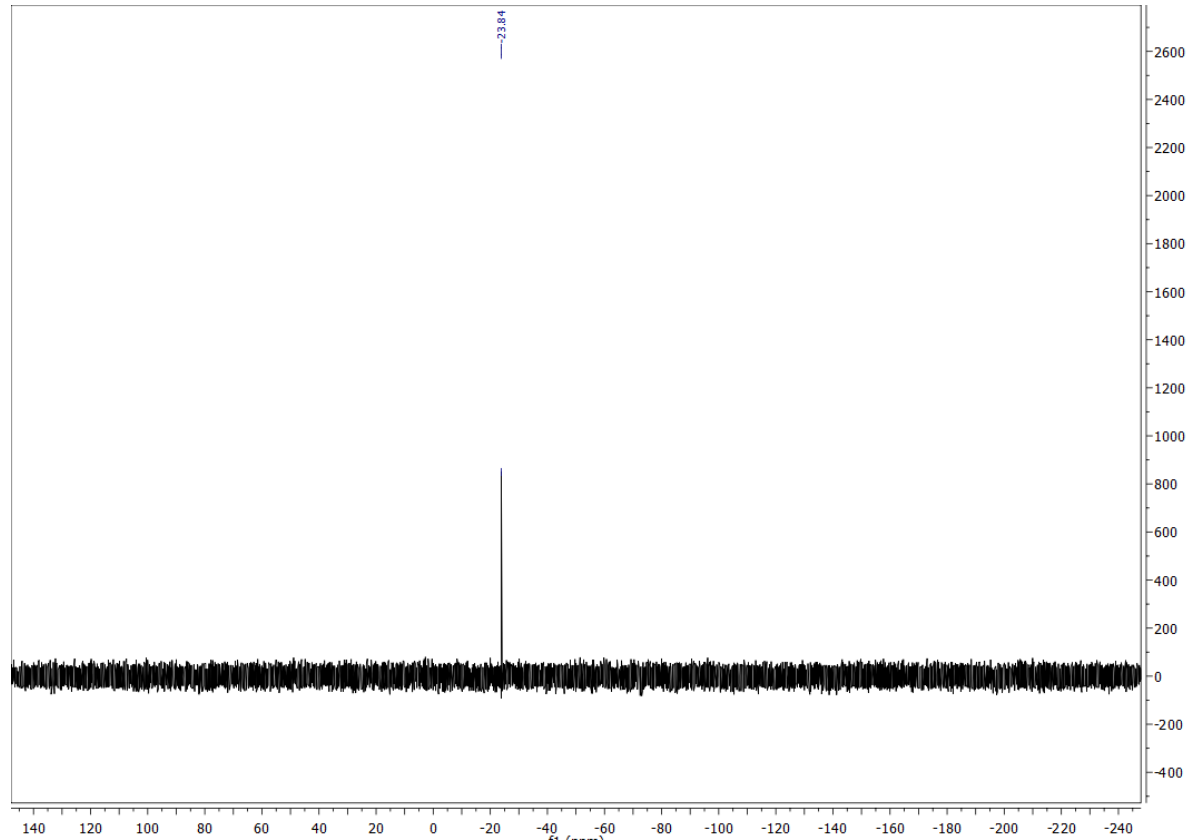


Figure S16: ^{31}P NMR (162 MHz, CD_2Cl_2 , 300 K) spectrum of L^{Dipp} .

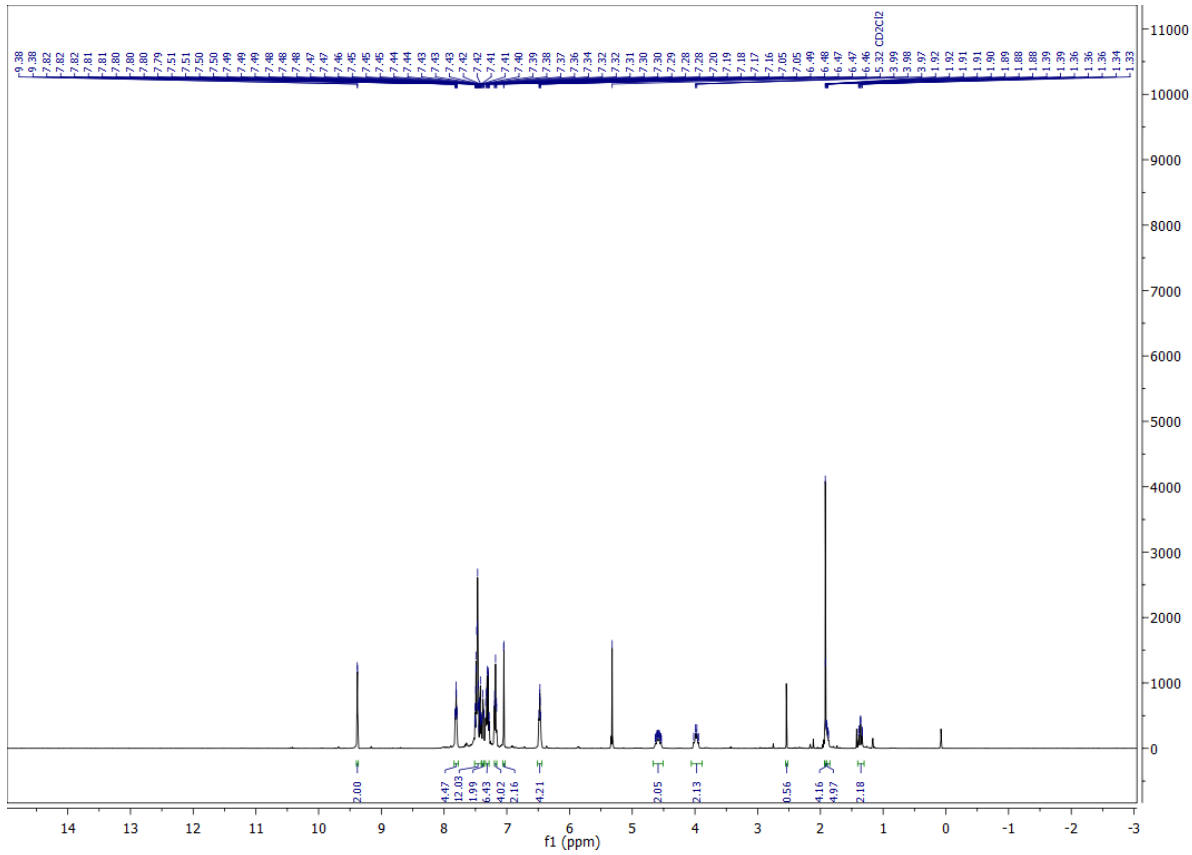


Figure S17: ^1H NMR (400 MHz, CD_2Cl_2 , 300 K) spectrum of **1**.

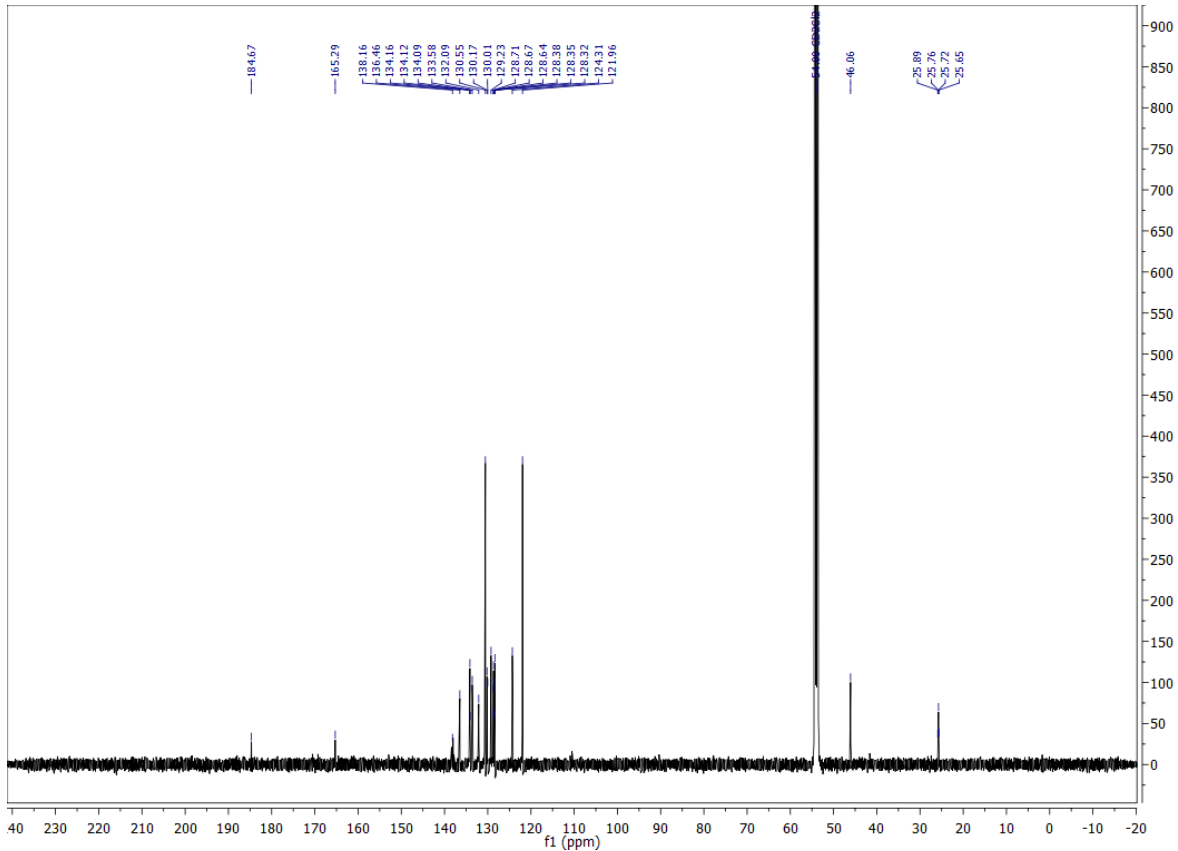


Figure S18: ^{13}C NMR (125 MHz, CD_2Cl_2 , 300 K) spectrum of **1**.

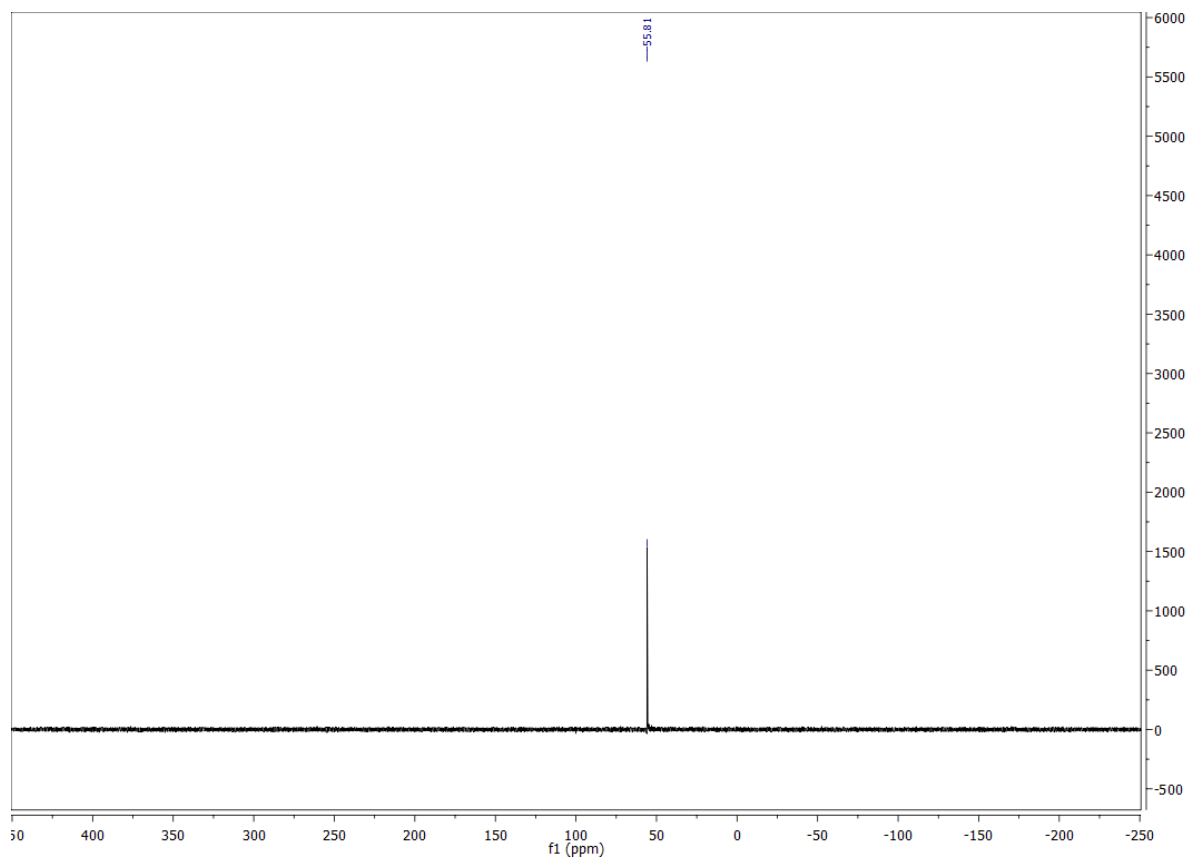


Figure S19: ^{31}P NMR (162 MHz, CD_2Cl_2 , 300 K) spectrum of **1**.

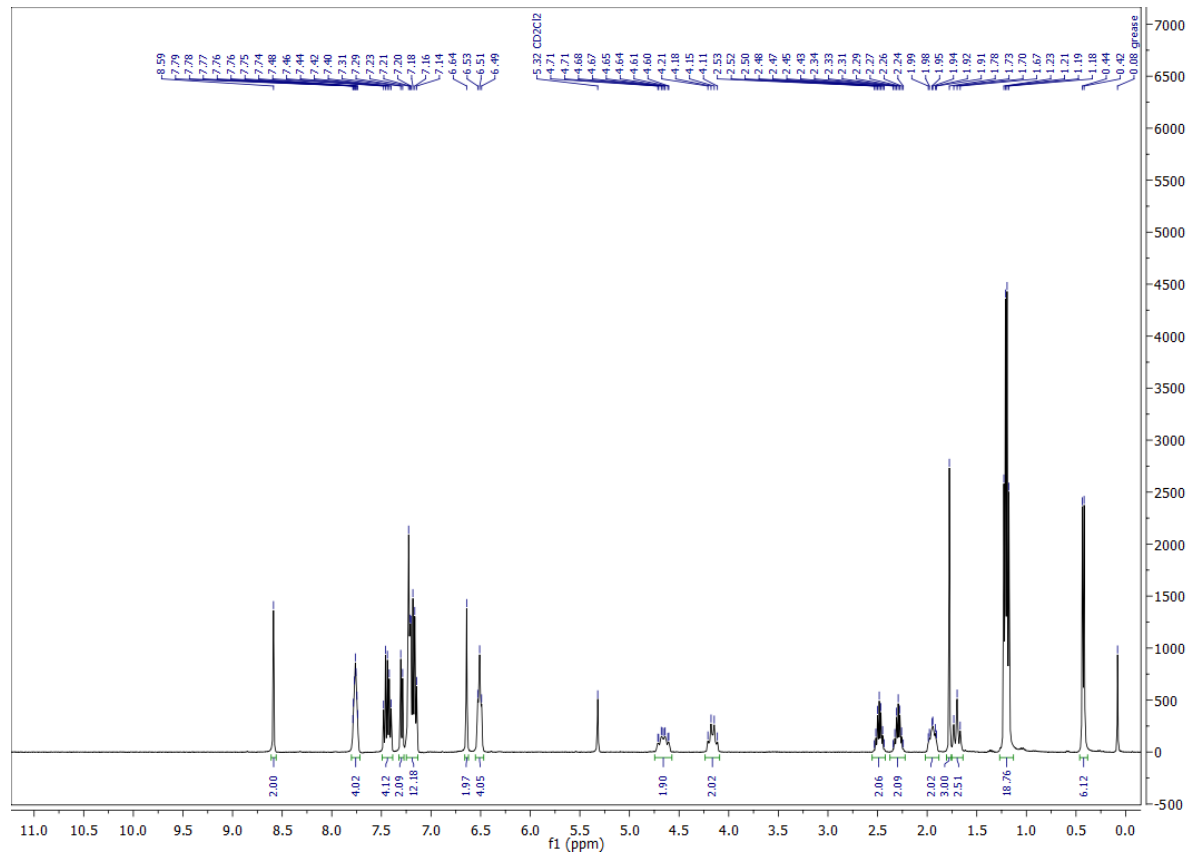


Figure S20: ^1H NMR (400 MHz, CD_2Cl_2 , 300 K) spectrum of **3**.

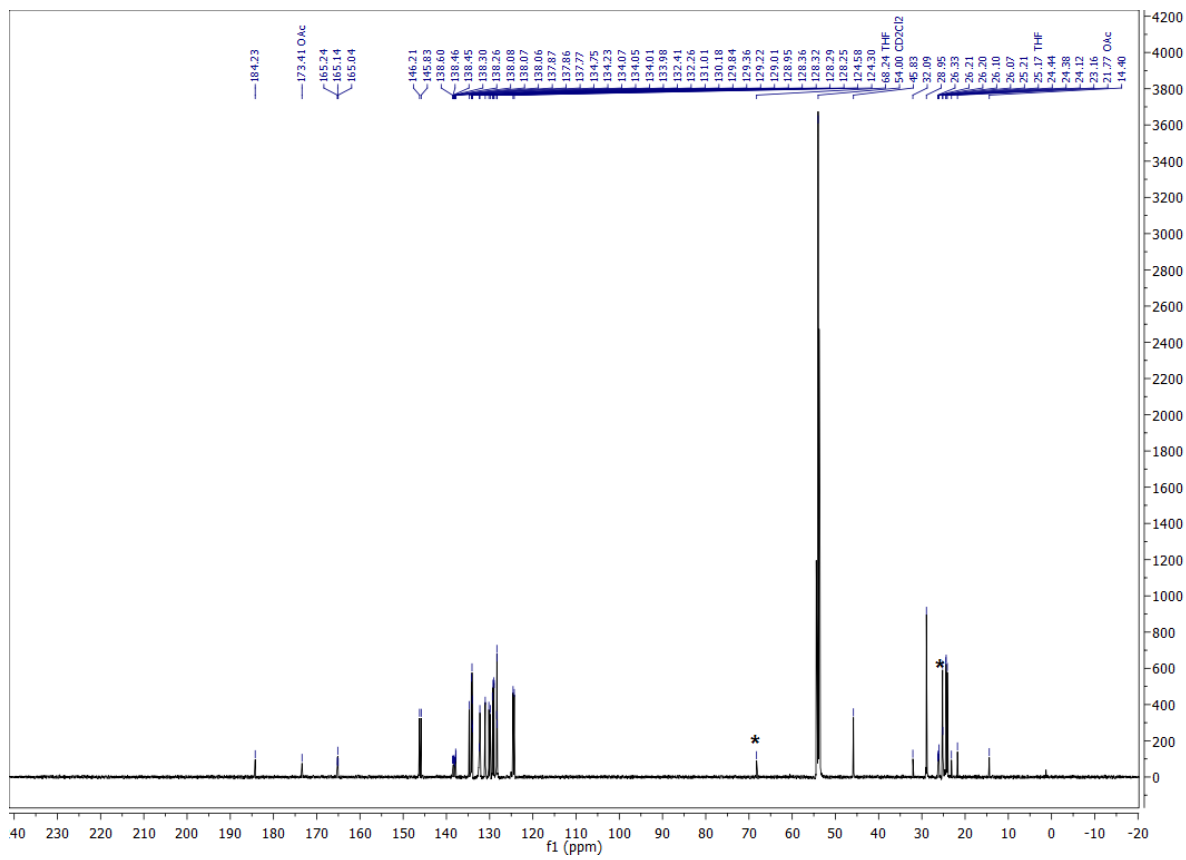


Figure S21: ^{13}C NMR (125 MHz, CD_2Cl_2 , 300 K) spectrum of **3**. Residual THF marked with asterisks (*).

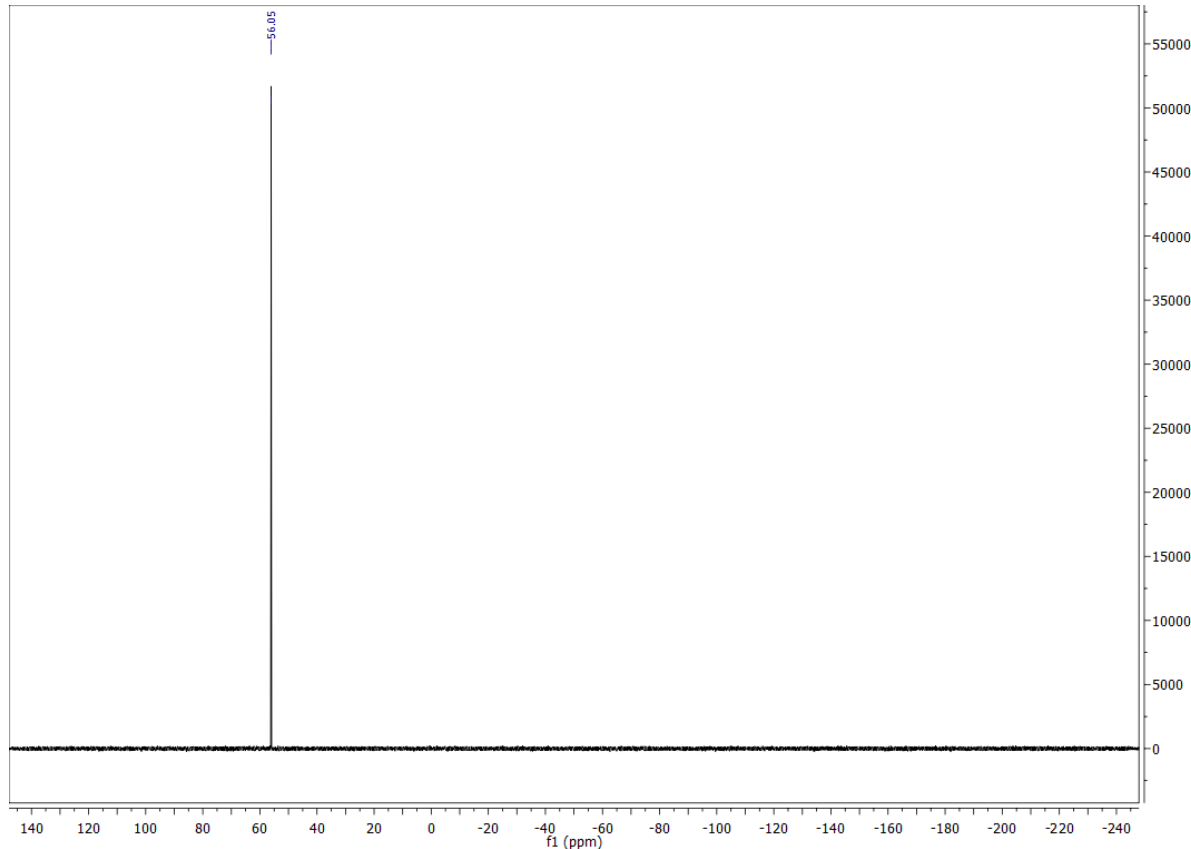


Figure S22: ^{31}P NMR (162 MHz, CD_2Cl_2 , 300 K) spectrum of **3**.

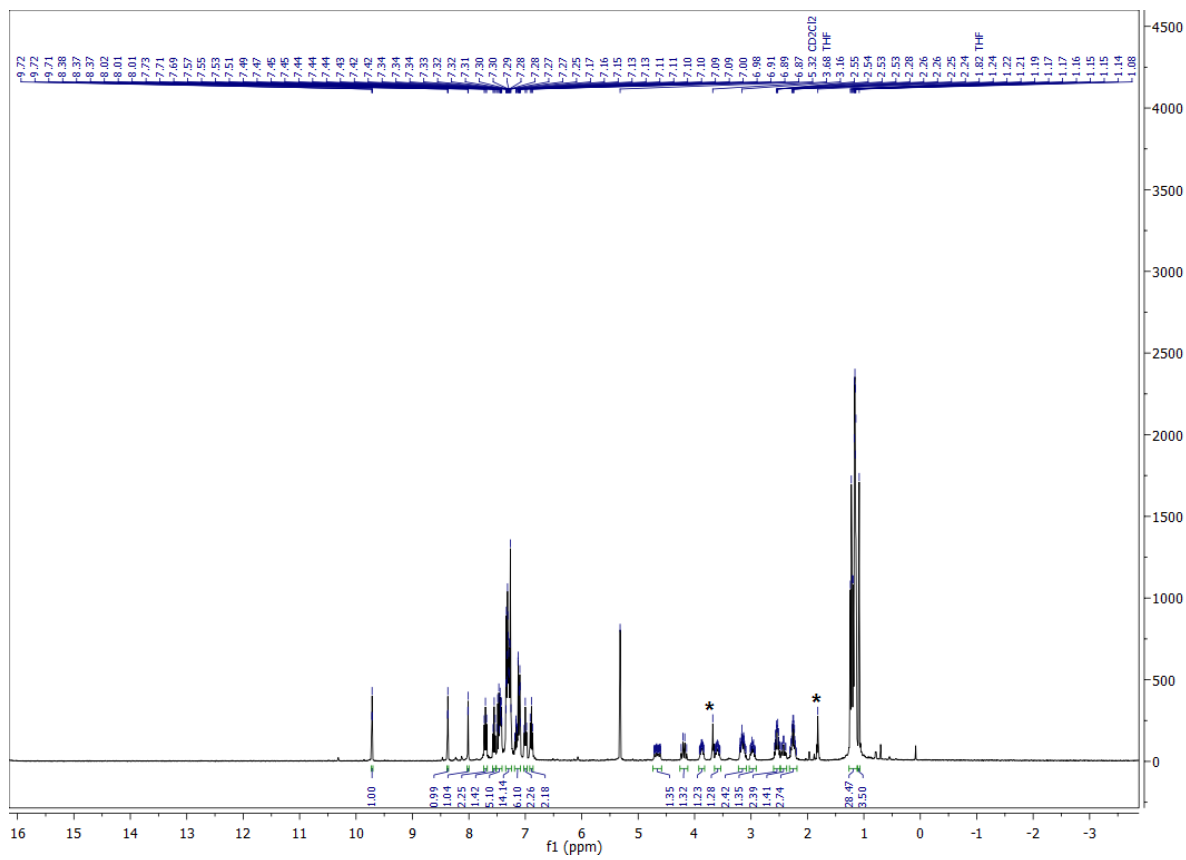


Figure S23: ^1H NMR (400 MHz, CD_2Cl_2 , 300 K) spectrum of **3a**. Residual THF marked with asterisks (*).

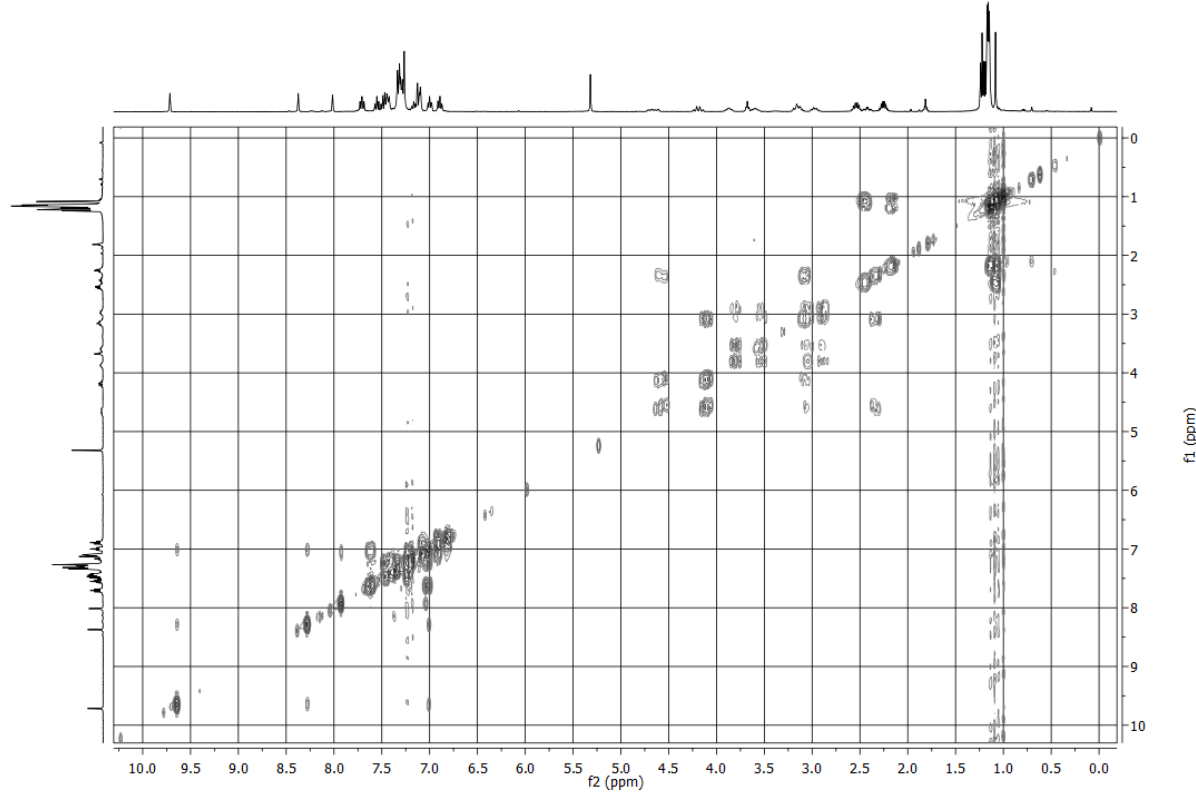


Figure S24: COSY NMR (400 MHz, CD_2Cl_2 , 300 K) spectrum of **3a**.

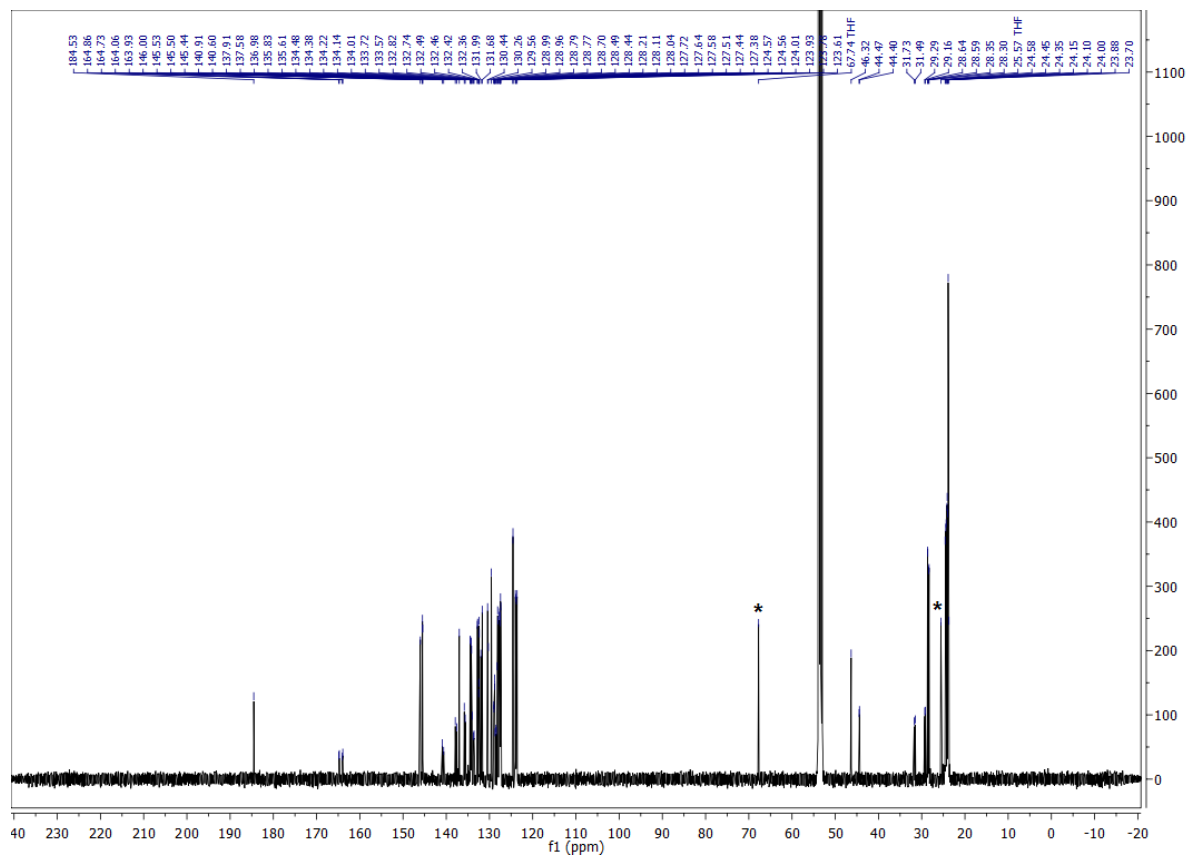


Figure S25: ^{13}C NMR (125 MHz, CD_2Cl_2 , 300 K) spectrum of **3a**. Residual THF marked with asterisks (*).

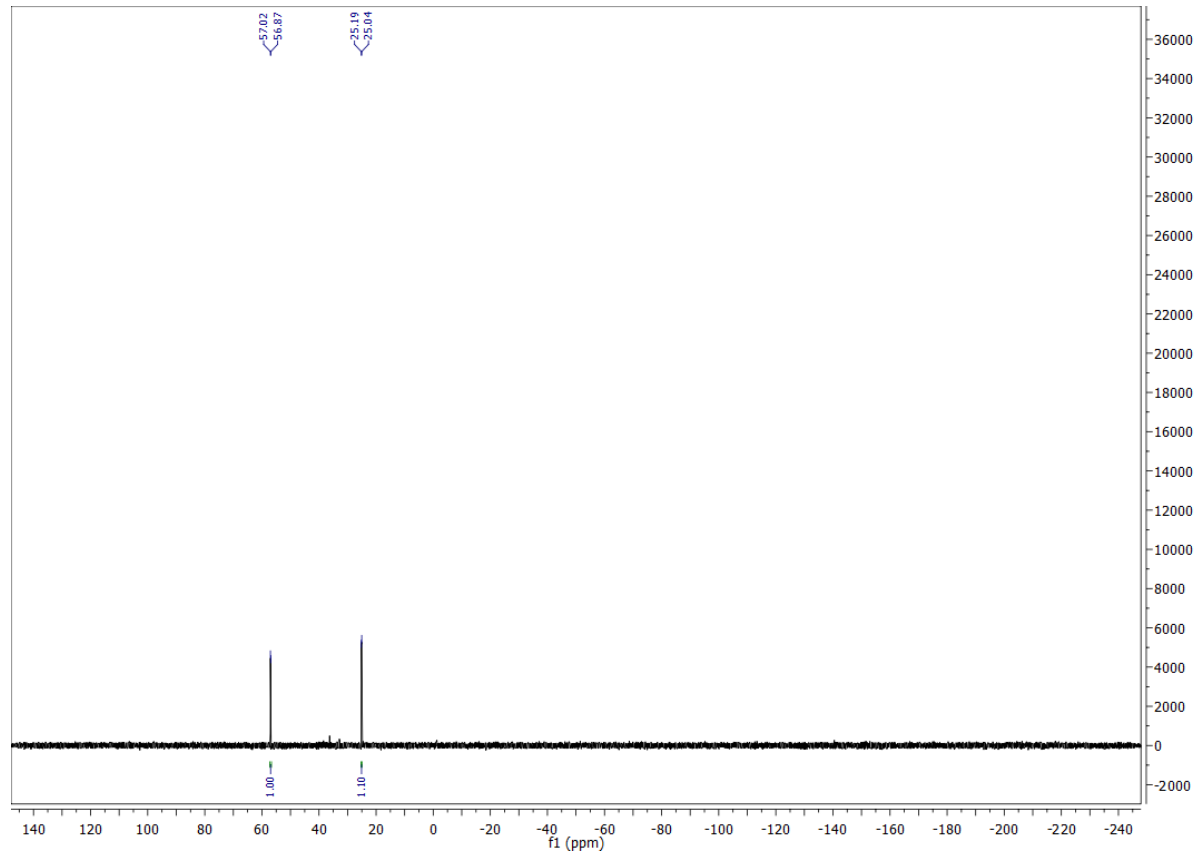


Figure S26: ^{31}P NMR (162 MHz, CD_2Cl_2 , 300 K) spectrum of **3a**.

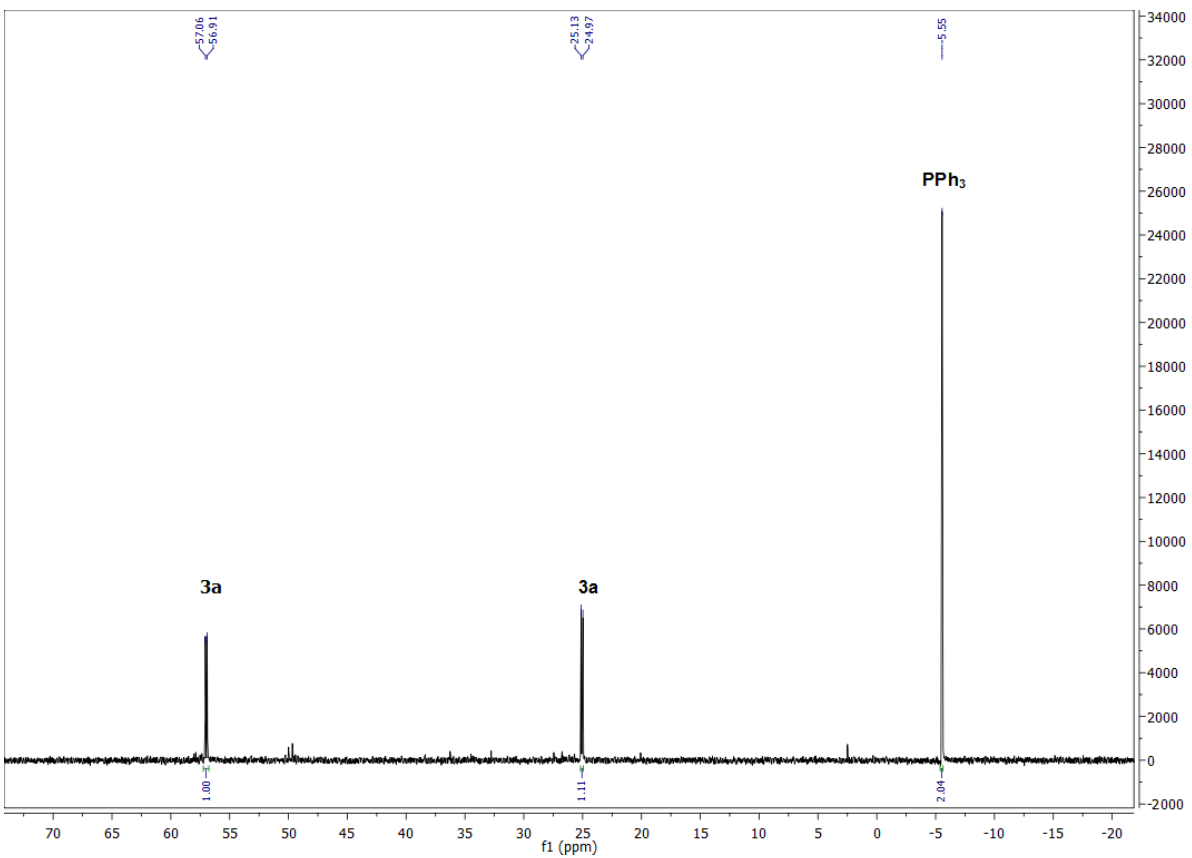


Figure S27: ^{31}P NMR control experiment showing full substitution of PPh_3 with L_{Dipp} , during preparation of **3a**.

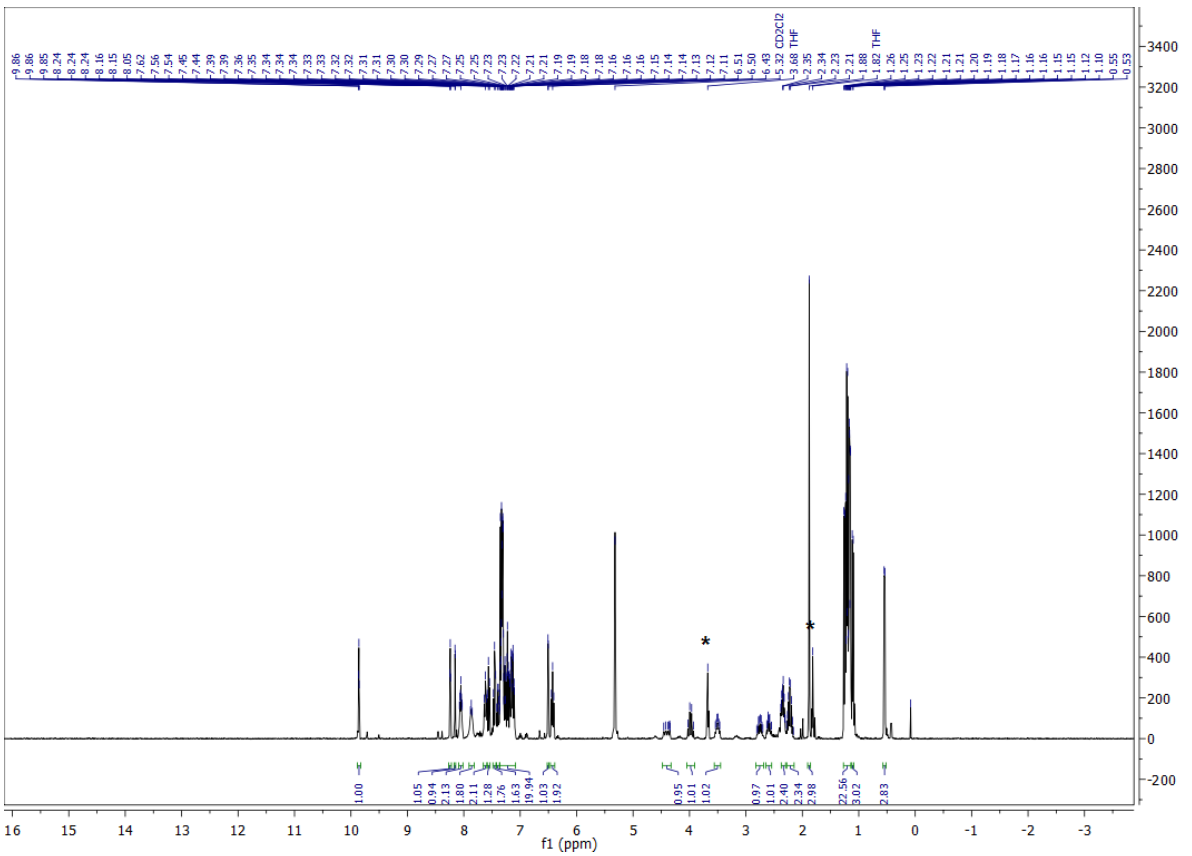


Figure S28: ^1H NMR (400 MHz, CD_2Cl_2 , 300 K) spectrum of **3b** with low formation of **3**. Residual THF marked with asterisks (*).

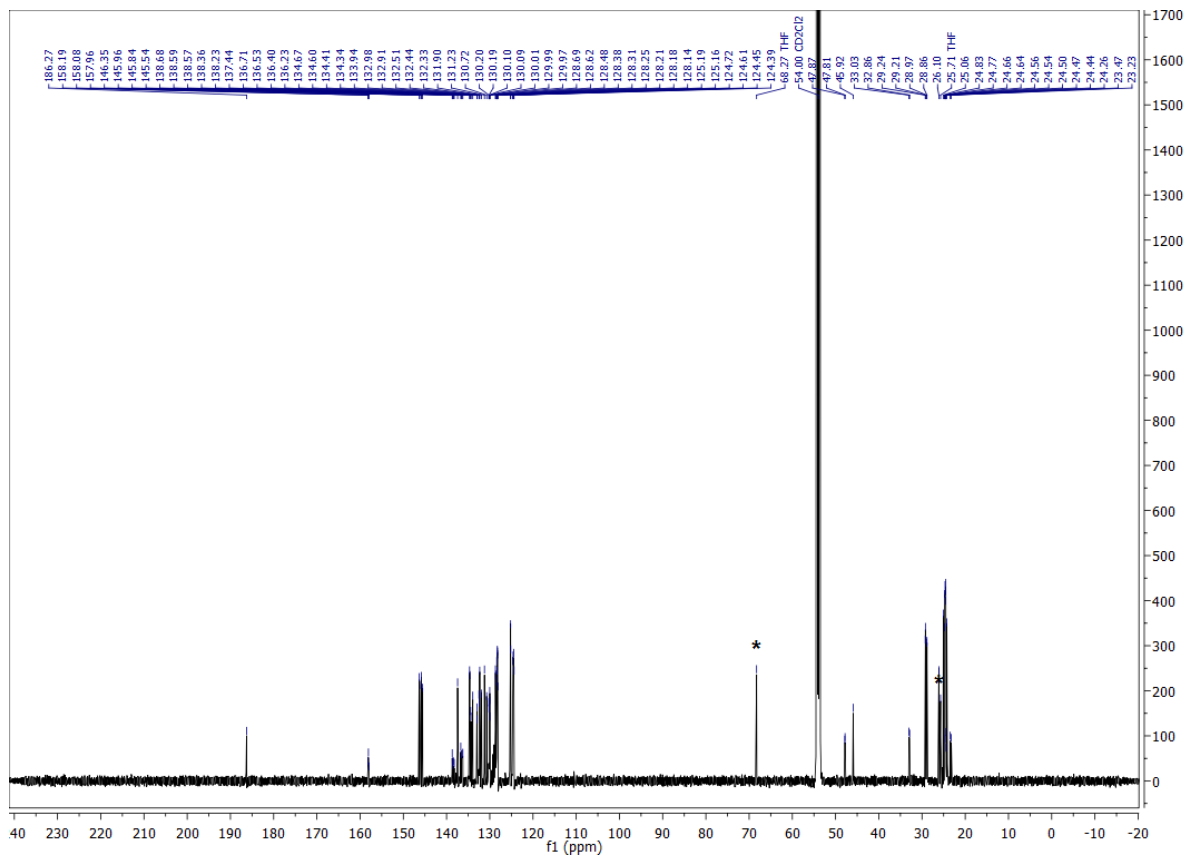


Figure S29: ¹³C NMR (125 MHz, CD₂Cl₂, 300 K) spectrum of **3b** with low formation of **3**. Residual THF marked with asterisks (*).

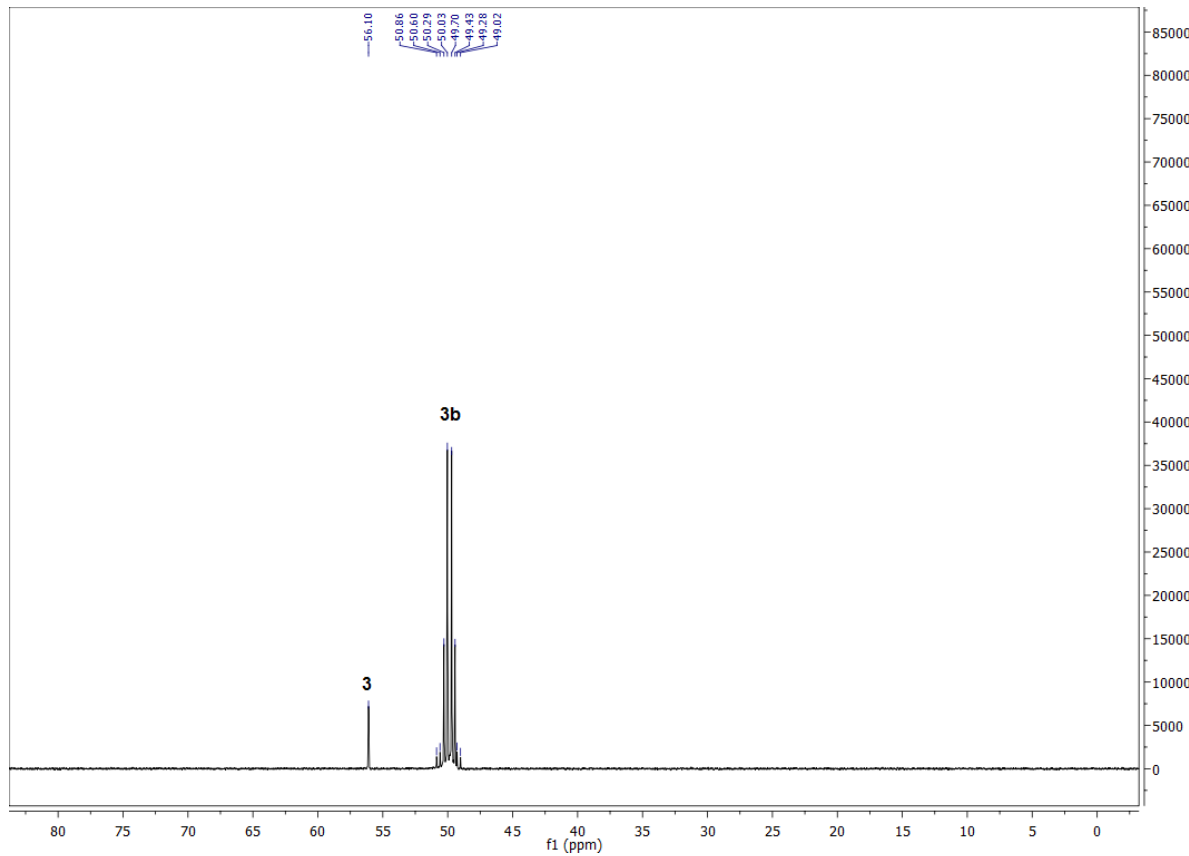


Figure S30: ³¹P NMR (162 MHz, CD₂Cl₂, 300 K) spectrum of **3b** with low formation of **3**.

Single Crystal X-Ray Structure Determination

The single crystal was grown by layering a solution of complex **3** in dichloromethane and a drop of benzene with *n*-pentane. X-ray crystallographic data was collected on a single crystal x-ray diffractometer with the following setup: A CMOS detector (Bruker APEX III, κ-CMOS), a TXS rotating anode and a Helios optic using the APEX3 software package.⁵ The measurement used MoK_α radiation ($\lambda = 0.71073 \text{ \AA}$) and was performed on a single crystal coated with perfluorinated ether. The crystal was fixed on top of a micromount sample holder and frozen under a stream of cold nitrogen at 100 K. A matrix scan was used to determine the initial lattice parameters. Reflections were corrected for Lorentz and polarisation effects, scan speed, and background using SAINT.⁶ Absorption corrections, including odd and even ordered spherical harmonics were performed using SADABS.⁷ Space group assignment was based upon systematic absences, E statistics, and successful refinement of the structure. The structure was solved by direct methods (SHELXT) with the aid of successive difference Fourier maps, and was refined against all data using SHELXL-2015 in conjunction with SHELXLE.⁸ Hydrogen atoms were calculated in ideal positions as follows: Methyl hydrogen atoms were refined as part of rigid rotating groups, with a C–H distance of 0.98 Å and $U_{\text{iso}(\text{H})} = 1.5 \cdot U_{\text{eq}(\text{C})}$. Other H atoms were placed in calculated positions and refined using a riding model, with methylene and aromatic C–H distances of 0.99 Å and 0.95 Å, respectively, other C–H distances of 1.00 Å and $U_{\text{iso}(\text{H})} = 1.2 \cdot U_{\text{eq}(\text{C})}$. Non-hydrogen atoms were refined with anisotropic displacement parameters. Full-matrix least-squares refinements were carried out by minimizing $\Sigma w(F_o^2 - F_c^2)^2$ with SHELXL weighting scheme. Neutral atom scattering factors for all atoms and anomalous dispersion corrections for the non-hydrogen atoms were taken from *International Tables for Crystallography*.⁹ The image of the crystal structure was generated with Mercury.¹⁰ CCDC 2163076 contains the supplementary crystallographic data for this paper. This data can be obtained free of charge *via* www.ccdc.cam.ac.uk/data_request/cif, or by emailing data_request@ccdc.cam.ac.uk, or by contacting The Cambridge Crystallographic Data Centre, 12 Union Road, Cambridge CB2 1EZ, UK; fax: +44 1223 336033.

Table S1: Crystallographic Data of Complex **3** CCDC: 2163076.

Sample and Crystal Data	
Chemical formula	C ₆₆ H ₈₁ BrCl ₁₂ N ₄ O ₂ P ₂ Ru
Formula weight	1630.66 g·mol ⁻¹
Temperature	100(2) K
Wavelength	0.71073 Å
Crystal size	0.286 mm x 0.300 mm x 0.430 mm
Crystal habit	clear yellow fragment
Crystal System	triclinic
Space group	P 1
Unit cell dimensions	a = 11.3315(7) Å α = 77.650(3) ° b = 12.2669(8) Å β = 88.094(3) ° c = 14.2038(10) Å γ = 75.630(2) °
Volume	1867.9(2) Å ³
Z	1
Density (calculated)	1.450 g·cm ⁻³
Absorption coefficient	1.261 mm ⁻¹
F(000)	834
Data Collection and Structure Refinement	
Diffractometer	Bruker D8 Venture
Radiation Source	TXS rotating anode, Mo
Theta range for data collection	2.34 to 25.35 °
Index ranges	-13<=h<=13, -14<=k<=14, -17<=l<=17
Reflections collected	77741
Independent reflections	13197 [R(int) = 0.0363]
Coverage of independent reflections	99.8%
Absorption correction	Multi-Scan
Max. and min. transmission	0.7140 and 0.6130
Structure solution technique	Direct methods
Structure solution program	SHELXT 2018/2 (Sheldrick, 2018)
Function minimized	Full-matrix least-squares on F ²
Refinement program	SHELXL-2018/3 (Sheldrick, 2018)
Data / restraints / parameters	13197 / 690 / 988
Goodness-of-fit on F ²	1.058
Final R indices	12932 data; I>2σ(I); R1 = 0.0359, wR2 = 0.0961 all data R1 = 0.0369, wR2 = 0.0973 w=1/[σ ² (F _o ²)+(0.0618P) ² +2.1130P] where P=(F _o ² +2F _c ²)/3
Weighting scheme	
Absolute structure parameter	0.4(0)
Largest diff. max. min.	0.904 and -0.805 eÅ ⁻³
R.M.S. deviation from mean	0.089 eÅ ⁻³

General Procedure for Catalytic Transfer Hydrogenation Reactions

In a typical experiment, a schlenk-tube (25.0 mL) is charged with catalyst stock solution (in *iso*-propanol, 1.00 mM) according to the desired loading. Acetophenone (116.7 μ L, 1.00 mmol) and *iso*-propanol (so that total volume equals 10.0 mL) are added. A small syringe is inserted through a septum with a long cannula. The argon valve (0.30 bar) is left open during the entire reaction for a constant overpressure. The mixture is stirred and heated to the desired temperature for 2 min. The reaction is started by addition of a 0.1 M solution of NaO*i*Pr in *iso*-propanol (200 μ L, 0.02 mmol, 2.00 mol%). Samples (0.50 mL) are taken at defined intervals using the syringe. The cannula is not removed from the reaction flask during this process, instead the syringe is detached from the cannula. The samples are quenched in a cooling solution (0 °C) of diethylether and filtered over a short pad of silica to remove residual catalyst. Analysis is performed *via* gas chromatography. Blanc experiments without catalyst or without base show no conversion within the investigated reaction times.

General Procedure for Catalytic Oppenauer-type Oxidation Reactions

In a typical experiment, a schlenk-tube (25.0 mL) is charged with catalyst stock solution (in DCM, 1.00 mM) according to the desired loading and the solvent removed under reduced pressure. KO*t*Bu (1.12 mg, 0.01 mmol, 2.00 mol%), substrate (0.50 mmol) and *t*BuOH (so that total volume equals 5.00 mL) are added. A small syringe is inserted through a septum with a long cannula. The argon valve (0.30 bar) is left open during the entire reaction for a constant overpressure. The mixture is stirred and heated to the desired temperature for 2 min. The reaction is started by addition of acetone (0.20 mL, 2.72 mmol). Samples (0.50 mL) are taken at defined intervals using the syringe. The cannula is not removed from the reaction flask during this process, instead the syringe is detached from the cannula. The samples are quenched in a cooling solution (0 °C) of diethylether and filtered over a short pad of silica to remove residual catalyst. Analysis is performed *via* gas chromatography. Blanc experiments without catalyst or without base show no conversion within the investigated reaction times.

TOF Calculations

For reactions reaching near to full conversion, calculation at the slope at 50% conversion (TOF₅₀, representing steepest slope), were calculated as “initial” TOFs. For lower conversions or long induction periods, in which this would misrepresent the “initial” TOF, the steepest slope of the kinetic curve was used for calculations, allowing for valid comparison of all results.

Catalytic Results

Transfer Hydrogenation

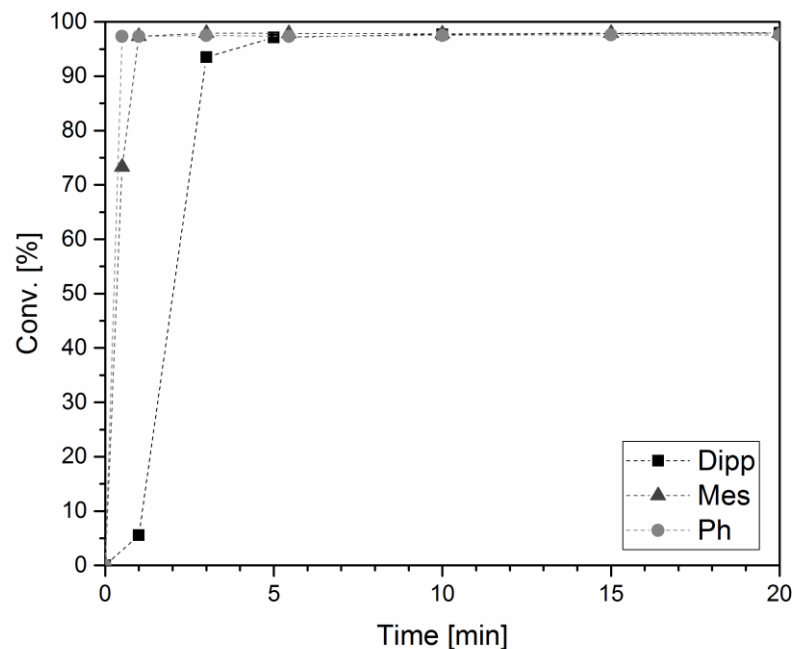


Figure S31: Catalytic TH of acetophenone with complexes **1**, **2** and **3** (Ph, Mes, Dipp respectively) at 80 °C with NaO*i*Pr (2.00 mol%) in *iso*-propanol at S/C = 1 000.

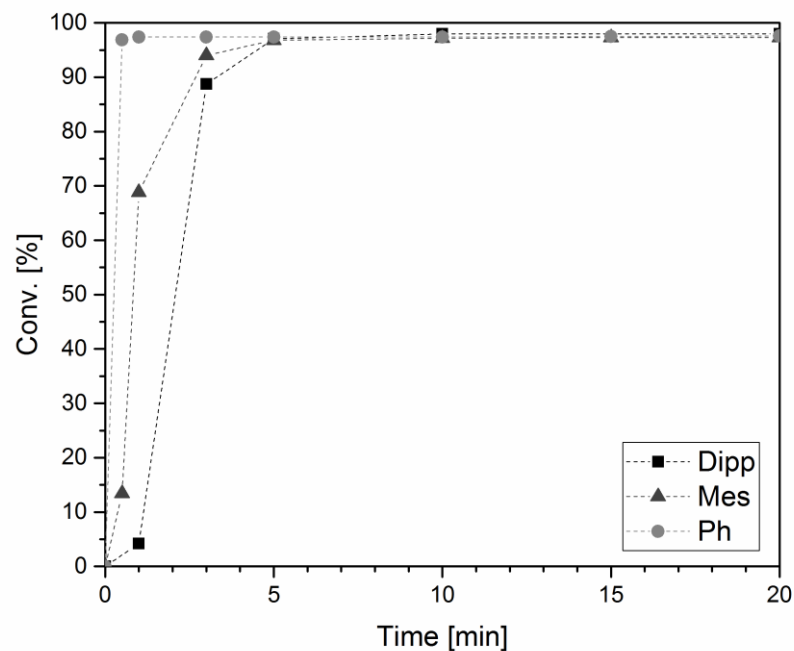


Figure S32: Catalytic TH of acetophenone with complexes **1**, **2** and **3** (Ph, Mes, Dipp respectively) at 80 °C with NaO*i*Pr (2.00 mol%) in *iso*-propanol at S/C = 2 000.

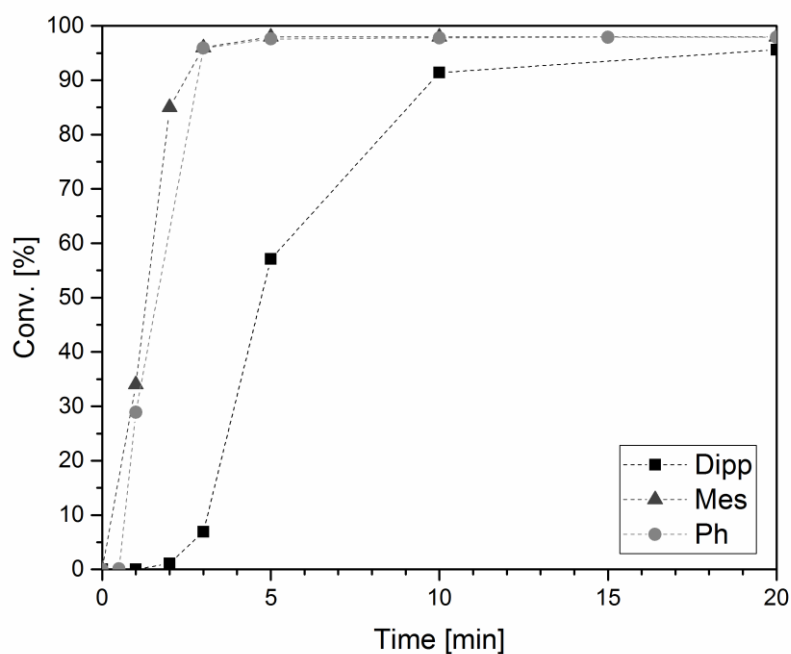


Figure S33: Catalytic TH of acetophenone with complexes **1**, **2** and **3** (Ph, Mes, Dipp respectively) at 80 °C with NaO*i*Pr (2.00 mol%) in *iso*-propanol at S/C = 10 000.

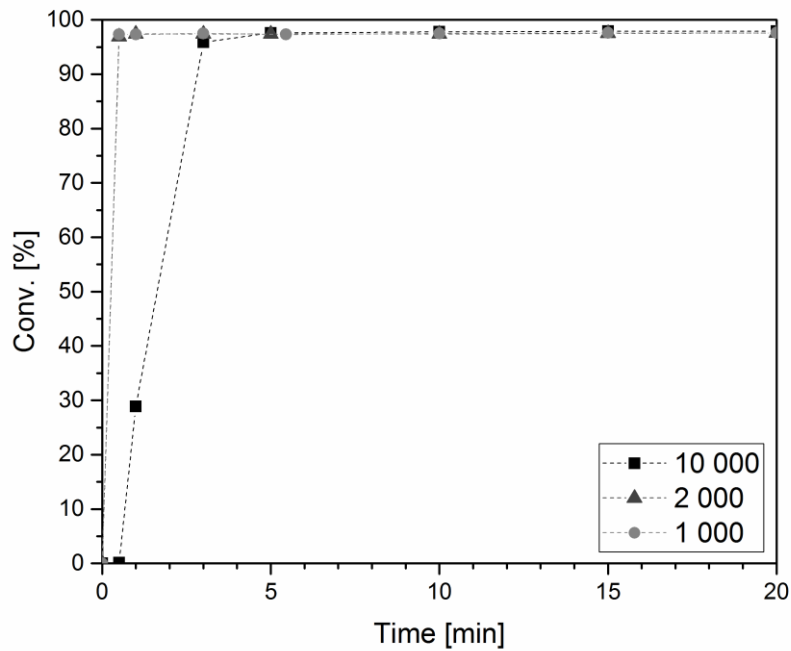


Figure S34: Catalytic TH of acetophenone with complex **1** (Ph) at 80 °C with NaO*i*Pr (2.00 mol%) in *iso*-propanol at S/C = 1 000, 2 000 and 10 000.

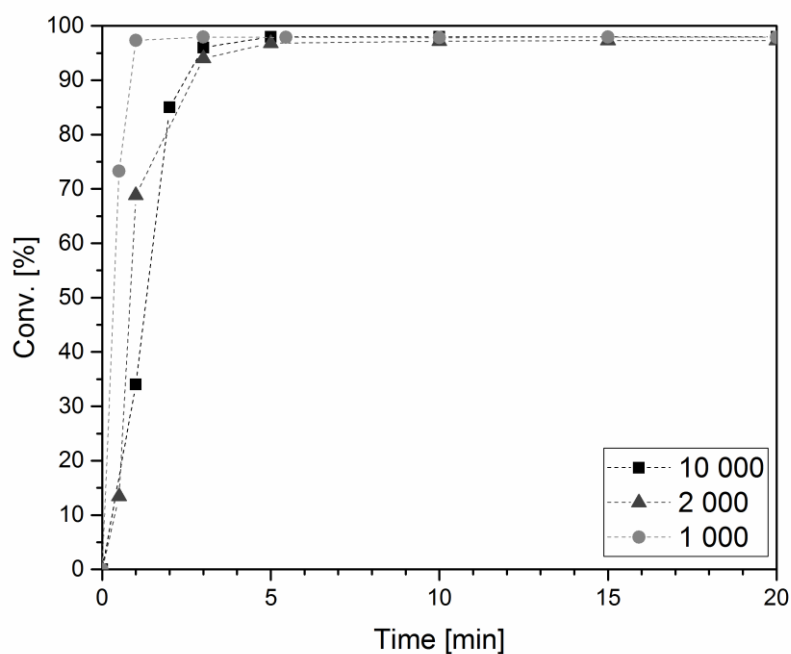


Figure S35: Catalytic TH of acetophenone with complex **2** (Mes) at 80 °C with NaO*i*Pr (2.00 mol%) in *iso*-propanol at S/C = 1 000, 2 000 and 10 000.

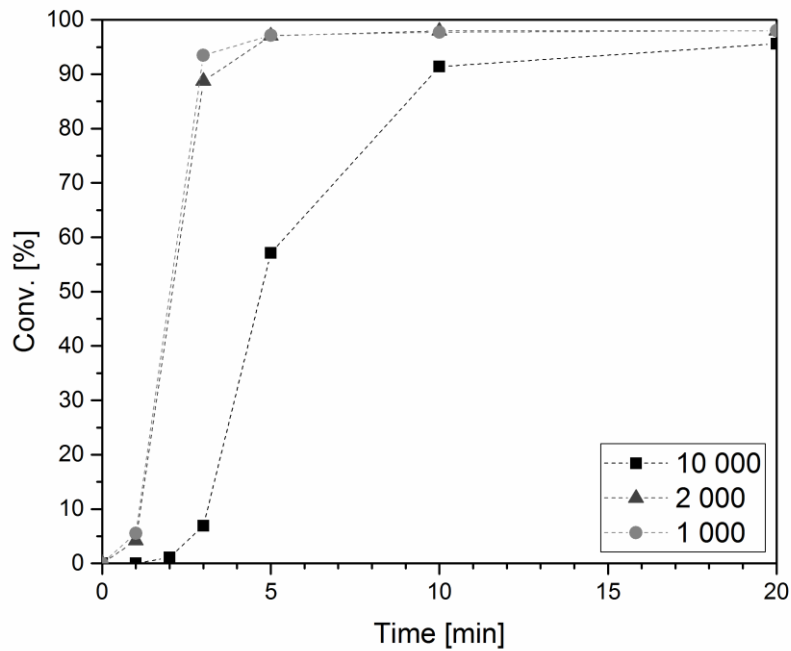


Figure S36: Catalytic TH of acetophenone with complex **3** (Dipp) at 80 °C with NaO*i*Pr (2.00 mol%) in *iso*-propanol at S/C = 1 000, 2 000 and 10 000.

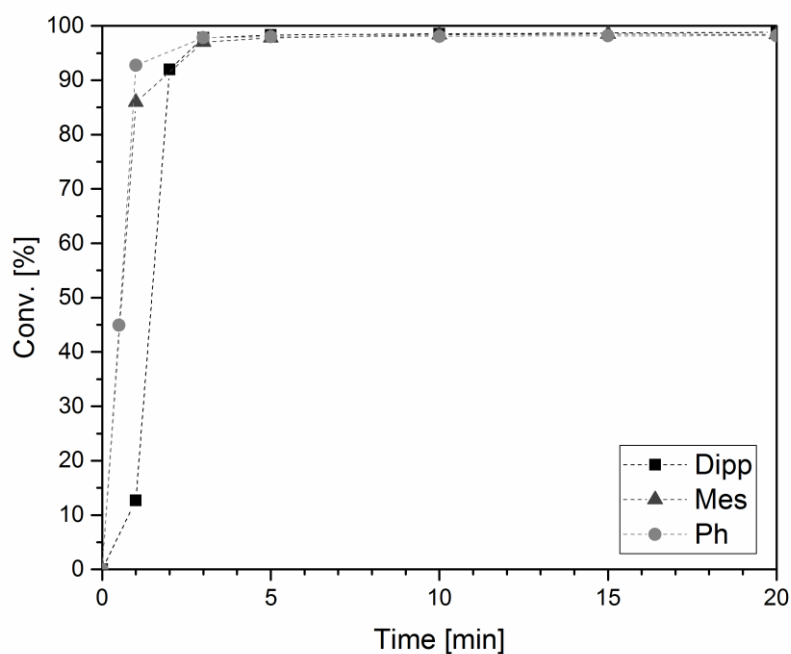


Figure S37: Catalytic TH of acetophenone with complexes **1**, **2** and **3** (Ph, Mes, Dipp respectively) at S/C = 10 000 with NaO*i*Pr (2.00 mol%) in *iso*-propanol at 90 °C.

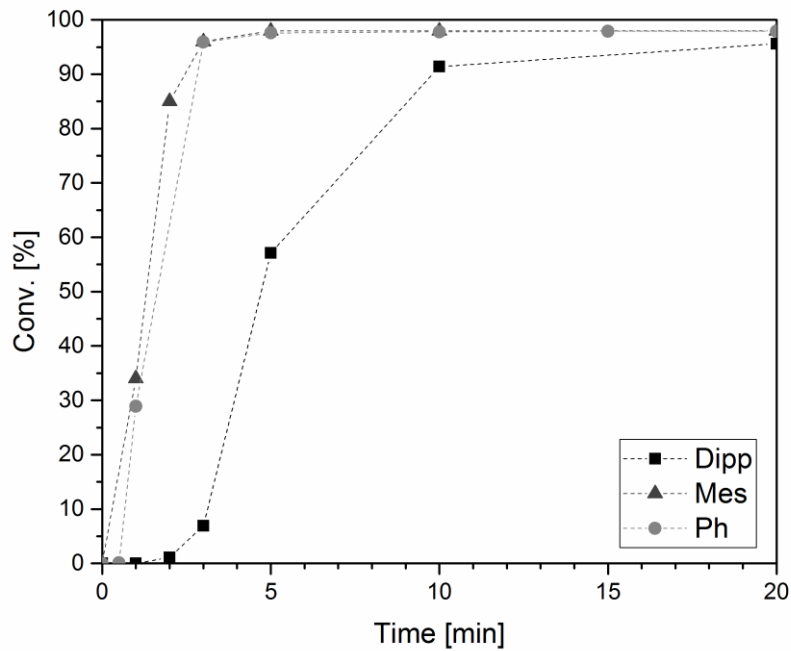


Figure S38: Catalytic TH of acetophenone with complexes **1**, **2** and **3** (Ph, Mes, Dipp respectively) at S/C = 10 000 with NaO*i*Pr (2.00 mol%) in *iso*-propanol at 80 °C.

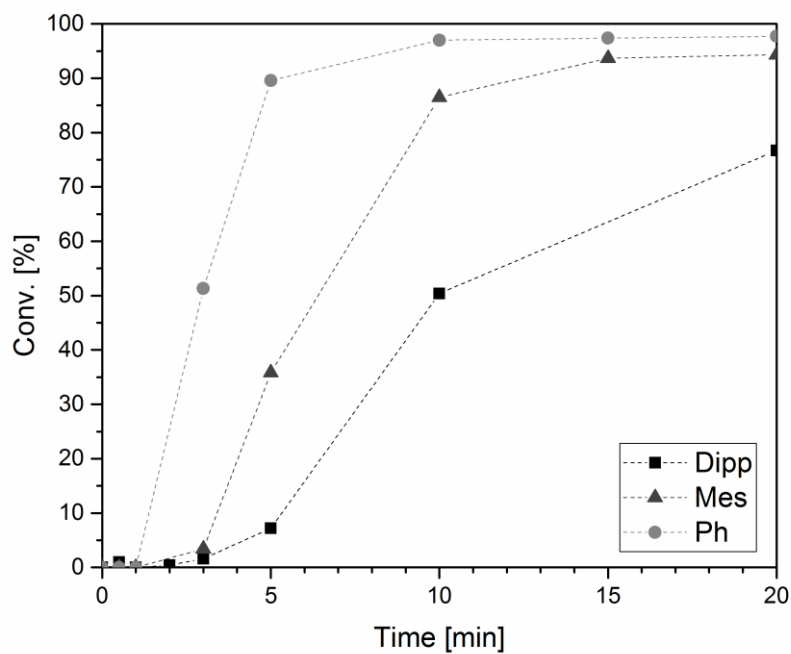


Figure S39: Catalytic TH of acetophenone with complexes **1**, **2** and **3** (Ph, Mes, Dipp respectively) at S/C = 10 000 with NaO*i*Pr (2.00 mol%) in *iso*-propanol at 70 °C.

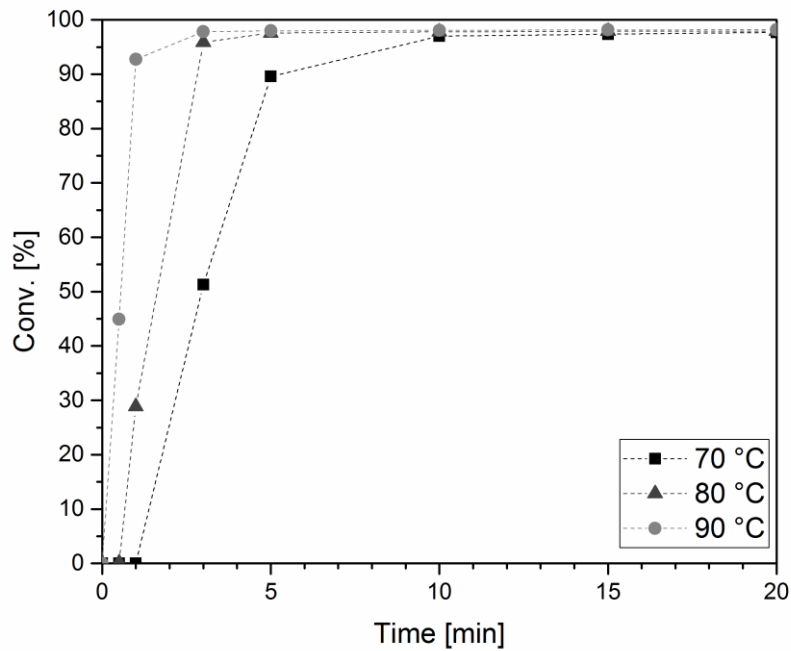


Figure S40: Catalytic TH of acetophenone with complex **1** (Ph) at S/C = 10 000 with NaO*i*Pr (2.00 mol%) in *iso*-propanol at 70 °C, 80 °C and 90 °C.

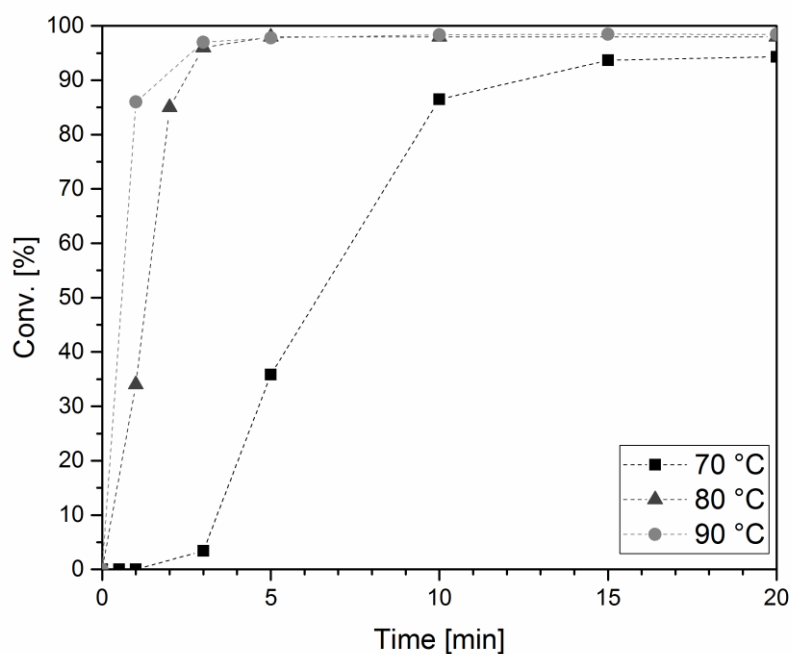


Figure S41: Catalytic TH of acetophenone with complex **2** (Mes) at S/C = 10 000 with NaO*i*Pr (2.00 mol%) in *iso*-propanol at 70 °C, 80 °C and 90 °C.

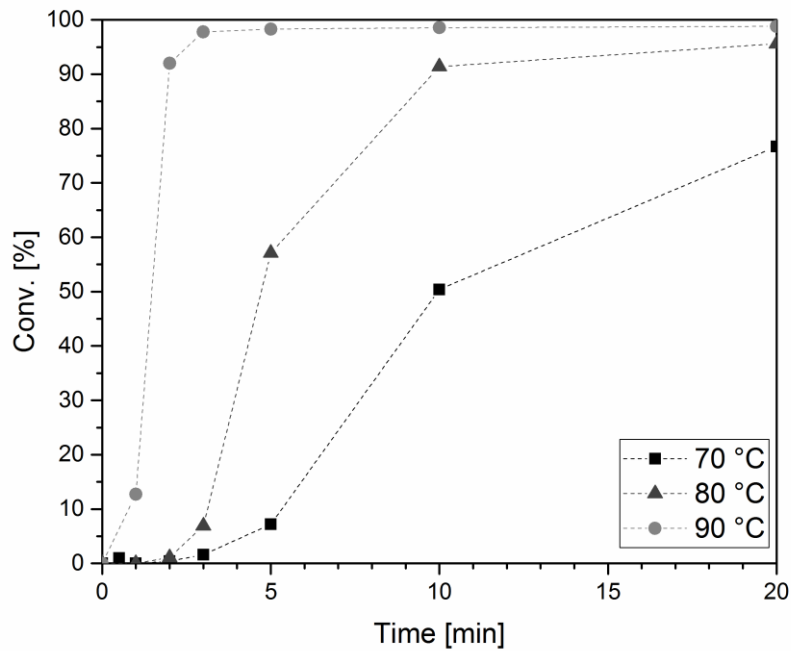


Figure S42: Catalytic TH of acetophenone with complex **3** (Dipp) at S/C = 10 000 with NaO*i*Pr (2.00 mol%) in *iso*-propanol at 70 °C, 80 °C and 90 °C.

Table S2: Activities of various ruthenium NHC complexes in TH reactions with acetophenone (AcPh) and *p*-chloroacetophenone (*p*-Cl-AcPh) as model substrates.

a

b

c

d

e

AcPh $\xrightarrow{[cat.], i\text{PrOH}}$ R-C(Me)-OH

R = H, Cl

Complex	Substrate	Loading [mol%]	TOF [h ⁻¹]	Conversion [%]	Time [min]
a ¹¹	AcPh	0.75	256	96	30
	p-Cl-AcPh	0.03	5 200	65	30
b ¹²	AcPh	0.50	199	99	120
c ¹³	AcPh	0.01	2 467	74	180
d ¹⁴	AcPh	0.50	580	98	80
e ¹⁵	AcPh	0.05	38 000	97	120
	AcPh*	0.01	140 000	86	60

*Ethylenediamine (EDA) as additive.

Oppenauer-Type Oxidation

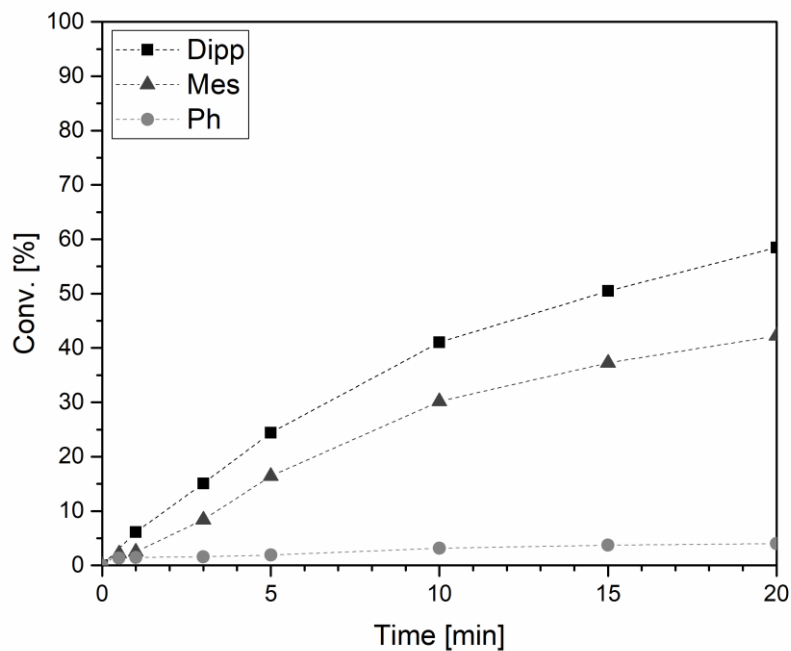


Figure S43: Catalytic *Oppenauer*-type oxidation of α -tetralol with complexes **1**, **2** and **3** (Ph, Mes, Dipp respectively) at S/C = 10 000 with KO^tBu (2.00 mol%) and acetone (6 eq.) in ^tBuOH at 40 °C.

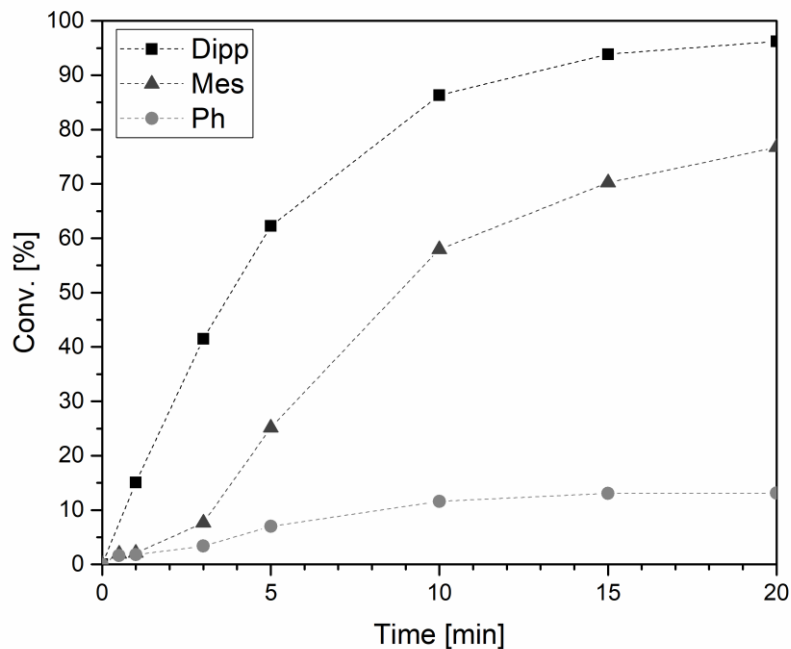


Figure S44: Catalytic *Oppenauer*-type oxidation of α -tetralol with complexes **1**, **2** and **3** (Ph, Mes, Dipp respectively) at S/C = 10 000 with KO^tBu (2.00 mol%) and acetone (6 eq.) in ^tBuOH at 50 °C.

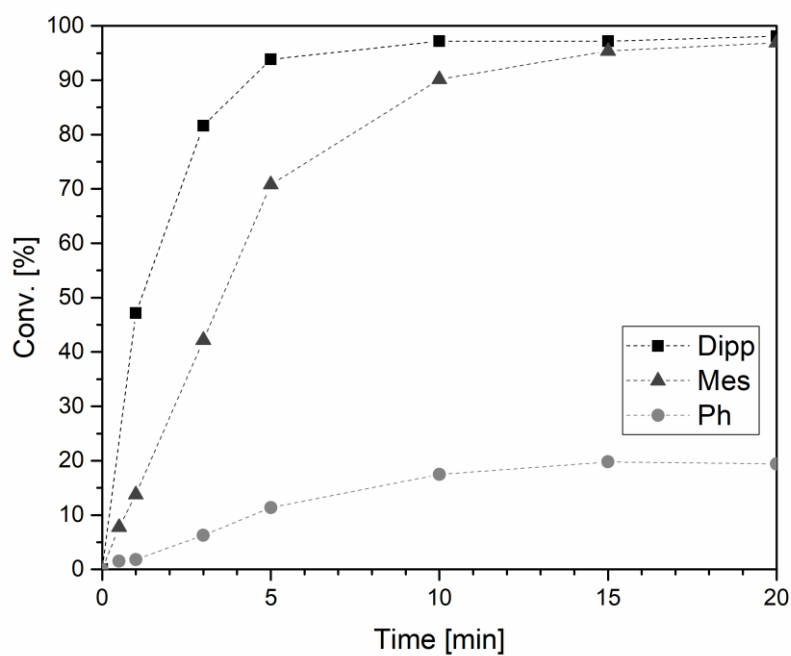


Figure S45: Catalytic Oppenauer-type oxidation of α -tetralol with complexes **1**, **2** and **3** (Ph, Mes, Dipp respectively) at S/C = 10 000 with KO^tBu (2.00 mol%) and acetone (6 eq.) in ^tBuOH at 60 °C.

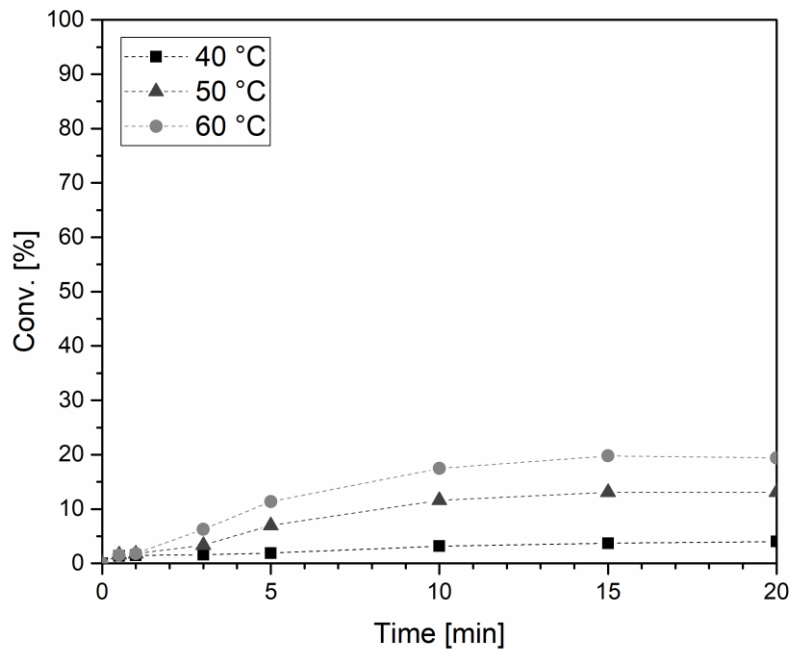


Figure S46: Catalytic Oppenauer-type oxidation of α -tetralol with complex **1** (Ph) at S/C = 10 000 with KO^tBu (2.00 mol%) and acetone (6 eq.) in ^tBuOH at 40 °C, 50 °C and 60 °C.

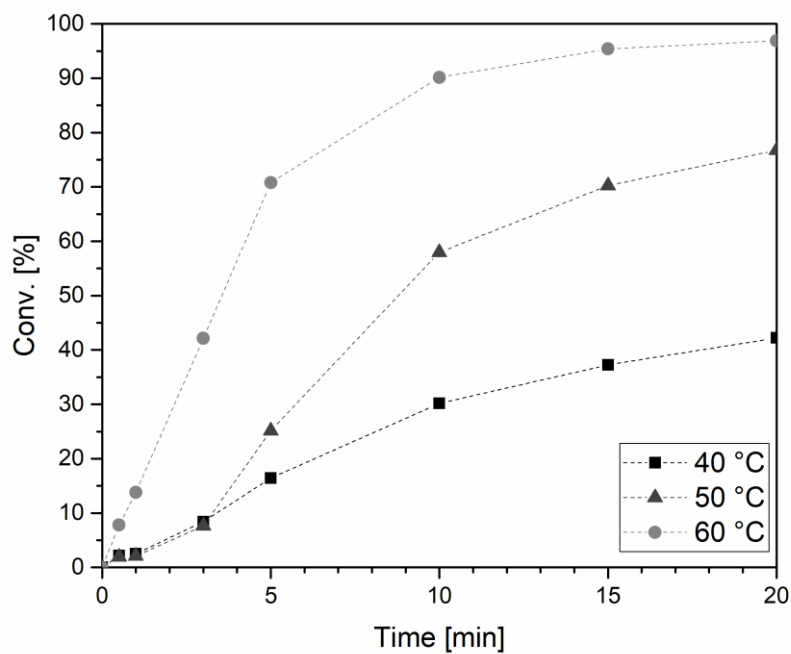


Figure S47: Catalytic Oppenauer-type oxidation of α -tetralol with complex **2** (Mes) at S/C = 10 000 with KO^tBu (2.00 mol%) and acetone (6 eq.) in ^tBuOH at 40 °C, 50 °C and 60 °C.

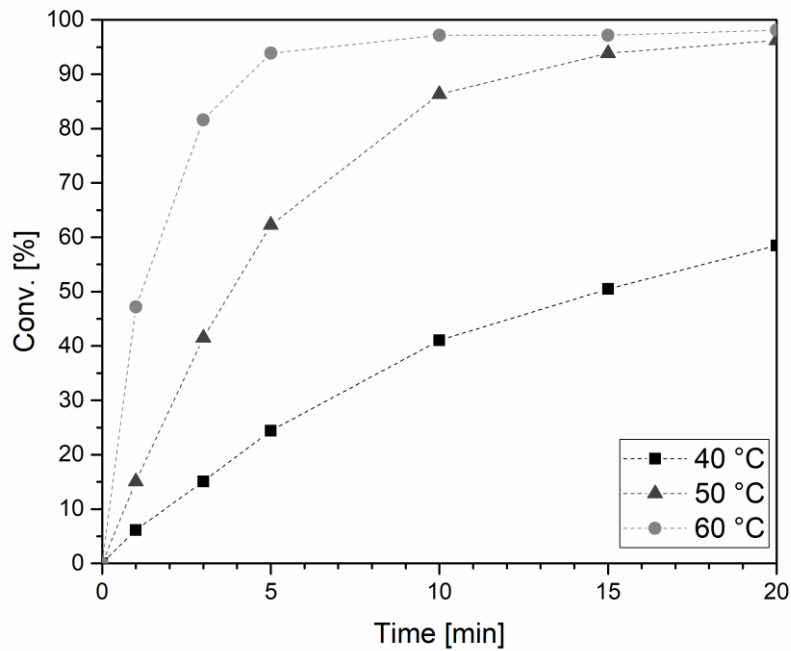
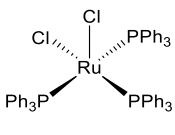
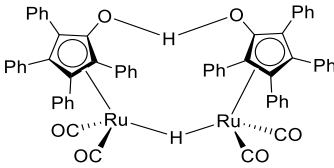
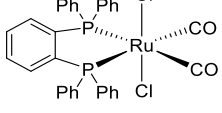
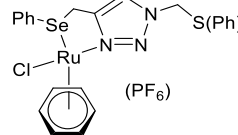
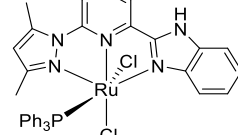
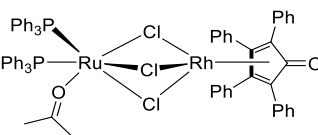
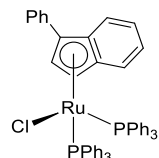
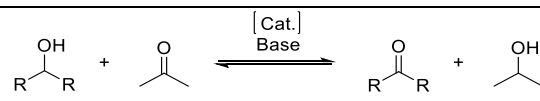


Figure S48: Catalytic Oppenauer-type oxidation of α -tetralol with complex **3** (Dipp) at S/C = 10 000 with KO^tBu (2.00 mol%) and acetone (6 eq.) in ^tBuOH at 40 °C, 50 °C and 60 °C.

Table S3: Activities of various ruthenium complexes in Oppenauer-type oxidation reactions with various substrates.

 f	 g	 h			
 i	 j	 k			
 l					
Complex	Substrate	Loading [mol%]	TOF [h^{-1}]	Conversion [%]	Time [h]
f ¹⁶	α -Tetralol	0.1	n.a. ^a	90	7
	1-Indanol	0.1	1 500	90	1.5
g ¹⁶	1-Indanol	0.1	n.a. ^a	87	17
h ¹⁷	Cyclohexanol	0.1	n.a. ^a	91	6
i ¹⁸	Benzylalcohol	0.1	2 300 ^b	98	3
j ¹⁹	α -Tetralol	0.5	792	99	0.25
k ²⁰	1-Indanol	0.1	n.a. ^a	96	24
l ²¹	1-Indanol	0.5	200	99	1

^aNot available/not reported by source. ^bCalculated manually from NMR conversion measurement.

DFT - Computational Structure Calculations

General Remarks

DFT calculations were performed with Gaussian-16²² and processed using GaussView-6.²³ Calculations were performed in a gas atmosphere, initial parameters were imported from the optimized DFT structure of the previously reported complex κ^2 -acetato-*bis*-(κ^2 -(1-(mesityl)-3-(2-diphenylphosphinoethyl)-imidazolium)-ruthenium(II) bromide **2**^{3a} and the wingtip structures altered to fit the wingtip structure of the desired complexes **1** or **3** (from mesityl to phenyl and di-*iso*-propylphenyl, respectively) in the GaussView-6 software. The same procedure was applied to the hydride analogues **1H** and **3H**, starting from the previously reported hydride **2H**.^{3a} Geometry optimizations were obtained without using constraint coordinates. The obtained structures are true ground states as no negative eigenvalues were found during vibrational analysis. In accordance to previous calculations,^{3a} the pure functional B97D3²⁴ was used. The basis set def2-SVP was applied to small atoms.²⁵ Ru was treated by the Stuttgart/Dresden 1997 SDD relativistic effective core potential (ECP) and its respective basis set.²⁶ The para-methyl groups of the mesityl moieties were removed from **2** and **2H** to facilitate convergence.

Coordinate Tables

Table S4: Coordinates of **1** calculated with B97D3/def2-SVP (charge 1, multiplicity 1, SCF: E = -3000.33 h).

Atom	Coordinates [Å]		
	x	y	z
Ru	-0.001152	-0.721289	0.003788
N	-2.163494	-0.506085	2.296147
C	-1.855528	-0.828043	0.954733
P	0.768749	0.805581	1.448612
P	-0.773700	0.792691	-1.453005
N	-4.066447	-1.112273	1.427994
C	-3.479039	-0.670762	2.560583
H	-3.990097	-0.454328	3.497542
O	0.493670	-2.681031	0.991710
O	-0.492962	-2.688521	-0.969948
C	-0.429081	1.196258	2.833404
H	0.129943	1.621924	3.683758
H	-1.148202	1.950190	2.473725
C	1.853807	-0.833697	-0.946759
C	3.477425	-0.683968	-2.553380
H	3.988200	-0.472851	-3.491717
C	-3.085322	-1.223557	0.440289

H	-3.338545	-1.587124	-0.551734
N	2.161367	-0.520910	-2.290497
C	-1.184031	-0.054459	3.290116
H	-0.488400	-0.887983	3.488429
H	-1.730055	0.150245	4.226344
N	4.065669	-1.116104	-1.417588
C	3.084437	-1.222976	-0.429406
H	3.338424	-1.577859	0.565573
C	1.180923	-0.078762	-3.287800
H	0.486852	-0.915143	-3.479314
H	1.726443	0.119517	-4.225705
C	0.423732	1.174152	-2.840851
H	-0.135850	1.592109	-3.694652
H	1.141559	1.932135	-2.487089
C	-5.463827	-1.358664	1.242006
C	-6.211999	-1.985367	2.251724
C	-7.580661	-2.210449	2.050907
H	-8.167760	-2.701209	2.835118
C	-8.191426	-1.829761	0.846108
C	-7.430307	-1.215944	-0.160862
H	-7.902594	-0.915499	-1.102918
C	-6.064592	-0.970998	0.031777
C	5.463543	-1.358023	-1.229367
C	6.062805	-0.961146	-0.021369
C	7.428912	-1.202009	0.173633
H	7.900023	-0.894394	1.113959
C	8.191882	-1.820871	-0.828840
C	7.582635	-2.210658	-2.031498
H	8.171232	-2.705242	-2.812174
C	6.213626	-1.989715	-2.234567
C	2.283038	2.518066	-0.154786
H	2.664040	1.580530	-0.570000
C	2.761389	3.744462	-0.631242
H	3.510851	3.763766	-1.431638
C	2.287916	4.946589	-0.080333
H	2.657771	5.908179	-0.454238
C	1.344298	4.908525	0.954832
H	0.967453	5.841042	1.389870
C	0.869615	3.679751	1.437973
H	0.129550	3.682346	2.242176
C	1.325096	2.472138	0.880600
C	3.346140	1.104470	2.678125
H	3.328906	2.140133	2.326070
C	4.467189	0.637264	3.381883
H	5.308532	1.315097	3.569623
C	4.511189	-0.686139	3.845736
H	5.388524	-1.050056	4.393183

C	3.423216	-1.539790	3.606033
H	3.448168	-2.576671	3.961476
C	2.304281	-1.080779	2.895428
H	1.496193	-1.777943	2.659916
C	2.256648	0.247418	2.419675
C	-2.260675	0.224413	-2.419531
C	-2.305266	-1.107042	-2.886369
H	-1.495334	-1.800632	-2.646713
C	-3.423478	-1.573601	-3.593151
H	-3.446092	-2.612910	-3.941581
C	-4.513747	-0.724319	-3.837857
H	-5.390531	-1.094118	-4.382232
C	-4.472793	0.602248	-3.382871
H	-5.315972	1.276686	-3.574560
C	-3.352502	1.076960	-2.682951
H	-3.337673	2.114967	-2.337791
C	-1.332654	2.462936	-0.898617
C	-2.290515	2.515726	0.136511
H	-2.669626	1.580971	0.559617
C	-2.771233	3.745166	0.602631
H	-3.520602	3.769749	1.402965
C	0.068913	-4.839403	-0.014450
H	1.023696	-5.151290	-0.477201
H	-0.754771	-5.253107	-0.617762
H	0.039155	-5.244829	1.009545
C	0.009483	-3.331679	0.008718
C	-0.879717	3.666675	-1.466340
H	-0.139905	3.663999	-2.270765
C	-1.356817	4.898550	-0.993590
H	-0.981991	5.828091	-1.436675
C	-2.300311	4.943516	0.041411
H	-2.672073	5.907507	0.407154
H	9.260646	-2.003539	-0.671774
H	-9.259906	-2.015644	0.690881
H	5.725826	-2.327797	-3.155157
H	5.468534	-0.459099	0.749253
H	-5.722896	-2.316568	3.174112
H	-5.471727	-0.472879	-0.742461

Table S5: Coordinates of **1_H** calculated with B97D3/def2-SVP (charge 0, multiplicity 1, SCF: E = -2773.45 h).

Atom	Coordinates [Å]		
	x	y	z
Ru	0.000007	0.332106	0.000005
P	-1.642051	-0.968692	-0.974044
C	1.058388	0.373409	-1.770999

P	1.642073	-0.968703	0.974032
N	-1.094590	-0.598472	2.762496
N	-1.994835	1.297252	2.237643
N	1.094598	-0.598398	-2.762514
N	1.994819	1.297329	-2.237632
C	-1.058379	0.373360	1.771005
C	2.366433	2.527854	-1.618316
C	3.725003	2.778533	-1.370291
C	3.157923	4.966404	-0.481563
C	1.396774	3.493516	-1.300706
C	-3.725045	2.778414	1.370281
C	-3.158010	4.966306	0.481578
C	-1.396835	3.493465	1.300749
C	-2.366472	2.527773	1.618334
C	2.230151	-2.472166	0.071174
C	-3.291103	-0.216363	-1.428897
C	-2.230108	-2.472185	-0.071221
C	3.291113	-0.216371	1.428927
C	0.330921	-1.847278	-2.755992
H	0.680938	-2.467863	-1.916847
H	0.590632	-2.381130	-3.685678
C	-1.176660	-1.626857	-2.667500
H	-1.496351	-0.870334	-3.405207
H	-1.718594	-2.562569	-2.890787
C	-0.330907	-1.847349	2.755945
H	-0.590621	-2.381226	3.685616
H	-0.680917	-2.467912	1.916781
C	1.176674	-1.626919	2.667467
H	1.496357	-0.870415	3.405197
H	1.718611	-2.562634	2.890730
C	4.387403	-1.033870	1.778203
H	4.295358	-2.124782	1.716590
C	5.598052	-0.463236	2.193929
H	6.443867	-1.110245	2.458183
C	5.728194	0.933909	2.271711
H	6.676387	1.380594	2.595857
C	4.641442	1.751419	1.930957
H	4.733357	2.842994	1.978683
C	3.430765	1.179080	1.510303
H	2.573998	1.803075	1.227695
C	3.131755	-2.299737	-1.004239
H	3.572677	-1.312834	-1.185219
C	1.676662	-3.752147	0.284531
H	0.969006	-3.919453	1.102169
C	3.452897	-3.368465	-1.848972
H	4.150136	-3.210464	-2.681173
C	2.881963	-4.635466	-1.638215

H	3.130038	-5.471978	-2.302256
C	1.998465	-4.822578	-0.563449
H	1.553183	-5.808961	-0.382483
C	-1.676596	-3.752153	-0.284597
H	-0.968931	-3.919432	-1.102234
C	-1.998388	-4.822605	0.563360
H	-1.553088	-5.808978	0.382379
C	-2.881900	-4.635529	1.638121
H	-3.129966	-5.472057	2.302144
C	-3.452857	-3.368542	1.848896
H	-4.150108	-3.210568	2.681093
C	-3.131724	-2.299792	1.004188
H	-3.572666	-1.312900	1.185181
C	-4.387393	-1.033865	-1.778168
H	-4.295337	-2.124778	-1.716578
C	-5.598057	-0.463234	-2.193855
H	-6.443871	-1.110246	-2.458103
C	-5.728216	0.933912	-2.271597
H	-6.676421	1.380594	-2.595711
C	-4.641466	1.751424	-1.930845
H	-4.733395	2.843000	-1.978542
C	-3.430772	1.179088	-1.510236
H	-2.574005	1.803086	-1.227633
C	-4.120157	4.000490	0.807378
H	-5.181787	4.185963	0.607270
C	-1.799596	4.707585	0.731876
H	-1.045412	5.463868	0.487493
C	1.799511	4.707644	-0.731833
H	1.045310	5.463904	-0.487431
C	4.120092	4.000618	-0.807391
H	5.181720	4.186121	-0.607303
C	2.588058	0.886804	-3.435643
H	3.325299	1.498575	-3.952278
C	2.012346	-0.302326	-3.765116
H	2.170082	-0.958030	-4.620612
C	-2.012348	-0.302431	3.765098
H	-2.170083	-0.958155	4.620579
C	-2.588073	0.886697	3.435644
H	-3.325328	1.498448	3.952284
H	-0.875595	1.614720	-0.462863
H	0.875597	1.614716	0.462904
H	3.463376	5.920459	-0.035839
H	-3.463481	5.920355	0.035854
H	0.343379	3.270056	-1.482823
H	4.464814	2.002186	-1.591349
H	-4.464837	2.002042	1.591318
H	-0.343437	3.270034	1.482884

Table S6: Coordinates of **2** calculated with B97D3/def2-SVP (charge 1, multiplicity 1, SCF: E = -3157.39 h).

Atom	Coordinates [Å]		
	x	y	z
Ru	-0.000904	-0.559926	0.002713
N	-2.255452	-0.380114	2.204970
C	-1.894400	-0.690739	0.873711
P	0.690350	0.968711	1.482841
P	-0.698348	0.958383	-1.484893
N	-4.101202	-1.069388	1.284188
C	-3.570433	-0.603581	2.429416
H	-4.115010	-0.449508	3.360295
O	0.447574	-2.529778	1.010081
O	-0.434095	-2.533924	-1.001638
C	-0.582640	1.366142	2.795225
H	-0.074000	1.815801	3.664600
H	-1.298266	2.099064	2.388468
C	1.893055	-0.687624	-0.867661
C	3.567708	-0.607387	-2.425105
H	4.111334	-0.458469	-3.357395
C	-3.092643	-1.136151	0.322940
H	-3.317150	-1.484013	-0.682434
N	2.252373	-0.385330	-2.201197
C	-1.327957	0.103584	3.233478
H	-0.620501	-0.710460	3.470332
H	-1.917463	0.304574	4.143746
N	4.100287	-1.064149	-1.277019
C	3.092636	-1.126469	-0.314544
H	3.318787	-1.466074	0.693311
C	1.322425	0.089623	-3.231648
H	0.617359	-0.728078	-3.463008
H	1.910482	0.287309	-4.143575
C	0.573520	1.352281	-2.799649
H	0.063448	1.795912	-3.671273
H	1.287079	2.089399	-2.396884
C	-5.481951	-1.422525	1.072963
C	-5.930918	-2.681731	1.524665
C	-7.276493	-3.012009	1.278716
H	-7.657683	-3.982870	1.615686
C	-8.122400	-2.121867	0.604884
C	-7.641432	-0.883399	0.159638
H	-8.309088	-0.193605	-0.369408
C	-6.304714	-0.506232	0.381907
C	-5.765254	0.818083	-0.100339
H	-6.573882	1.451742	-0.497790

H	-5.015255	0.684529	-0.900544
H	-5.265898	1.371799	0.715157
C	5.481364	-1.414465	-1.063970
C	-5.000868	-3.632975	2.238591
H	-5.440458	-4.641317	2.299172
H	-4.794794	-3.298471	3.272919
H	-4.025818	-3.708075	1.724662
C	6.304727	-0.490804	-0.383647
C	7.641781	-0.865468	-0.159095
H	8.310084	-0.170049	0.361697
C	8.122191	-2.108734	-0.591412
C	7.275368	-3.006503	-1.253962
H	7.656110	-3.981143	-1.580361
C	5.929537	-2.678823	-1.501783
C	5.764931	0.837805	0.086307
H	6.573671	1.476248	0.475789
H	5.016778	0.711071	0.889440
H	5.263133	1.382860	-0.733513
C	4.997846	-3.638071	-2.202854
H	5.437938	-4.646680	-2.254703
H	4.787358	-3.314272	-3.239674
H	4.024638	-3.708389	-1.684516
C	2.312783	2.658925	-0.026199
H	2.708589	1.713737	-0.408260
C	2.835225	3.877591	-0.474889
H	3.638874	3.885470	-1.221219
C	2.335995	5.087474	0.035638
H	2.741038	6.043339	-0.315866
C	1.320942	5.064744	1.001662
H	0.923262	6.003654	1.403168
C	0.801043	3.843380	1.456602
H	0.003939	3.856190	2.204392
C	1.285248	2.629160	0.939979
C	3.107120	1.335548	2.978983
H	3.067170	2.383211	2.665187
C	4.162826	0.902158	3.795247
H	4.933478	1.616769	4.107861
C	4.234927	-0.436852	4.207584
H	5.062751	-0.774214	4.842057
C	3.240479	-1.340282	3.802942
H	3.288601	-2.389318	4.118475
C	2.185715	-0.914520	2.981348
H	1.447407	-1.640474	2.631215
C	2.112054	0.429186	2.557453
C	-2.118224	0.409861	-2.557394
C	-2.190245	-0.936765	-2.972144
H	-1.452118	-1.659795	-2.615580

C	-3.242929	-1.368606	-3.793252
H	-3.289966	-2.419837	-4.101569
C	-4.236673	-0.468394	-4.206656
H	-5.062824	-0.810486	-4.840773
C	-4.166081	0.873481	-3.803479
H	-4.936280	1.585579	-4.122860
C	-3.112619	1.312902	-2.987567
H	-3.073988	2.362701	-2.680787
C	-1.297641	2.619929	-0.950725
C	-2.324931	2.651351	0.015618
H	-2.717356	1.706784	0.402662
C	-2.851021	3.870646	0.458279
H	-3.654433	3.879843	1.204843
C	0.095161	-4.684675	-0.029104
H	1.076635	-4.985024	-0.441340
H	-0.690192	-5.102674	-0.678895
H	0.014769	-5.097066	0.989452
C	0.020844	-3.176801	-0.000618
C	-0.817218	3.832950	-1.473639
H	-0.020346	3.844359	-2.221710
C	-1.340800	5.054981	-1.024759
H	-0.946161	5.993087	-1.431116
C	-2.355693	5.079442	-0.058592
H	-2.763611	6.035825	0.288149
H	9.167066	-2.382570	-0.405970
H	-9.167014	-2.397793	0.421041

Table S7: Coordinates of **2_H** calculated with B97D3/def2-SVP (charge 0, multiplicity 1, SCF: E = -2930.53 h).

Atom	Coordinates [Å]		
	x	y	z
Ru	-0.000010	0.105012	0.000012
P	-1.660084	-1.220858	-0.926453
C	0.920366	0.239780	-1.838123
P	1.659874	-1.221082	0.926465
N	-0.925951	-0.684982	2.872368
N	-1.670519	1.282861	2.374088
N	0.925916	-0.685175	-2.872291
N	1.670827	1.282538	-2.374016
C	-0.920305	0.239937	1.838167
C	2.069286	2.480760	-1.689727
C	3.386257	2.545689	-1.182187
C	2.904507	4.805845	-0.400132
C	1.175758	3.571333	-1.609738
C	-3.385839	2.546122	1.182202
C	-2.903859	4.806185	0.400032

C	-1.175227	3.571559	1.609674
C	-2.068865	2.481084	1.689733
C	2.216430	-2.731176	0.012586
C	-3.306920	-0.471736	-1.402410
C	-2.216858	-2.730861	-0.012583
C	3.306807	-0.472176	1.402408
C	4.337224	1.388995	-1.351482
H	4.709340	1.322337	-2.391211
H	5.203657	1.483582	-0.678927
H	3.834597	0.436928	-1.124352
C	-0.214141	3.479380	-2.171202
H	-0.227370	2.979756	-3.155441
H	-0.824472	2.858383	-1.488884
H	-0.680447	4.473426	-2.260274
C	0.272893	-1.993460	-2.822856
H	0.720773	-2.576870	-2.005082
H	0.516442	-2.510392	-3.766755
C	-1.237006	-1.884601	-2.638022
H	-1.657202	-1.173436	-3.369965
H	-1.725016	-2.860226	-2.807006
C	-4.336870	1.389476	1.351463
H	-4.708789	1.322627	2.391249
H	-5.203414	1.484255	0.679075
H	-3.834347	0.437421	1.124048
C	0.214713	3.479434	2.171005
H	0.227985	2.979805	3.155243
H	0.824878	2.858365	1.488598
H	0.681164	4.473415	2.260026
C	-0.273160	-1.993381	2.822935
H	-0.516759	-2.510246	3.766858
H	-0.721179	-2.576747	2.005203
C	1.236746	-1.884785	2.638038
H	1.657108	-1.173736	3.369999
H	1.724581	-2.860510	2.806939
C	4.478212	-1.243341	1.540957
H	4.463032	-2.310032	1.290718
C	5.669436	-0.654170	1.990981
H	6.577309	-1.263572	2.081611
C	5.699625	0.707922	2.331107
H	6.630963	1.166612	2.685447
C	4.531571	1.476629	2.213561
H	4.543109	2.543105	2.468629
C	3.347470	0.891339	1.744596
H	2.440426	1.488104	1.605348
C	3.084214	-2.582081	-1.094359
H	3.525755	-1.602919	-1.305502
C	1.654322	-4.002540	0.252953

H	0.968641	-4.153535	1.092037
C	3.371515	-3.663521	-1.935048
H	4.046988	-3.522165	-2.787837
C	2.791502	-4.921079	-1.695091
H	3.009966	-5.767337	-2.357088
C	1.935547	-5.084444	-0.594904
H	1.480827	-6.062236	-0.392267
C	-1.655011	-4.002332	-0.252975
H	-0.969360	-4.153450	-1.092061
C	-1.936449	-5.084187	0.594873
H	-1.481931	-6.062070	0.392222
C	-2.792360	-4.920664	1.695071
H	-3.010987	-5.766888	2.357058
C	-3.372101	-3.662987	1.935066
H	-4.047528	-3.521506	2.787871
C	-3.084579	-2.581594	1.094393
H	-3.525885	-1.602332	1.305568
C	-4.478425	-1.242743	-1.540976
H	-4.463389	-2.309438	-1.290751
C	-5.669578	-0.653405	-1.990972
H	-6.577533	-1.262685	-2.081601
C	-5.699586	0.708691	-2.331086
H	-6.630862	1.167511	-2.685423
C	-4.531422	1.477232	-2.213561
H	-4.542817	2.543707	-2.468633
C	-3.347397	0.891783	-1.744605
H	-2.440274	1.488425	-1.605364
C	-3.783110	3.723251	0.523358
H	-4.794328	3.781805	0.104084
C	-1.617683	4.731979	0.948511
H	-0.935974	5.586446	0.868345
C	1.618331	4.731741	-0.948629
H	0.936739	5.586314	-0.868582
C	3.783645	3.722814	-0.523400
H	4.794865	3.781278	-0.104113
C	2.106153	1.005290	-3.670608
H	2.703050	1.715930	-4.239868
C	1.630505	-0.233438	-3.984532
H	1.728190	-0.827921	-4.892435
C	-1.630354	-0.233067	3.984653
H	-1.728103	-0.827514	4.892573
C	-2.105778	1.005748	3.670728
H	-2.702523	1.716509	4.239996
H	-0.931896	1.377771	-0.350561
H	0.932025	1.377681	0.350583
H	3.227149	5.717199	0.117939
H	-3.226404	5.717537	-0.118102

Table S8: Coordinates of **3** calculated with B97D3/def2-SVP (charge 1, multiplicity 1, SCF: E = -3471.49 h).

Atom	Coordinates [Å]		
	x	y	z
Ru	-0.004724	-0.328988	0.001704
N	-2.359922	-0.150375	2.092524
C	-1.930547	-0.454647	0.781195
P	0.620373	1.197189	1.511987
P	-0.620507	1.190124	-1.519298
N	-4.139781	-0.894270	1.088863
C	-3.677806	-0.410492	2.255952
H	-4.266716	-0.286275	3.163747
O	0.370217	-2.303920	1.039696
O	-0.420359	-2.308776	-1.010054
C	-0.720823	1.605397	2.752492
H	-0.257872	2.060985	3.644051
H	-1.413009	2.335998	2.303227
C	1.922650	-0.480023	-0.777886
C	3.675073	-0.423538	-2.247201
H	4.266484	-0.293211	-3.152529
C	-3.088500	-0.931641	0.175545
H	-3.258533	-1.276722	-0.841110
N	2.355356	-0.171256	-2.087692
C	-1.489917	0.348016	3.163652
H	-0.795627	-0.461948	3.449355
H	-2.128475	0.560376	4.037538
N	4.136182	-0.908244	-1.080325
C	3.081220	-0.955653	-0.170897
H	3.250332	-1.302413	0.845474
C	1.488062	0.323976	-3.162611
H	0.791860	-0.485686	-3.444156
H	2.128471	0.528387	-4.037049
C	0.721970	1.586531	-2.761779
H	0.260786	2.036311	-3.657219
H	1.415451	2.319083	-2.317820
C	-5.490360	-1.324223	0.824477
C	-5.841793	-2.655445	1.146276
C	-7.160628	-3.052779	0.859908
H	-7.478813	-4.074130	1.091340
C	-8.070341	-2.162664	0.276329
C	-7.681166	-0.857524	-0.049507
H	-8.403270	-0.179529	-0.515181
C	-6.373666	-0.408314	0.208574
C	5.492299	-1.320096	-0.813656
C	6.361262	-0.393764	-0.192092

C	7.675242	-0.823786	0.065172
H	8.385895	-0.136785	0.535186
C	8.086084	-2.120613	-0.267389
C	7.191400	-3.021049	-0.857536
H	7.525457	-4.036204	-1.094471
C	5.866751	-2.642707	-1.143416
C	2.317880	2.878678	0.075186
H	2.722350	1.931746	-0.293715
C	2.860419	4.094939	-0.356498
H	3.688897	4.097464	-1.074217
C	2.345058	5.307505	0.131023
H	2.766149	6.261241	-0.207170
C	1.291585	5.290171	1.055002
H	0.880536	6.231173	1.437731
C	0.748683	4.071412	1.489627
H	-0.080223	4.088688	2.201859
C	1.250251	2.854109	0.996867
C	2.931052	1.566511	3.162685
H	2.908730	2.614681	2.848440
C	3.921106	1.138816	4.059539
H	4.658994	1.857946	4.433613
C	3.971645	-0.201085	4.471973
H	4.749109	-0.533730	5.169571
C	3.021387	-1.111612	3.985448
H	3.054084	-2.161719	4.299594
C	2.028497	-0.690386	3.087891
H	1.320602	-1.418875	2.684076
C	1.976347	0.655102	2.666095
C	-1.979418	0.644000	-2.668438
C	-2.028355	-0.701469	-3.090858
H	-1.315430	-1.427399	-2.691715
C	-3.026518	-1.127521	-3.980154
H	-3.056528	-2.177733	-4.294170
C	-3.985886	-0.221867	-4.457810
H	-4.767820	-0.558350	-5.148533
C	-3.938628	1.118069	-4.045175
H	-4.683308	1.833654	-4.412546
C	-2.942936	1.550601	-3.156864
H	-2.923479	2.598789	-2.842805
C	-1.247322	2.851051	-1.013712
C	-2.317676	2.882657	-0.095225
H	-2.724583	1.938461	0.277956
C	-2.861008	4.102072	0.326289
H	-3.692805	4.109725	1.040280
C	-0.008456	-4.460720	0.015715
H	0.998748	-4.801766	-0.286450
H	-0.741062	-4.861201	-0.702429

H	-0.207326	-4.851356	1.026804
C	-0.030494	-2.950747	0.018254
C	-0.743315	4.064559	-1.513081
H	0.087200	4.076385	-2.223570
C	-1.286244	5.286619	-1.087712
H	-0.873187	6.224745	-1.475318
C	-2.342804	5.310982	-0.167388
H	-2.764346	6.267326	0.162795
H	9.114526	-2.435815	-0.056518
H	-9.093953	-2.493073	0.065161
C	4.862693	-3.641888	-1.709764
H	4.030237	-3.069344	-2.156315
C	5.903516	1.021184	0.147833
H	4.806285	0.993583	0.265687
C	-4.816942	-3.638238	1.705197
H	-4.020070	-3.051126	2.196148
C	-5.935096	1.013817	-0.127111
H	-4.837703	1.000161	-0.246391
C	4.264869	-4.492831	-0.569296
H	5.053925	-5.077160	-0.062347
H	3.768875	-3.860497	0.187084
H	3.517799	-5.202918	-0.968176
C	5.453133	-4.526406	-2.820074
H	5.918860	-3.919482	-3.616467
H	6.219338	-5.220115	-2.430701
H	4.659086	-5.143552	-3.276315
C	6.226302	1.986091	-1.011052
H	5.738813	1.670704	-1.950539
H	5.884037	3.008648	-0.771098
H	7.315107	2.026075	-1.195001
C	6.477505	1.538381	1.475889
H	6.296647	0.822211	2.295000
H	7.563998	1.727221	1.411891
H	5.993360	2.493287	1.746002
C	-5.401658	-4.585140	2.765499
H	-5.917671	-4.027683	3.567031
H	-6.123686	-5.297606	2.328396
H	-4.595265	-5.183263	3.225248
C	-4.153492	-4.425445	0.554454
H	-4.904407	-5.026495	0.010313
H	-3.665406	-3.750185	-0.168664
H	-3.384187	-5.112908	0.950186
C	-6.267179	1.971585	1.035014
H	-5.778264	1.656357	1.973793
H	-5.932626	2.997968	0.799786
H	-7.356476	2.002173	1.217970
C	-6.516924	1.527258	-1.453232

H	-6.326538	0.816107	-2.274641
H	-7.605970	1.700436	-1.388240
H	-6.046513	2.489851	-1.720601

Table S9: Coordinates of **3_H** calculated with B97D3/def2-SVP (charge 0, multiplicity 1, SCF: E = -3244.62 h).

Atom	Coordinates [Å]		
	x	y	z
Ru	-0.000359	0.303273	-0.000055
P	1.646940	1.672250	-0.933500
C	-0.873677	0.162725	-1.868649
P	-1.648459	1.671547	0.932860
N	0.867827	1.127488	2.870768
N	1.457100	-0.920907	2.517303
N	-0.867887	1.124954	-2.871848
N	-1.455699	-0.923676	-2.517353
C	0.873588	0.164515	1.868283
C	-1.793209	-2.218871	-1.986329
C	-3.083198	-2.419061	-1.430786
C	-2.574130	-4.808861	-1.305544
C	-0.884709	-3.282249	-2.178642
C	3.084721	-2.416843	1.431744
C	2.576362	-4.806899	1.308907
C	0.886500	-3.279892	2.180495
C	1.794754	-2.216472	1.987234
C	-2.383681	3.034783	-0.079452
C	3.190016	0.924586	-1.684587
C	2.382079	3.035784	0.078485
C	-3.191451	0.923817	1.684015
C	-4.028009	-1.248542	-1.167036
H	-3.390324	-0.439683	-0.766675
C	0.492636	-3.060810	-2.785667
H	0.631181	-1.972391	-2.879677
C	-0.374401	2.491880	-2.716648
H	-0.877324	2.942715	-1.854034
H	-0.687087	3.054300	-3.612716
C	1.134612	2.549014	-2.533002
H	1.640212	2.037682	-3.369078
H	1.485999	3.594553	-2.530487
C	4.029073	-1.246265	1.166646
H	3.390930	-0.437821	0.766183
C	-0.490884	-3.058215	2.787341
H	-0.629937	-1.969715	2.879680
C	0.372645	2.493751	2.715134
H	0.685024	3.056945	3.610821
H	0.874655	2.944841	1.852106

C	-1.136522	2.548812	2.532172
H	-1.640932	2.036524	3.368386
H	-1.489547	3.593808	2.530017
C	-4.399534	1.632017	1.833461
H	-4.526995	2.606346	1.348944
C	-5.439707	1.105672	2.616129
H	-6.379021	1.663594	2.717085
C	-5.275465	-0.119313	3.280997
H	-6.084083	-0.521974	3.902866
C	-4.072630	-0.827923	3.137285
H	-3.936772	-1.791296	3.643785
C	-3.047390	-0.316552	2.330533
H	-2.116183	-0.869449	2.178259
C	-3.311854	2.694939	-1.090053
H	-3.685827	1.668866	-1.154599
C	-1.900914	4.359747	-0.030881
H	-1.161778	4.648745	0.724233
C	-3.737203	3.647061	-2.024042
H	-4.454603	3.358543	-2.802207
C	-3.242019	4.960959	-1.972239
H	-3.570221	5.705713	-2.706886
C	-2.325007	5.312807	-0.968927
H	-1.934779	6.336916	-0.916339
C	1.899459	4.360787	0.029640
H	1.160350	4.649713	-0.725529
C	2.323643	5.314003	0.967491
H	1.933535	6.338144	0.914670
C	3.240574	4.962259	1.970908
H	3.568839	5.707128	2.705412
C	3.735600	3.648313	2.023000
H	4.452928	3.359851	2.801252
C	3.310190	2.696058	1.089182
H	3.684089	1.669980	1.153933
C	4.398075	1.632842	-1.833929
H	4.525464	2.607157	-1.349361
C	5.438312	1.106573	-2.616568
H	6.377609	1.664538	-2.717450
C	5.274172	-0.118406	-3.281474
H	6.082844	-0.521005	-3.903311
C	4.071376	-0.827097	-3.137818
H	3.935586	-1.790470	-3.644338
C	3.046062	-0.315787	-2.331127
H	2.114869	-0.868733	-2.178923
C	3.454178	-3.734533	1.108043
H	4.441299	-3.928181	0.679443
C	1.298870	-4.577586	1.823389
H	0.608258	-5.417092	1.960706

C	-1.296724	-4.579718	-1.820298
H	-0.605885	-5.419168	-1.956827
C	-3.452263	-3.736539	-1.105784
H	-4.439354	-3.930067	-0.677060
C	-1.720397	-0.652762	-3.862051
H	-2.163433	-1.399883	-4.517401
C	-1.348942	0.639024	-4.082183
H	-1.399902	1.255552	-4.978916
C	1.350438	0.642914	4.081027
H	1.401717	1.260192	4.977225
C	1.722798	-0.648720	3.861553
H	2.167020	-1.394969	4.517091
H	0.918120	-0.980643	-0.365549
H	-0.917747	-0.981255	0.366022
H	-2.885811	-5.826314	-1.040017
H	2.888320	-5.824534	1.044405
C	-5.094659	-1.560101	-0.109087
H	-4.657805	-2.016097	0.791582
H	-5.596244	-0.628564	0.202198
H	-5.871357	-2.241430	-0.503707
C	-4.722166	-0.731995	-2.444769
H	-4.009411	-0.339034	-3.185283
H	-5.306112	-1.541397	-2.921259
H	-5.425294	0.082441	-2.189066
C	0.585945	-3.663046	-4.199759
H	0.460006	-4.761402	-4.177815
H	-0.191058	-3.248197	-4.866371
H	1.572588	-3.445130	-4.649240
C	1.600563	-3.586986	-1.861703
H	1.527218	-4.678167	-1.708730
H	2.597650	-3.380957	-2.288664
H	1.542501	-3.096615	-0.878514
C	-1.598690	-3.586362	1.864354
H	-1.524836	-4.677743	1.713033
H	-2.595810	-3.380220	2.291173
H	-1.541073	-3.097457	0.880410
C	-0.583677	-3.658362	4.202356
H	-0.457164	-4.756685	4.182027
H	0.193206	-3.242104	4.868224
H	-1.570364	-3.440265	4.651655
C	5.095058	-1.558203	0.108130
H	4.657653	-2.014874	-0.791935
H	5.596182	-0.626731	-0.204076
H	5.872219	-2.239087	0.502599
C	4.723921	-0.728748	2.443603
H	4.011487	-0.335623	3.184348
H	5.308447	-1.537679	2.920180

H 5.426588 0.085794 2.186975

Calculated Structures

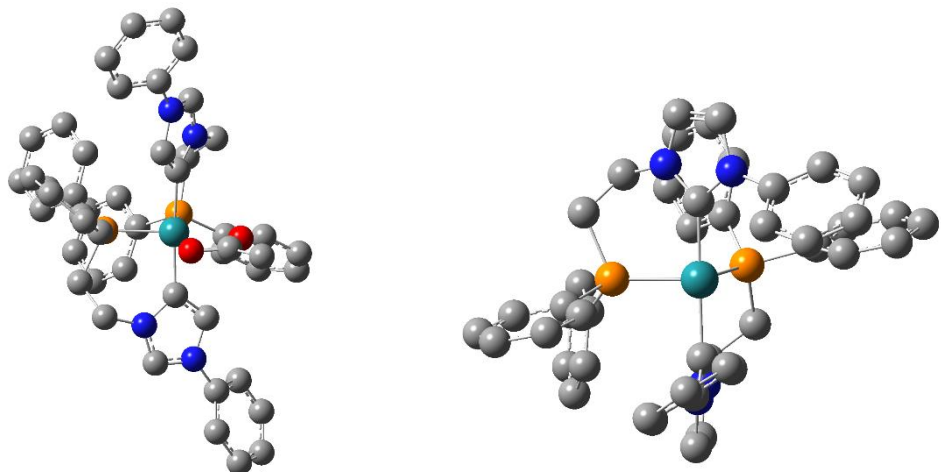


Figure S49: Calculated structures for **1** (left) and **1_H** (right). H atoms removed for clarity.

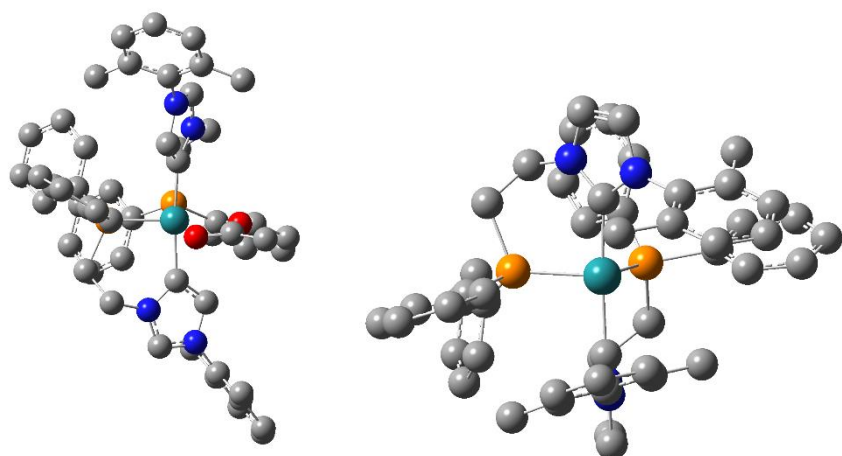


Figure S50: Calculated structures for **2** (left) and **2_H** (right). H atoms removed for clarity.

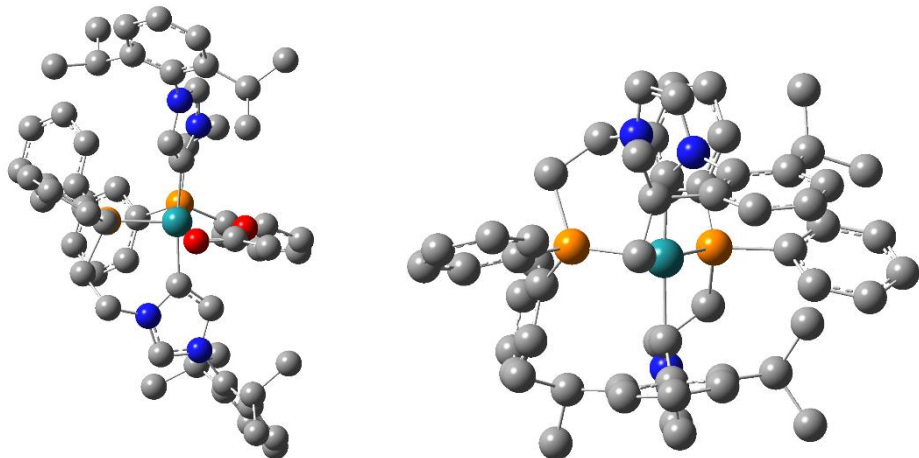


Figure S51: Calculated structures for **3** (left) and **3_H** (right). H atoms removed for clarity.

DFT - Buried Volume and Steric Map Calculations

General Remarks

For determination of the buried volumes²⁷ as well as the steric maps²⁸ of complexes **1**, **2** and **3**, as well as their respective hydrides **1_H**, **2_H** and **3_H**, the SambVca 2.0 tool²⁹ is applied. Hereby, the atoms were loaded into the tool as .xyz files. The Ru atom was chosen as coordination point to the center of the sphere (distance 0.00 Å) and the carboxylic acetate carbon or the hydrides selected as z-positive z-axis definition, respectively. One abnormal coordinating aNHC carbene carbon or normal coordinating NHC carbene carbon was selected for xz-plane definition for **1**, **2**, **3** and **1_H**, **2_H**, **3_H**, respectively. The ruthenium central atoms as well as the acetates in compounds **1**, **2** and **3** and the hydrides in compounds **1_H**, **2_H** and **3_H**, were removed. The bondi radii were scaled by 1.17 and sphere radii of 3.5 Å, 5 Å and 7 Å chosen. A mesh spacing for numerical integration of 0.10 Å was applied. Hydrogens were neglected from the calculations. The calculated steric maps therefore represent a viewpoint along the z-axis, from positive to negative.

It is to be noted, that whilst calculations using a sphere radius of 3.5 Å and 5 Å are representative of the steric shielding of the coordination site of the complexes, calculations using a sphere radius of 7 Å take into account nearly the whole complex surface (Figure S52) and hence do not represent the active site but the whole complex. Nevertheless, these results were reported for completeness; however, trends describe the buried volume regarding the whole complex rather than that of the active center.

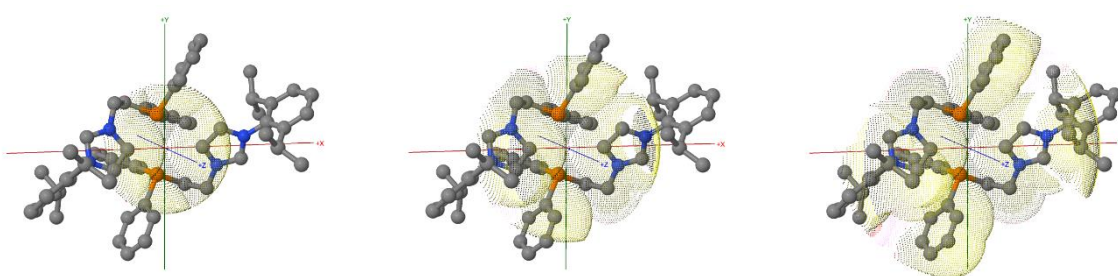


Figure S52: Comparison of steric maps with varying sphere radii (3.5 Å left, 5 Å center and 7 Å right) on calculated structures of **3**.

Furthermore, steric map calculations for the hydride complexes **1_H**, **2_H** and **3_H** using sphere radii of 3.5 Å and 5 Å all resulted in an area that did not lie in the defined color range. This is hence depicted by a white color in the center of the steric maps in the SambVca 2.0 tool. Other than the color change, test calculations using the SambVca 2.1 tool did not yield any notable

differences in calculated buried volume (values deviate a maximum of 0.1%) or in the topographic form of the steric maps (Figure S53). The validity is also confirmed in the SambVca 2.1 release notes.³⁰ All herein reported calculations were performed in SambVca 2.0 for comparability.

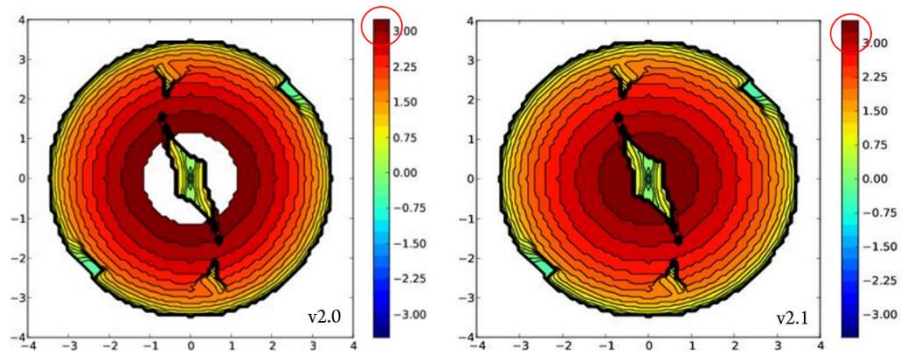
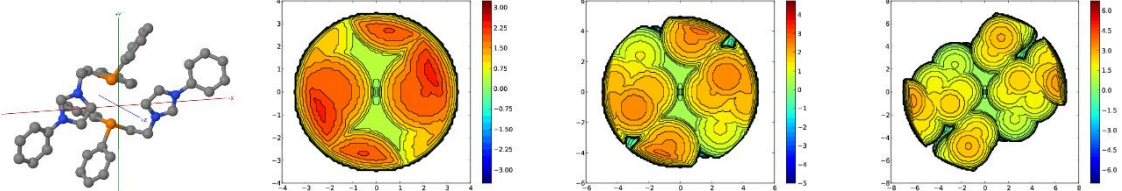


Figure S53: Comparison of steric maps of the hydride complex **3H** (left) at a sphere radius of 3.5 Å using the SambVca 2.0 (left) and SambVca 2.1 (right) tool versions. The increase in color increments can be observed in the red circles on the color scale.

It is worth pointing out that the di-hydride complex **2H** formed from **2** via *iso*-propoxide β-H elimination and isomerization of the abnormal to normal carbene ligand occurs through a deactivation pathway.^{3a} Calculations performed on **1H**, **2H** and **3H** show a significantly higher buried volume compared to their active abnormal carbene catalyst counterparts whilst their steric maps indicate a shielding of the active center.

Buried Volume Tables

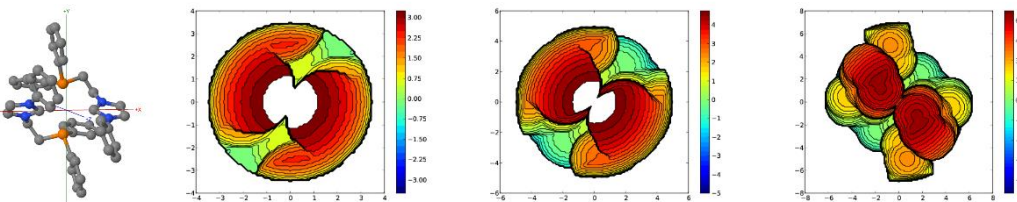
Table S10: Calculated buried volume for complex 1.



The figure shows a 3D molecular model of complex 1 on the left, and three 2D contour plots on the right representing buried volume distributions at different radii. The top plot is for a radius of 3.5 Å, the middle for 5 Å, and the bottom for 7 Å. Each plot has axes ranging from -4 to 4 or -6 to 6. Color scales indicate the magnitude of the buried volume, with values ranging from -3.00 to 3.00 for the top plot, -5 to 5 for the middle, and -6.0 to 6.0 for the bottom.

Radius [Å]	Buried Volume				
	V Free	V Buried	V Total	V Exact	
3.5	36.5	143	179.5	179.6	
	%V_Free	%V_Bur	% Tot/Ex		
	20.3	79.7	100		
	Quadrant	V_f	V_b	V_t	%V_f %V_b
	SW	7.8	37.1	44.9	17.3 82.7
	NW	10.5	34.3	44.9	23.5 76.5
	NE	7.7	37.2	44.8	17.1 82.9
	SE	10.5	34.4	44.9	23.3 76.7
5	V Free	V Buried	V Total	V Exact	
	160.2	363.1	523.3	523.6	
	%V_Free	%V_Bur	% Tot/Ex		
	30.6	69.4	99.9		
	Quadrant	V_f	V_b	V_t	%V_f %V_b
	SW	34.5	96.3	130.8	26.4 73.6
	NW	45.8	85	130.8	35 65
	NE	34.3	96.5	130.8	26.2 73.8
	SE	45.5	85.2	130.8	34.8 65.2
7	V Free	V Buried	V Total	V Exact	
	795.2	641.1	1436.3	1436.8	
	%V_Free	%V_Bur	% Tot/Ex		
	55.4	44.6	100		
	Quadrant	V_f	V_b	V_t	%V_f %V_b
	SW	155.6	203.5	359.1	43.3 56.7
	NW	242.6	116.4	359	67.6 32.4
	NE	155	204	359	43.2 56.8
	SE	242	117.1	359	67.4 32.6

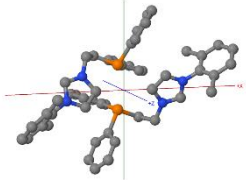
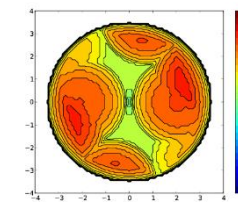
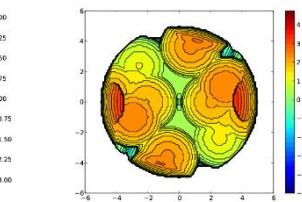
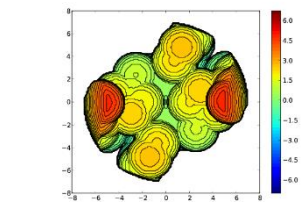
Table S11: Calculated buried volume for complex **1_H**.



The figure shows a 3D molecular model of complex **1_H** on the left, and four 2D contour plots on the right representing buried volume distributions at different radii. The top-left plot is a 3D ball-and-stick model. The other three plots are 2D contour maps with axes labeled x, y, and z. The color scale for the plots ranges from blue (low value) to red (high value). The first plot (radius 3.5 Å) has axes from -4 to 4. The second plot (radius 5 Å) has axes from -6 to 6. The third plot (radius 7 Å) has axes from -8 to 8.

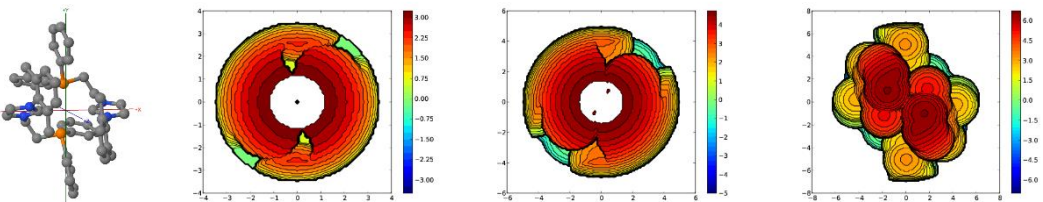
Radius [Å]	Buried Volume				
	V Free	V Buried	V Total	V Exact	
3.5	22.7	156.8	179.5	179.6	
	%V_Free	%V_Bur	% Tot/Ex		
	12.6	87.4	100		
	Quadrant	V_f	V_b	V_t	%V_f
	SW	8.4	36.5	44.9	18.6
	NW	3	41.9	44.9	6.6
	NE	8.4	36.5	44.8	18.6
	SE	3	41.9	44.9	6.6
					%V_b
					81.4
5	97.9	425.4	523.3	523.6	
	%V_Free	%V_Bur	% Tot/Ex		
	18.7	81.3	99.9		
	Quadrant	V_f	V_b	V_t	%V_f
	SW	39.5	91.3	130.8	30.2
	NW	9.5	121.3	130.8	7.2
	NE	39.4	91.3	130.8	30.2
	SE	9.5	121.3	130.8	7.2
					%V_b
					69.8
7	691.8	744.5	1436.3	1436.8	
	%V_Free	%V_Bur	% Tot/Ex		
	48.2	51.8	100		
	Quadrant	V_f	V_b	V_t	%V_f
	SW	238.6	120.4	359.1	66.5
	NW	107.2	251.8	359	29.9
	NE	238.6	120.4	359	66.5
	SE	107.2	251.8	359	29.9
					%V_b
					33.5

Table S12: Calculated buried volume for complex 2.

Radius [Å]	Buried Volume				
	V Free	V Buried	V Total	V Exact	
3.5	36	143.5	179.5	179.6	
	%V_Free	%V_Bur	% Tot/Ex		
	20.1	79.9	100		
	Quadrant	V_f	V_b	V_t	%V_f
	SW	7.7	37.2	44.9	17.1
	NW	10.5	34.3	44.9	23.5
	NE	7.5	37.4	44.8	16.7
	SE	10.3	34.5	44.9	23
					77
5	V Free	V Buried	V Total	V Exact	
	154.1	369.2	523.3	523.6	
	%V_Free	%V_Bur	% Tot/Ex		
	29.5	70.5	99.9		
	Quadrant	V_f	V_b	V_t	%V_f
	SW	32.5	98.3	130.8	24.9
	NW	45.1	85.7	130.8	34.5
	NE	32	98.8	130.8	24.5
	SE	44.5	86.3	130.8	34
					66
7	V Free	V Buried	V Total	V Exact	
	743.1	693.2	1436.3	1436.8	
	%V_Free	%V_Bur	% Tot/Ex		
	51.7	48.3	100		
	Quadrant	V_f	V_b	V_t	%V_f
	SW	137.6	221.4	359.1	38.3
	NW	235	124	359	65.5
	NE	136.5	222.6	359	38
	SE	233.9	125.2	359	65.1
					34.9

Table S13: Calculated buried volume for complex **2_H**.

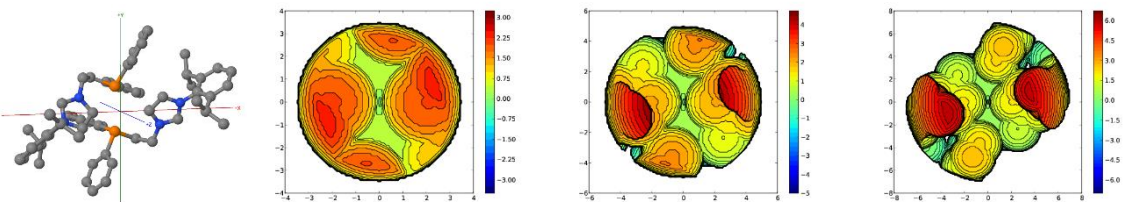


The figure shows a 3D molecular model of complex **2_H** on the left, and four corresponding 2D contour plots on the right. Each plot displays the calculated buried volume distribution across a 2D plane, with color scales indicating the volume values.

The first plot (top-left) shows a circular distribution with a central white hole, a green ring, and a red/orange outer region. The second plot (top-right) shows a similar pattern but with a larger central white hole and more extensive green and red regions. The third plot (bottom-left) shows a more complex, multi-lobed distribution with a large central white hole and several distinct colored lobes. The fourth plot (bottom-right) shows a highly localized, high-volume region centered near the origin, represented by a large red/orange area.

Radius [Å]	Buried Volume					
	V Free	V Buried	V Total	V Exact		
3.5	16.5	163.1	179.5	179.6		
	%V_Free	%V_Bur	% Tot/Ex			
	9.2	90.8	100			
	Quadrant	V_f	V_b	V_t	%V_f	%V_b
	SW	4.6	40.3	44.9	10.1	89.9
	NW	3.6	41.2	44.9	8.1	91.9
	NE	4.6	40.3	44.8	10.1	89.9
	SE	3.7	41.2	44.9	8.1	91.9
	5	59.8	463.5	523.3	523.6	
	%V_Free	%V_Bur	% Tot/Ex			
11.4	88.6	99.9				
Quadrant	V_f	V_b	V_t	%V_f	%V_b	
SW	22	108.8	130.8	16.9	83.1	
NW	7.8	123	130.8	6	94	
NE	22	108.7	130.8	16.9	83.1	
SE	7.8	123	130.8	6	94	
7	619.3	817	1436.3	1436.8		
	%V_Free	%V_Bur	% Tot/Ex			
	43.1	56.9	100			
	Quadrant	V_f	V_b	V_t	%V_f	%V_b
	SW	206.4	152.6	359.1	57.5	42.5
	NW	103.2	255.8	359	28.7	71.3
	NE	206.4	152.6	359	57.5	42.5
	SE	103.2	255.8	359	28.7	71.3

Table S14: Calculated buried volume for complex 3.



Radius [Å]	Buried Volume				
3.5	V Free		V Buried		V Total
	35.7		143.8		179.5
	%V_Free		%V_Bur		% Tot/Ex
	19.9		80.1		100
Quadrant		V_f	V_b	V_t	%V_f
SW		7.4	37.5	44.9	16.4
NW		10.3	34.6	44.9	22.9
NE		7.5	37.3	44.8	16.8
SE		10.4	34.4	44.9	23.3
5	V Free		V Buried		V Total
	147.7		375.6		523.3
	%V_Free		%V_Bur		% Tot/Ex
	28.2		71.8		99.9
Quadrant		V_f	V_b	V_t	%V_f
SW		29.2	101.6	130.8	22.4
NW		43.6	87.2	130.8	33.4
NE		30.4	100.4	130.8	23.2
SE		44.4	86.4	130.8	33.9
7	V Free		V Buried		V Total
	687.4		748.9		1436.3
	%V_Free		%V_Bur		% Tot/Ex
	47.9		52.1		100
Quadrant		V_f	V_b	V_t	%V_f
SW		112.2	246.9	359.1	31.2
NW		229.7	129.3	359	64
NE		114.2	244.8	359	31.8
SE		231.2	127.8	359	64.4

Table S15: Calculated buried volume for complex **3_H**.

Radius [Å]	Buried Volume				
	V Free	V Buried	V Total	V Exact	
3.5	19	160.5	179.5	179.6	
	%V_Free	%V_Bur	% Tot/Ex		
	10.6	89.4	100		
	Quadrant	V_f	V_b	V_t	%V_f
	SW	4.4	40.5	44.9	9.7
	NW	5.1	39.8	44.9	11.4
	NE	4.4	40.5	44.8	9.7
	SE	5.1	39.7	44.9	11.4
					88.6
5	47.7	475.6	523.3	523.6	
	%V_Free	%V_Bur	% Tot/Ex		
	9.1	90.9	99.9		
	Quadrant	V_f	V_b	V_t	%V_f
	SW	14.5	116.3	130.8	11.1
	NW	9.4	121.4	130.8	7.2
	NE	14.5	116.3	130.8	11.1
	SE	9.3	121.5	130.8	7.1
					88.9
7	503.4	933	1436.3	1436.8	
	%V_Free	%V_Bur	% Tot/Ex		
	35.0	65.0	100		
	Quadrant	V_f	V_b	V_t	%V_f
	SW	158.2	200.9	359.1	44
	NW	93.5	265.6	359	26
	NE	158.2	200.9	359	44.1
	SE	93.4	265.6	359	26
					56

Steric Maps

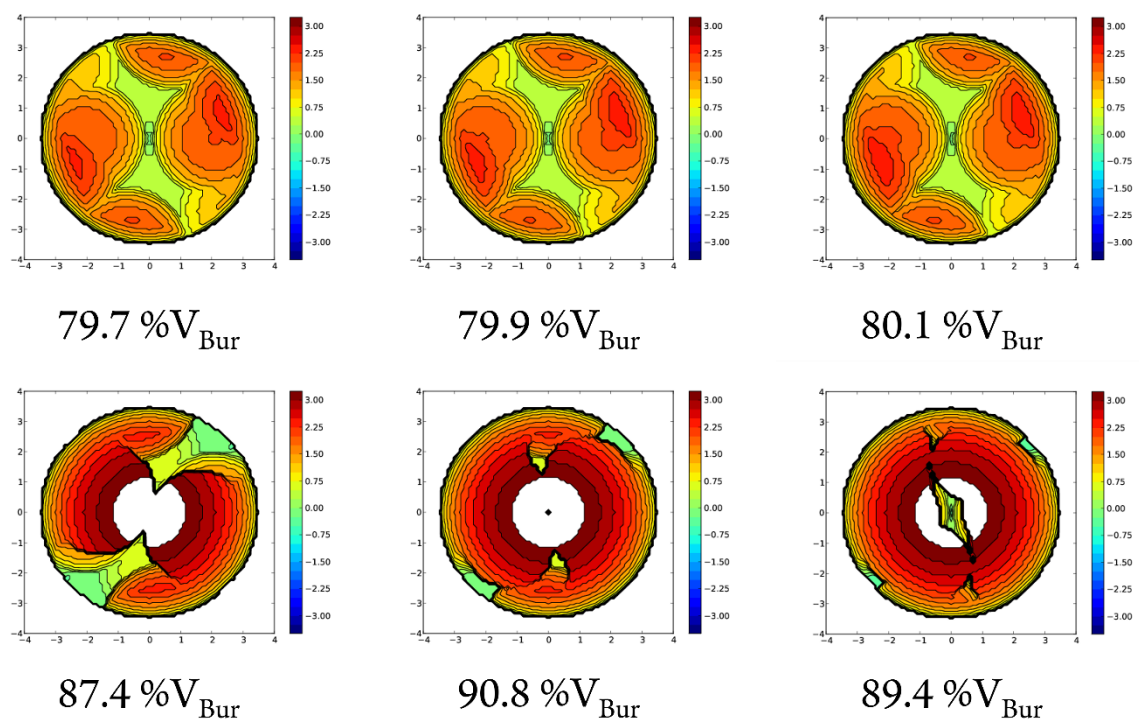


Figure S54: Steric maps at 3.5 Å for complexes **1** (top left), **2** (top center) and **3** (top right) as well as their corresponding hydrides **1_H**, **2_H** and **3_H** below. Axes are in Å. The relative values for buried volume are given below each map.

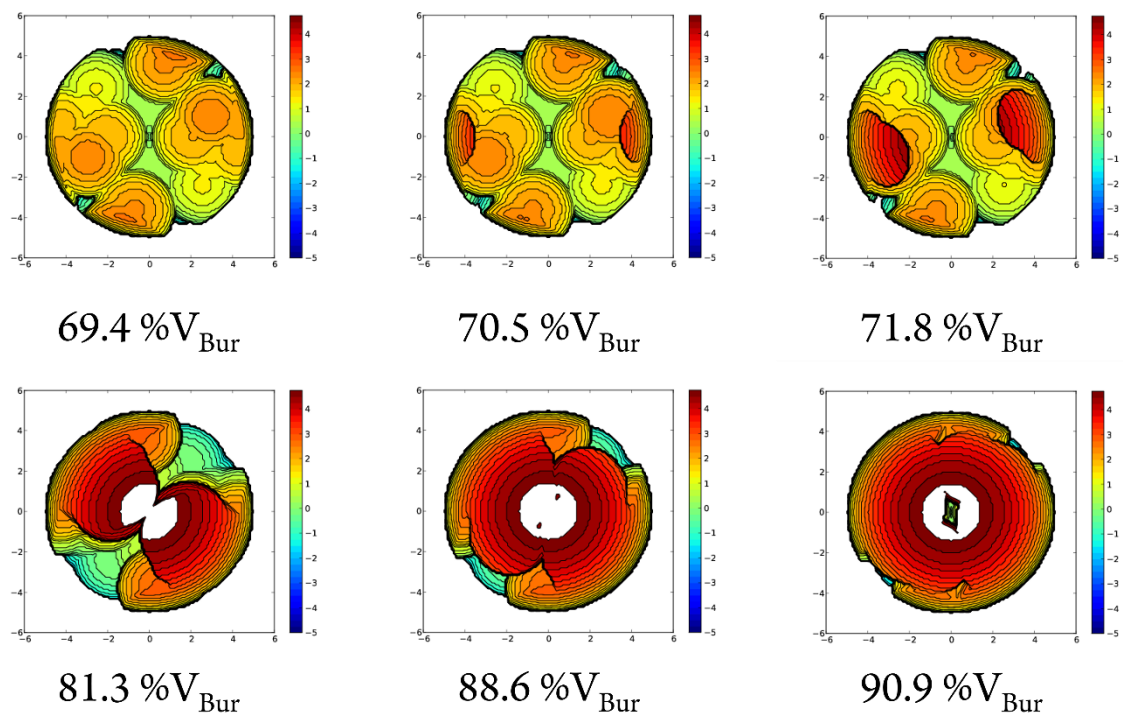


Figure S55: Steric maps at 5 Å for complexes **1** (top left), **2** (top center) and **3** (top right) as well as their corresponding hydrides **1_H**, **2_H** and **3_H** below. Axes are in Å. The relative values for buried volume are given below each map.

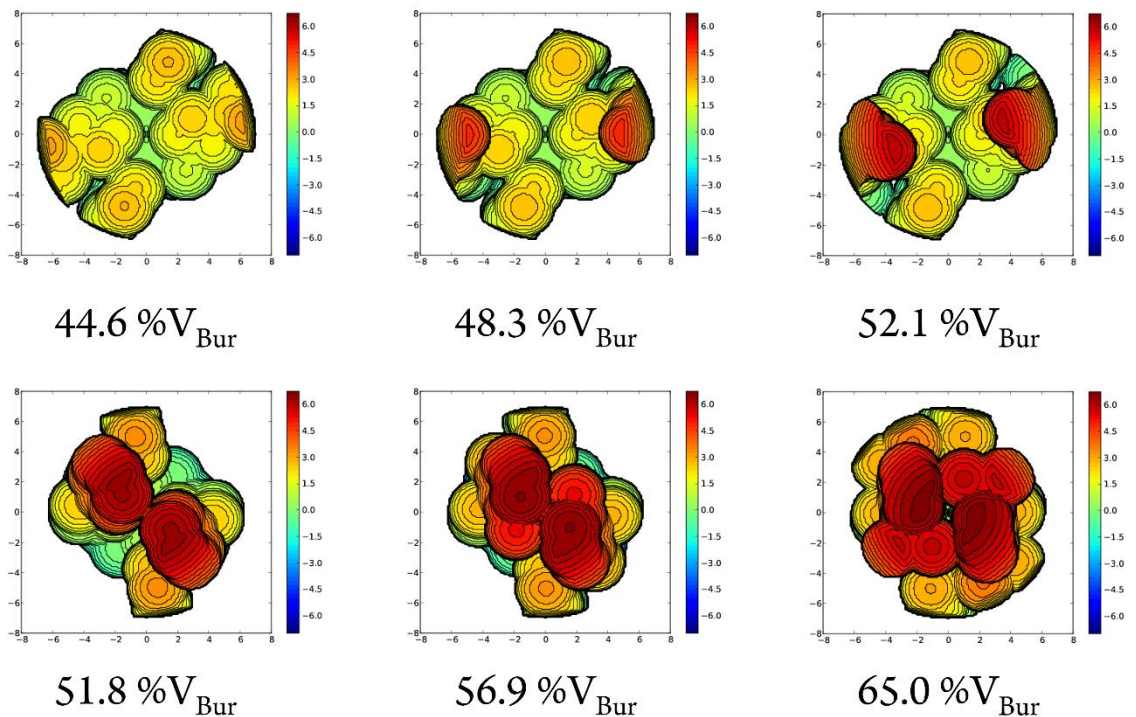


Figure S56: Steric maps at 7 Å for complexes **1** (top left), **2**(top center) and **3** (top right) as well as their corresponding hydrides **1_H**, **2_H** and **3_H** below. Axes are in Å. The relative values for buried volume are given below each map.

Mechanisms

The proposed mechanisms for both TH and *Oppenauer*-type oxidation applying complexes **1**, **2** and **3** are depicted (Figure S57 and S58, respectively). The Ru-bis-aNHC complexes applied in catalysis are technically all singular positive complexes with a bromide counterion (excluded for clarity). As the carbenes “donate” their electrons towards the Ru center, they can formally be considered as positively charged, whilst the acetate ligand has a negative charge. During TH, the complex can directly coordinate to *iso*-propanolate, which acts as hydrogen donor for the reaction. For the *Oppenauer*-type oxidation however, a competing coordination of *tert*-butanolate most likely occurs. This however cannot act as hydrogen donor *via* β-H-elimination so that an exchange with the sterically demanding substrate (in comparison to sterically less demanding *iso*-propanolate during TH) is required. Both active species can undergo a β-H-elimination step and form a mono-hydride as well as the ketone. From here, the mono-hydride species can either follow the catalytic cycle, likely in accordance to the inner-sphere mechanism as proposed by Noyori,³¹ or form a di-hydride species which has been shown to be inactive in TH and *Oppenauer*-type oxidation,^{3a} representing a deactivation pathway.

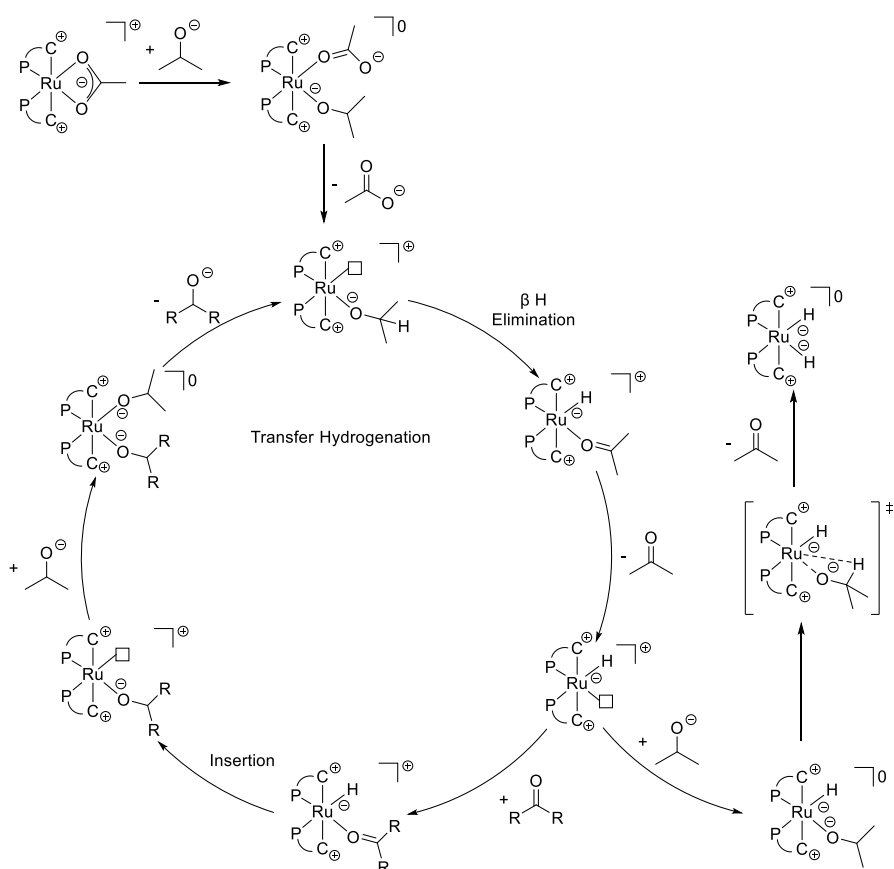


Figure S57: Inner-sphere catalytic mechanism for TH as originally proposed by Noyori³¹ including additional di-hydride deactivation pathway. Coordination of the 1-(2-diphenylphosphino-ethyl)-3-aryl-imidazolium ligands depicted as P-C and counter ion bromide excluded for clarity. The substrate acetophenone is represented abbreviated as R.

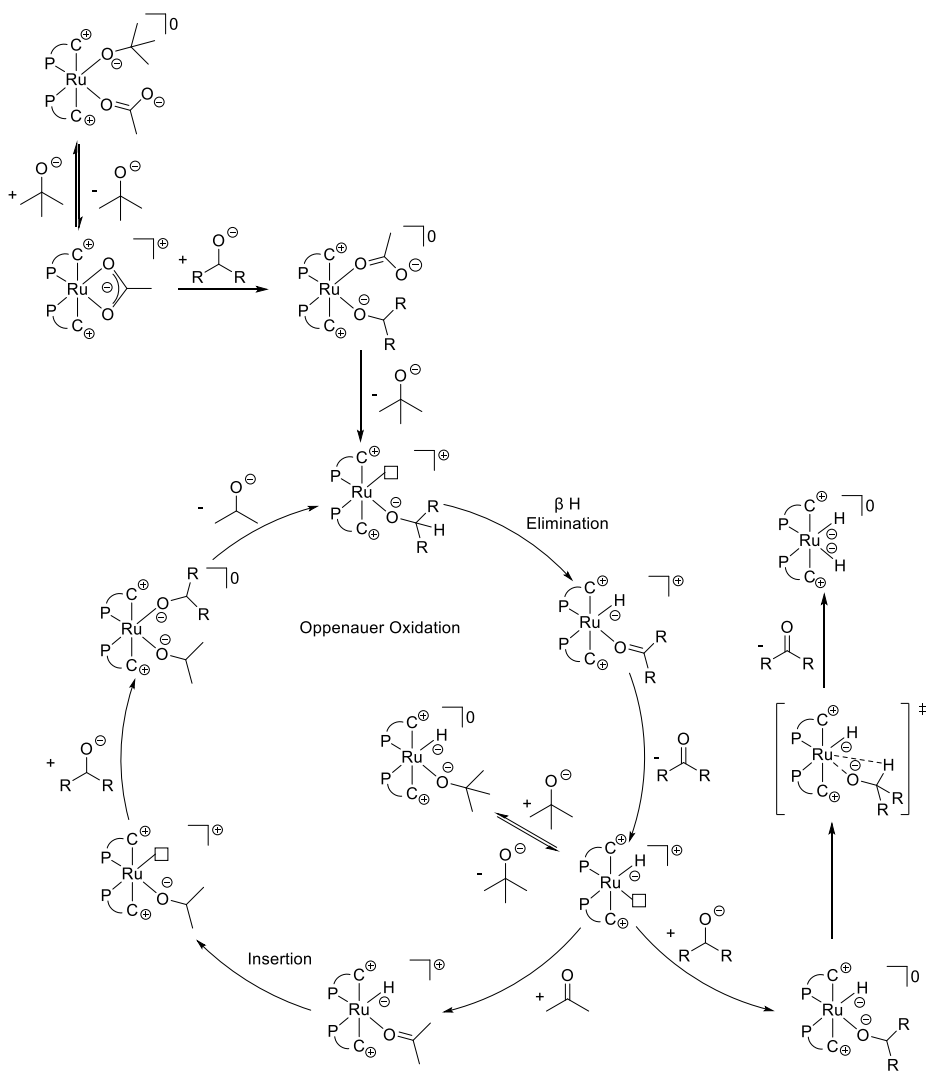


Figure S58: Inner-sphere catalytic mechanism for Oppenauer type oxidation as originally proposed in by Noyori³¹ including additional di-hydride deactivation pathway as well as potential coordination of ${}^t\text{BuOH}$ solvent. Coordination of the 1-(2-diphenylphosphino-ethyl)-3-aryl-imidazolium ligands depicted as P-C and counter ion bromide excluded for clarity. The substrate α -tetralol is represented abbreviated as R.

References

1. Mitchell, R. W.; Spencer, A.; Wilkinson, G., *J Chem Soc Dalton* **1973**, 846-854.
2. Wang, Z.; Zhang, M.; Li, Y. Ionic conductors containing phenyl/biphenyl and hydroxyalkyl as well as preparation method and application of ionic conductors. CN108383794 (A), 2018.
3. (a) Pardatscher, L.; Hofmann, B. J.; Fischer, P. J.; Hözl, S. M.; Reich, R. M.; Kühn, F. E.; Baratta, W., *ACS Catal.* **2019**, 9, 11302-11306; (b) Zhao, Y.; Gilbertson, S. R., *Org. Lett.* **2014**, 16, 1033-1035; (c) Wolf, J.; Labande, A.; Daran, J. C.; Poli, R., *J. Organomet. Chem.* **2006**, 691, 433-443; (d) Wolf, J.; Labande, A.; Natella, M.; Daran, J. C.; Poli, R., *J Mol Catal a-Chem* **2006**, 259, 205-212.
4. (a) Liu, J. P.; Chen, J. B.; Zhao, J. F.; Zhao, Y. H.; Li, L.; Zhang, H. B., *Synthesis-Stuttgart* **2003**, 2661-2666; (b) Hameury, S.; de Fremont, P.; Breuil, P. A. R.; Olivier-Bourbigou, H.; Braunstein, P., *Dalton Trans.* **2014**, 43, 4700-4710.
5. *APEX suite of crystallographic software*, APEX 3, Version 2019-11.0; Bruker AXS Inc.: Madison, Wisconsin, USA, 2019.
6. *SAINT*, Version 8.38A; Bruker AXS Inc.: Madison, Wisconsin, USA, 2017.
7. *SADABS*, Version 2016/2; Bruker AXS Inc.: Madison, Wisconsin, USA, 2016.
8. (a) Sheldrick, G. M., *Acta Cryst. C* **2015**, 71, 3-8; (b) Hübschle, C. B.; Sheldrick, G. M.; Dittrich, B., *J. Appl. Cryst.* **2011**, 44, 1281-1284; (c) Sheldrick, G. M., *Acta Cryst. A* **2015**, 71, 3-8.
9. Wilson, A. J., *International Tables for Crystallography*. Kluwer Academic Publishers: Dordrecht, The Netherlands, 1992; Vol. C.
10. Macrae, C. F.; Sovago, I.; Cottrell, S. J.; Galek, P. T. A.; McCabe, P.; Pidcock, E.; Platings, M.; Shields, G. P.; Stevens, J. S.; Towler, M.; Wood, P. A., *J. Appl. Cryst.* **2020**, 53, 226-235.
11. Yasar, S.; Cekirdek, S.; Ozdemir, I., *J. Coord. Chem.* **2014**, 67, 1236-1248.
12. Viji, M.; Tyagi, N.; Naithani, N.; Ramaiah, D., *New. J. Chem.* **2017**, 41, 12736-12745.
13. Hollering, M.; Albrecht, M.; Kühn, F. E., *Organometallics* **2016**, 35, 2980-2986.
14. Kleinhans, G.; Guisado-Barrios, G.; Peris, E.; Bezuidenhout, D. I., *Polyhedron* **2018**, 143, 43-48.
15. Witt, J.; Pöthig, A.; Kühn, F. E.; Baratta, W., *Organometallics* **2013**, 32, 4042-4045.
16. Almeida, M. L. S.; Beller, M.; Wang, G. Z.; Bäckvall, J. E., *Chem. Eur. J.* **1996**, 2, 1533-1536.
17. Mukherjee, A.; Bhattacharya, S., *RSC Adv.* **2021**, 11, 15617-15631.
18. Saleem, F.; Rao, G. K.; Kumar, S.; Singh, M. P.; Singh, A. K., *Dalton Trans.* **2015**, 44, 19141-19152.
19. Wang, Q.; Du, W.; Liu, T.; Chai, H.; Yu, Z., *Tetrahedron Lett.* **2014**, 55, 1585-1588.
20. Gauthier, S.; Scopelliti, R.; Severin, K., *Organometallics* **2004**, 23, 3769-3771.
21. Manzini, S.; Urbina-Blanco, C. A.; Nolan, S. P., *Organometallics* **2013**, 32, 660-664.
22. Frisch, M. J.; Trucks, G. W.; Schlegel, H. B.; Scuseria, G. E.; Robb, M. A.; Cheeseman, J. R.; Scalmani, G.; Barone, V.; Petersson, G. A.; Nakatsuji, H.; Li, X.; Caricato, M.; Marenich, A. V.; Bloino, J.; Janesko, B. G.; Gomperts, R.; Mennucci, B.; Hratchian, H. P.; Ortiz, J. V.; Izmaylov, A. F.; Sonnenberg, J. L.; Williams, Ding, F.; Lipparini, F.; Egidi, F.; Goings, J.; Peng, B.; Petrone, A.; Henderson, T.; Ranasinghe, D.; Zakrzewski, V. G.; Gao, J.; Rega, N.; Zheng, G.; Liang, W.; Hada, M.; Ehara, M.; Toyota, K.; Fukuda, R.; Hasegawa, J.; Ishida, M.; Nakajima, T.; Honda, Y.; Kitao, O.; Nakai, H.; Vreven, T.; Throssell, K.; Montgomery Jr., J. A.; Peralta, J. E.; Ogliaro, F.; Bearpark, M. J.; Heyd, J.

- J.; Brothers, E. N.; Kudin, K. N.; Staroverov, V. N.; Keith, T. A.; Kobayashi, R.; Normand, J.; Raghavachari, K.; Rendell, A. P.; Burant, J. C.; Iyengar, S. S.; Tomasi, J.; Cossi, M.; Millam, J. M.; Klene, M.; Adamo, C.; Cammi, R.; Ochterski, J. W.; Martin, R. L.; Morokuma, K.; Farkas, O.; Foresman, J. B.; Fox, D. J. *Gaussian 16 Rev. B.01*, Wallingford, CT, 2016.
- 23. Dennington, R.; Keith, T. A.; Milliam, J. M. *GaussView, Version 6.0.16*, Semichem Inc.: Shawnee Missions, KS, 2016.
 - 24. Grimme, S.; Ehrlich, S.; Goerigk, L., *J. Comput. Chemie* **2011**, *32*, 1456-1465.
 - 25. (a) Weigend, F., *Phys. Chem. Chem. Phys.* **2006**, *8*, 1057-1065; (b) Weigend, F.; Ahlrichs, R., *Phys. Chem. Chem. Phys.* **2005**, *7*, 3297-3305.
 - 26. Bergner, A.; Dolg, M.; Küchle, W.; Stoll, H.; Preuß, H., *Mol. Phys.* **1993**, *80*, 1431-1441.
 - 27. Poater, A.; Ragone, F.; Giudice, S.; Costabile, C.; Dorta, R.; Nolan, S. P.; Cavallo, L., *Organometallics* **2008**, *27*, 2679-2681.
 - 28. Poater, A.; Ragone, F.; Mariz, R.; Dorta, R.; Cavallo, L., *Chem. Eur. J.* **2010**, *16*, 14348-14353.
 - 29. Poater, A.; Cosenza, B.; Correa, A.; Giudice, S.; Ragone, F.; Scarano, V.; Cavallo, L., *Eur. J. Inorg. Chem.* **2009**, *2009*, 1759-1766.
 - 30. Falivene, L.; Cao, Z.; Petta, A.; Serra, L.; Poater, A.; Oliva, R.; Scarano, V.; Cavallo, L., *Nat. Chem.* **2019**, *11*, 872-879.
 - 31. Noyori, R.; Hashiguchi, S., *Acc. Chem. Res.* **1997**, *30*, 97-102.

Author Contributions

Alexander D. Böth: Synthesis, computational chemistry, catalysis, manuscript preparation; Michael J. Sauer: X-ray diffraction measurements/analysis; Walter Baratta: Project design and experimental strategy planning; Fritz E. Kühn: Project design and controlling.